Gina Almås Gundersen

The intestinal uptake of polystyrene (PS) and polyethylene terephthalate (PET) nanaoplastic particles in the Atlantic salmon (*Salmo salar*) parr and post-smolt, and translocation of PET nanoplastic particles to the circulatory system and liver in parr

Master's thesis

NTNU
Norwegian University of Science and Technology
Faculty of Natural Sciences
Department of Biology

Master's thesis in Physiology
Supervisor: Rolf Erik Olsen, Signe Dille Løvmo, Fredrik Jutfelt
May 2019

NTNU
Kunnskap for en bedre verden

Gina Almås Gundersen

The intestinal uptake of polystyrene (PS) and polyethylene terephthalate (PET) nanaoplastic particles in the Atlantic salmon (*Salmo salar*) parr and post-smolt, and translocation of PET nanoplastic particles to the circulatory system and liver in parr

Master's thesis in Physiology
Supervisor: Rolf Erik Olsen, Signe Dille Løvmo, Fredrik Jutfelt
May 2019

Norwegian University of Science and Technology
Faculty of Natural Sciences
Department of Biology

NTNU
Norwegian University of
Science and Technology

Abstract

Micro- (20 µm – 5 mm) and nano- (< 20 µm) plastics pose a great environmental concern as it accumulates in marine and aquatic environments. Recently, several studies have also confirmed that marine vertebrates and invertebrates ingest and translocate these plastic particles to various organs with potentially harmful effects. However, knowledge regarding uptake mechanisms over the intestinal epithelium remains unknown. The present study aimed to examine the uptake of polystyrene (PS) and polyethylene terephthalate (PET) nanoplastic particles over the intestinal epithelium in the Atlantic salmon (*Salmo salar*) parr and post-smolt, and translocation of the latter to the circulatory system, liver, head kidney and spleen in parr. An *ex vivo* pilot study using the Ussing chamber confirmed intestinal uptake of PS (0.5 µm) and PET nano particles in post-smolt. The *in vivo* feeding experiment further confirmed intestinal uptake of ≤ 2 µm PET nanoplastic particles and translocation to the circulatory system and liver in parr. Particles translocated to the intestinal tissue and circulatory system were associated with intraepithelial and blood leucocytes, respectively, potentially indicating initiation of the immune system. The results highlight the extended need for further research on cellular uptake mechanisms and effects in the Atlantic salmon exposed to nanoplastic particles and increased knowledge regarding health and welfare consequences.

Acknowledgement

I would first like to thank my main supervisor Professor Rolf Erik Olsen for letting me work with such interesting and highly relevant project, for constructive feedback, inputs and supervision. Thanks also to my co-supervisors Signe Dille Løvmo and Fredrik Jutfelt. I especially appreciate all the help and feedback from Signe regarding the practical work during my thesis and in the writing process. Thank you for your patience and positivity! Thanks to Fredrik for lending me the polystyrene nanoplastic particles, for scientific inspiration and for always being so supportive. I have the greatest gratitude for all help and support form Dag Altin who has spent time and resources in making my results as good as possible by lending me fluorescence microscope, computers and associated equipment for my analysis. I´m so thankful for the all feedback, discussions and the always-positive mood! I couldn't have done this without!

In addition, I would like to thank Martin Wagner for the PET particles, informative articles and feedback. Thanks also to Trude Johansen for good help with the coulter counter analysis at Gløshaugen and Tora Bardal for instructions and follow-up at the histology-lab. Thanks to Iurgi Imanol Salaverria-Zabalegui for helping me trying to get some PET information at the very end of my writing process.

And of course, thanks to my lovely family, friends and fellow students for all support during these years at NTNU. I especially appreciate all the good times with my fellow students at Sealab, who made my masters work so much easier. Thank you, folks, for being so motivating and amazing.

Finally, I would thank my amazing boyfriend Torstein Brandth for always encouraging and supporting me. You are the best!

Thank you all for believing in me!

Trondheim, May 2019

Gina Almås Gundersen

Table of contents

1. Introduction

1.1 Plastics:

Plastics (from Greek "*plasticos*") are synthetic or semi-synthetic organic polymers derived from petrochemicals (e.g. crude oil and gas), and plastics production make up 4 – 6% of the annual petroleum composition (PlasticsEurope, 2017). The chemical and physical properties make plastics lightweight and flexible with a great resistance against degradation over a range of temperatures, pressures and chemicals. These properties and the relatively low cost of production, make plastics indispensable in numerous industrial applications, such as construction, transport, agri- and aquaculture (Andrady and Neal, 2009, PlasticsEurope, 2018). Plastics serve social benefits in safe conservation of food and water through temperature and atmosphere-controlled packing, in health care products and medical technology (Muralisrinivasan, 2016). Unfortunately, as many of these properties are based on the high resistance against degradation, discards will accumulate in nature and are now considered one of the world`s biggest environmental issues regarding waste hazards (Andrady, 2003b).

The total annual production of plastics is steadily increasing, reaching a total of 348 million tons in 2017 (PlasticsEurope, 2018). Assuming an increase in the global population to 10 billion by 2100, simple extrapolation suggests that the annual plastics production could amount to 500 million tons by then (Andrady, 2003a). An estimated 10% of the annual plastic produced end up in the marine environment (Thompson, 2006, Jambeck *et al*., 2015), where large amounts accumulate as macro- (> 25 mm) and microplastics (20 µm – 5 mm) (Wagner *et al*., 2014) debris in the water column, on the seabed and on beaches (Thiel *et al*., 2013, Topçu *et al*., 2013). Of the total amount of plastics present in the world's oceans, 92.4% are estimated to be microplastic particles (Eriksen *et al*., 2014). More recently, plastics in the microscopic range has also been reported from surface waters in the Arctic Polar circle as well as embedded in the polar ice, illustrating the great and concerning spread to non-populated areas (Cózar *et al*., 2017, Peeken *et al*., 2018).

Microplastics reach the marine environment in high quantities from different sources. Primary microplastics, such as microbeads from cosmetics (Fendall and Sewell, 2009, Napper *et al*., 2015) and synthetic clothing (e. g polyester) (Browne *et al*., 2011, Napper and Thompson,

2016) enter the environment through waste water and drainage systems. Secondary microplastics are produced via fragmentation of macroplastics through thermooxidation, photooxidation, mechanical abrasion and, to a lesser extent, microbial and enzymatic degradation (Shah *et al*., 2008, Andrady, 2011). Microplastics, and even smaller nanoplastic particles (< 20 µm, Wagner *et al*., 2014), are persistent and pose a great concern regarding marine biota and habitats (Moore, 2008, Eerkes-Medrano *et al*., 2015). Several field and laboratory studies have shown the presence of nano and micro sized plastic particles in different organs of marine vertebrates and invertebrates and have indicated harmful effects to cells and tissues (Browne *et al*., 2008, Brennecke *et al*., 2015, Jovanović, 2017).

1.1.2 Plastic polymers

Plastics consist of a great range of polymers, in which studies on uptake, translocation and effects in organisms have dealt with only some of these. Polystyrene (PS), polyethylene (PE) and polypropylene (PP) are common thermoplastics often reported in the literature regarding uptake studies (Lei *et al*., 2018). These are the most abundant plastic polymers, also expected to be widely distributed in marine and aquatic environments (Andrady, 2011). PS, the most common polymer used in uptake studies, has a hard, amorphous structure with a bulk density of 1.05 g/cm^3. It's a suitable polymer for low-density packing materials, contributing for approximately 6.6% of the European plastic demand (PlasticsEurope, 2018). PS latex particles are also used as model delivery vehicles in research on oral drug administration (Olivier *et al*., 2003) and the physiochemical properties of the PS polymer are therefore well known. Polyethylene terephthalate (PET) is another abundant polymer, constituting for approximately 7.4% of the European plastic demand (PlasticsEurope, 2018). It has a bulk density of 1.29 – 1.40 g/cm^3 and is used in synthetic clothing (e.g. fleece) and in soda bottles due to its excellent transparency and good CO_2-barriers (Andrady, 2003a). PET has recently been used in an invertebrate uptake study, but is to a lesser extent than PS mentioned as a used polymer in relation to such studies (Weber *et al*., 2018).

1.2 Ingestion and translocation of micro- and nanoplastic particles in marine biota

The high density of small plastic particles in the aquatic environment makes many fish vulnerable to exposure and ingestion. Field studies from the North Sea (Foekema *et al*., 2013), the North Pacific Gyre (Moore *et al*., 2001, Boerger *et al*., 2010, Davison and Asch,

2011) and the North Atlantic Gyre (Reisser *et al*., 2015) report findings of microplastics in the gastrointestinal tract of numerous pelagic, mesopelagic and demersal fish species. The reported size distribution of the particles varies greatly between studies. For example, ranges from 0.04 – 4.8 mm (Foekema *et al*., 2013) and 0.13 – 14.3 mm (Lusher *et al*., 2013) have been reported. The variation is probably in part caused by variations in sampling procedures and extraction protocols (Avio *et al*., 2015). The establishment of reproducible and accurate analytical protocols are therefore a prioritized current research area. Regardless of methodology, the average number of particles in the gastrointestinal tract of each fish appears constant at 1 – 2 particles (Boerger *et al*., 2010, Davison and Asch, 2011, Lusher *et al.*, 2013, Bellas *et al*., 2016).

The relatively low number of particles may indicate that they only stay in the digestive tract for a short period (Foekema *et al.*, 2013), either as a result of excretion (i.e. in feces) or translocation to the circulatory system and other organs (Yin *et al*., 2018). The latter is likely dependent on the polymer's physiochemical properties and species specific differences (Kashiwada, 2006, Browne *et al.*, 2008, Doyle-McCullough *et al.*, 2007, Andrady, 2017). The size is considered an important characteristic and laboratory studies indicate that small sized particles translocate into organs to a greater extent than larger ones. For instance, 39.4 nm water-suspended PS nanoparticles were distributed to the liver, gallbladder, gonads and brain of Medaka (*Oryzias latipes*) (Kashiwada, 2006). Translocation to the liver was also observed in adult zebrafish (*Danio rerio*) following exposure to 70 nm and 5 µm PS particles in the surrounding water (Lu *et al*., 2016). The same was reported from exposed zebrafish embryos, in addition to translocation to the pancreas, gallbladder and the brain (Pitt *et al*., 2018). On the contrary, larger PS particles of 15 and 20 µm translocated to the circulatory system of water-exposed juvenile jacopever (*Sebastes schlegelii*) and adult zebrafish, respectively, showed no distribution to the liver (Lu *et al*., 2016, Yin *et al.*, 2018). Particle translocation to the liver was nor observed in injected zebrafish larvae exposed to 700 nm PS particles (Veneman *et al*., 2017). Nevertheless, larger particles have been found in organs of wild fish species. PE particles in the size range of 124 – 438 µm were observed in livers of European anchovies (*Engraulis encrasicolus*), and even larger 200 – 600 µm PS and PE particles were reported randomly located in the hepatic cells of mullets (*Mugil cephalus*) form the Adriatic sea (Avio *et al*., 2015, Collard *et al*., 2017).

Exposure time is considered another important variable regarding translocation, and exposure times of 7 – 30 days have mainly been reported from the previous studies (Kashiwada, 2006, Lu *et al.*, 2016, Yin *et al.*, 2018). Nevertheless, even shorter and longer exposure times of 0.5 hours and 2 months have been reported in studies of exposed Sprague-Dawley rats and fiddler crabs (*Una rapax*), respectively (Hodges *et al.*, 1995, Brennecke *et al*., 2015). Brown *et al*., (2008) reported accumulation of 3 µm PS particles in the gut and digestive tubules of the blue mussel (*Mytilus edulis*) 12 hours after exposure, with translocation to the circulatory system after 3 days. The study also observed highest abundance of particles after 12 days, before a decline followed (Browne *et al*., 2008). A decline in translocated particles was also observed in the rat intestinal tissue from 0.5 hours to 24 hours after oral administration (Hodges *et al.*, 1995). An 18 – 30 days feeding experiment with PS nanoplastic particles confirmed that at least 22 days of exposure was necessary for metabolic effects to be observed in zebrafish (Cedervall *et al*., 2012).

Several studies indicate that particle translocations have harmful effects, and altered metabolic profiles, endocrine and behavioral disruptions have been reported in exposed fish (Rochman *et al.*, 2014, Jovanović, 2017, Mattsson *et al.*, 2017, Yin *et al*., 2018). For instance, zebrafish exposed to PS nanoparticles had altered lipid metabolism after binding to apolipoprotein A-I in fish serum (Cedervall *et al*., 2012) in addition to signs of inflammation and accumulation of lipids in the liver (Lu *et al*., 2016). There is still debated whether nano and micro sized particles cause any hazard *per se*, but some chemicals embedded into the particles are known to be toxic. These include plasticizers and flame retardants. Nano and micro sized particles have large surface area to volume ratios, which will increase the exposure of these additives. Nano- and microparticles have also been shown to absorb persistent organic pollutants from the aquatic environment which may then leak into organisms when ingested (Jovanović, 2017). Recent studies also suggest interactions between micro and nano sized particles and immune cells (von Moos *et al*., 2012, Greven *et al.*, 2016, Veneman *et al.*, 2017), in addition to increased activation of superoxide dismutase and catalase (Lu *et al*., 2016), indicating mobilization of oxidative stress systems in exposed organisms.

1.3 Physiology of the Atlantic salmon

1.3.1 The intestine

The vertebrate intestine is a continuous muscular layer representing a barrier between the surroundings and the interior of the organism. In fish, the intestine is divided in an anterior midgut and a posterior hindgut. The main function of the midgut is absorption of nutrients from the enzymatically degraded food (chyme) in the lumen. Some nutrient uptake is maintained in the hindgut of salmonids, but water absorption is to a greater extent the main function of the proximal segment. This is further reflected in the decreased epithelial permeability observed from the midgut to the hindgut segment. The intestine also has important roles as a first line defense system against pathogens (Bone, 2008, Jutfelt, 2011).

The intestinal wall has distinct layers with different morphology and functions (Figure 1). The mucosa, with the epithelium and mucus layer, face the luminal side of the intestine. The mucosal epithelium, composed of one layer of cells, contains numerous mucosal folds which increase the surface area and nutrient uptake capacity. Located on the mucosal folds are the absorptive enterocytes, mucus-secreting goblet cells and enteroendocrine cells. The goblet cells continuously produce mucus (mainly consisting of acid glycoproteins) that lubricate and protects the epithelium against pathogens. They also ease the transport of luminal content down the intestinal canal. These cells have shown to increase their production in situations of stress or as a response to inflammatory stimuli (Edelblum and Turner, 2015). Under the mucosal epithelium is the lamina propria, a connective tissue rich in blood cells and nerve fibers. It absorbs nutrients from the enterocytes, leading them towards the circulatory system. In addition, the lamina propria has important immunological functions through the presence of numerous phagocytotic cells that phagocytose and destroys potentially harmful agents that have crossed the epithelial barrier before entering the circulation. External to the lamina propria is the muscularis mucosae, a layer of smooth muscles important for movement of the mucosa. The serosa is the outermost layer of connective tissue and epithelium, facing the circulatory system (Jutfelt, 2011, Marieb, 2016).

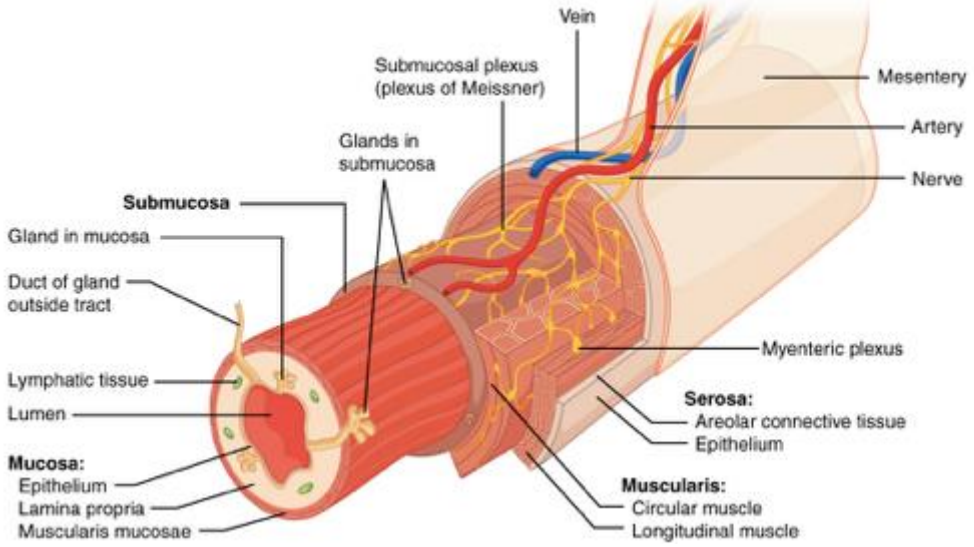

Figure 1. Illustration of the intestinal anatomy in vertebrates, including fish. The intestine is a long hollow tube making up a barrier between the outside (lumen) and the inside of the organism. The mucosa is the innermost layer, facing the lumen. It consists of the epithelium, lamina propria and muscularis mucosae. Underneath are the submucosa and muscularis (circular and longitudinal muscles). The serosa is the outermost layer of connective tissue and epithelium, facing the circulation. The intestine is also supplied with nerve fibers, blood vessels and mesenteries (OpenStax, 2016).

The enterocytes lay in close proximity connected by tight junction (TJ) protein complexes, acting as diffusion barriers (Figure 2). Nutrients mainly pass through the enterocytes, termed the transcellular rout. Small hydrophobic substances (e.g. fatty acids) can pass freely through passive diffusion, while hydrophilic substances (e.g. glucose and many amino acids) are transported through adenosine-triphosphate (ATP)-dependent active transport or cotransport via specialized transporter molecules (Jutfelt, 2011, Marieb, 2016). Lager molecules can be transported via transcytosis, mainly endocytosis at the apical membrane and exocytosis at the basolateral membrane. Some hydrophilic particles can also pass between enterocytes (paracellular rout) through pores formed in the TJ complexes (Jutfelt, 2011, Zihni *et al*., 2016). The paracellular transport mechanism has been shown to discriminate particles on the basis of charge and size. Pores with radius of approximately 0.6 nm are reported in the tight junctions at the apical part of villi in rats, while larger pores (radius 1 – 5 nm) are present further down the villus-crypt-axis. Macromolecules with radius up to 3 – 6 nm are also suggested to cross this barrier, indicating a potential transport of molecules of different size through the paracellular rout (Fihn *et al*., 2000, Zihni *et al*., 2016).

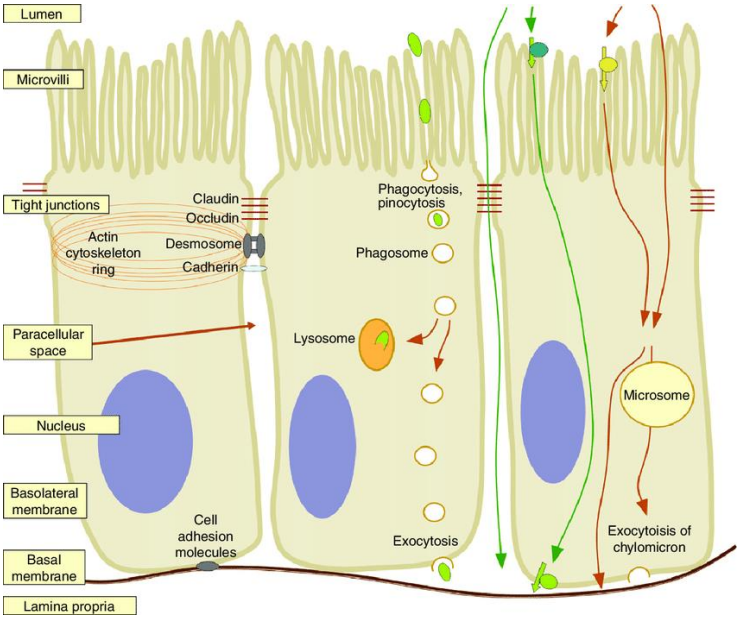

Figure 2. Schematic representation of enterocytes and their associated structures. Protein complexes termed tight junctions and desmosomes connect the individual enterocytes. Nutrients enter the enterocytes (transcellular rout) at the apical membrane (with microvilli) through active adenosine-triphosphate (ATP)-dependent transport, as passive diffusion or as endo-, phago-, or pinocytosis, and leaves the enterocytes on the basolateral side (e. g through exocytosis). Some hydrophilic substances can pass between the enterocytes, termed the paracellular rout. Illustration: Jutfelt, 2011.

1.3.2 The circulatory system and blood filtration

The circulatory system represents the main transport system in fish, in which it delivers O_2 and nutrients to working cells and removes CO_2, lactate and other metabolites excreted from the cells. The blood is made up of plasma and formed elements. Plasma mainly consists of various proteins (e.g. lipoproteins, albumin and fibrinogen), organic compounds (e.g. amino acids, vitamins, hormones) and inorganic salts. The formed elements are the red blood cells (erythrocytes), white blood cells (leukocytes) and platelets. Erythrocytes are the most abundant of the formed elements, constituting approximately 20 – 40 % of the blood volume (hematocrit) in fish (Kryvi and Poppe, 2016). They contain numerous hemoglobin pigments that bind O_2 to its four heme-groups for transportation, which is facilitated by the cells concave shape and increased surface area. The erythrocyte membrane (plasmalemma) consists of various lipids and glycoproteins, in which the carboxylated glycoprotein sialic acid creates an overall negative charge of the blood cell (Fernandes *et al.*, 2011). Leucocytes are immune cells divided into two

main groups: granulocytes (e.g. eosinophils, basophiles and neutrophils) and agranulocytes (lymphocyte and monocytes). Leucocytes have different protective mechanisms but are all involved in the humoral and cellular defense system by detecting and destroying foreign agents and materials in the organism. The blood is continuously filtrated through the liver, spleen and kidneys. The liver detoxifies the blood, while the kidney filtrates the blood for excess water, ions and other water-soluble substance. Aged erythrocytes are filtrated and degraded in the spleen by the end of their functional lifetime (Janqueira and Carneiro, 2005, Kryvi and Poppe, 2016).

1.4 Possible uptake routes for micro- and nanoplastic particles

It has been heavily debated to what extent the intestine or the respiratory gill epithelia are important as uptake routes for nano – and microplastics in fish (Kashiwada, 2006, Lu *et al*., 2016, Yin *et al*., 2018). Furthermore, many studies fail to distinguish between the two possible uptake routes in experiments with fish exposed to plastic particles in water. An uptake study using zebrafish embryos exposed to 25, 50, 250 and 700 nm PS particles showed accumulation in both the gastrointestinal tract and gills after oral and dermal (over the gills) exposure. Nevertheless, translocation of particles into the organisms only occurred after oral administration, suggesting uptake only through the intestinal epithelium (van Pomeren *et al*., 2017). Despite indications of uptake through the intestine, the cellular mechanisms behind such uptake remain unknown. Hodges *et al*., (1995) observed translocation of 2 µm PS particles to the lamina propria, enterocytes and goblet cells in rats after oral administration, and suggested transepithelial transport mechanisms as possible cellular uptake routs. However, observations in blue mussels showed indications of intestinal endocytosis of high-density polyethylene (HDPE) particles of > 0 – 80 µm, in addition to formation of granulocytomas. The latter indicates particle uptake by phagocytotic immune cells and migration into the tissue (von Moos *et al*., 2012).

Nano- and microplastic particles have been suggested to cause functional and structural alterations of the intestinal tissue, which may represent another route of entrance for these particles. An increase in goblet cells and mucus production was the first sign after 30 days exposure to polyvinyl chloride (PVC) microplastic particles in European seabass (*Dicentrarchus labrax*), indicating a first line defense reaction against synthetic polymers. Even

longer exposure of 60 and 90 days, respectively, further caused moderate to severe histological alterations including edema in the seromuscular layer, vacuolation of enterocytes and detachment of the epithelium (Pedà *et al*., 2016). Lei *et al*., (2018) exposed zebrafish to 70 nm PE, PP and PVC particles and showed intestinal injury, mainly of the mucosal folds. However, exposure to 0.1, 1.0 and 5 µm PS particles did not cause any histological alterations. Nor did 28 days exposure to PS microplastics of 100 – 400 µm in rainbow trout (*Oncorhynchus mykiss*) (Ašmonaitė *et al*., 2018), indicating that the type of polymer is another important factor regarding physiological effects. Nevertheless, none of these studies reported translocation of particles into the tissue after observations of physical injury.

The fact that many observations on nano- and microplastics uptake and translocation seems unclear and contradictory may be a result of incomprehensible methodological approaches and analytical protocols, as well as lack of knowledge regarding the polymers physiochemical properties. Establishment of accurate and credible methods are therefore an important and prioritized research area. The majority of translocation studies report histology and fluorescence microscopy as analytical approaches, which enables detection of fluorescent polymers and their location in the tissue (Lu *et al*., 2016, Veneman *et al*., 2017, Pitt *et al*., 2018). Nevertheless, such approach do not reveal whether particles are located inside cells or organelles, and is not suitable for quantification of particles (Delie, 1998). van Pomeren *et al*., (2017) combined fluorescence microscopy and confocal microscopy in order to detect absorbed and biodistributed particles after oral and dermal exposure. The latter offers a three-dimensional view and more informative localization of the particles in study (Delie, 1998). Confocal microscopy was also used in a 2005 – study to confirm intracellular uptake of 0.2 µm nanoplastic particles into human erythrocytes. Furthermore, histology in combination with polarized light microscopy proved to be a useful tool for microplastic detection in organs and tissues of blue mussel (*M. edulis*) (von Moos *et al*., 2012).

2. Aims of study

Nano- and microplastics are becoming a major contaminant issue in the marine and aquatic environment. The mechanisms behind uptake and excretion are to a large extent unknown. This is particularly true for Atlantic salmon where there are no published results on intestinal uptake of nano- or microplastic particles. The objective of these master thesis was to investigate the intestine as a possible route of uptake of the fluorescing nanoplastic Polyethylene terephthalate (PET) and Polystyrene (PS) particles in parr and post-smolt of the Atlantic salmon. Both *in vivo* (Feeding) and *ex vivo* (Ussing) experiments were conducted to examine the potential uptake. The hypotheses were:

1) There is an uptake of PET and PS nanoplastic particles (< 20 µm) in the intestine, from the mucosa side to the serosa side, through the enterocytes.
2) PET microparticles are distributed through the circulatory system to the liver, spleen and head kidney

A potential uptake over the gills will not be examined in this task.

Examination and analysis were conducted using the Ussing chamber, histology and fluorescence microscopy.

3. Materials and methods

All experiments were carried out as laboratory studies on Atlantic salmon (*Salmo salar*) parr and post-smolt at NTNU SeaLab (Senter for Fiskeri og Havbruk), Brattørkaia, Trondheim, in accordance with the Norwegian Regulations for use of Experimental Animals.

3.1 Ussing experiment

The Ussing chamber represents a physiological system for measurements of the active and passive transport of e.g. drugs, nutrients and electrolytes across various epithelial tissues (Clarke, 2009). In this experiment, the Ussing chamber was used to investigate the permeability and potential transport of plastic particles (40 nm PS, 0.5 μm PS and PET) over the fish intestinal epithelium *ex vivo*.

3.1.1 Smolt care and husbandry

Smolt, originally from Marine Harvest, dpt. Slørdalen were transported to the fish holding facilities at NTNU SeaLab. After 3 days on brackish water, the fish were transferred into seawater at approximately 11°C with 24:0 h (light:dark) light regime and O_2- concentrations at 80 – 85%. Experimental fish feed (Biomar) (see appendix S1) was fed continuously to satiation, using Arvo – Tec T Drum 2000 (Arvo – Tec Oy, Huutokoski, Finland) automatic feeders. The fish were monitored twice daily by manual inspection. The fish had previously been part of a feeding experiment and had been fed a diet with Soy HP48, and therefore likely had a small inflammation in the intestine. The experiment was approved by the Norwegian Food Safety Authority (FODS-ID: 13640).

3.1.2 Dissection

Upon reaching approximately 320 g, all fish (n = 12) were gently hauled into a 20L bucket (2 fish at a time) and euthanized with an overdose Metacain (FINQUEL^R vet. 1000 mg/g. Scannvac, Norway, Årnes). Care was taken not to stress the fish. The intestine was dissected out immediately after the fish were euthanized and fat, mesenteries and blood vessels were removed from the surface with point tweezers. The intestine was cut longitudinal using a microscissor and the luminal content washed out using ice-cold physiological Ringer solution (see appendix S2). The intestine was than subdivided into mid- and hindgut segments (Figure

3) and kept in ice-cold physiological Ringer solution. Before mounting the Ussing chamber, the intestinal sections were gently stretched out with needles and held under a loupe (Leica M80) to remove the seromuscular layer with tweezers. The tissue was constantly embedded in Ringer solution.

Figure 3. Illustration of the mid- and hindgut segments in fish.

Illustration: Gina Almås Gundersen.

3.1.3 Plastic particles and concentrations

The plastic particles were of three types, in which two were fluorescent PS plastic bullets (ThermoFisher Scientific, Norway): 0.04 µm FluoSpheres™ Carboxylate-Modified Micropheres, yellow-green fluorescent (505/515), 5% solids and 0.5 µm FluoSpheres™ Carboxylate-Modified Micropheres, red fluorescent (580/605), 2% solids. The third type was PET particles of different size and shapes made from a Mountain Dew soda bottle (see 3.2.2 Feed manufactory and PET particles). A High concentration of particles were used in the study to ensure adequate tissue exposure.

The number of the FluoSpheres™ particles per ml was calculated with equation (I) (Polyscience Inc.)

$$\text{Particles/ml} = \frac{6x*10^{12}}{y*\pi*z^3} \qquad \text{(I)}$$

Where

x = weight of the particles (g)/ml

y = density (g/ml) (~1.05 for PS)

z = diameter (μm)

The calculated number of PS particles in the stock solution from the manufacturer and in the pre-made Ringer solution used in the experiment are given in table 1 based on equation (I)

Table 1. Calculated number of FluoSphere Polystyrene (PS) particles pr ml (pl/ml) stock solution from the manufacturer, and per ml (pl/ml) in the pre-made Ringer solution made for the experiment. All calculations are based on equation (I)

	Stock solution (pl/ml)	**1 ml Ringer (pl/ml)**
0.05 µm PS particles	$3.1*10^{11}$	$7.3*10^{9}$
0.04 µm PS particles	$9.4*10^{14}$	$9.4*10^{12}$

3.1.4 Ussing chamber experiment

The Ussing chambers were cooled with a continuous water flow of 3 – 4ºC (2219 Multitemp Thermostatic circulator) before and during the experiment to maintain a temperature of approximately 10℃ inside the chambers. This was controlled to avoid temperature related damage to the tissue. The intestinal segments were gently placed on small pins on the donor chamber (Figure 4A), kept on ice. The two chamber-halves were put together with the tissue in between. A total of four chambers with midgut and hindgut segments from two fish ran at same time (Figure 4B). Six ml Ringer solution (3 ml/chamber half) was added and electrodes for measurements of PD (the transepithelial voltage potential) and R (transepithelial conductance) were placed in each chamber. AGA special gas with 0.3% CO_2 was supplied through tubes in injection ports to provide oxygenation and circulation of the Ringer solution. The intestine was then left for one hour to stabilize the PD / R (see appendix S3). Then, 200 μl of a pre-made solution of plastic particles (see 3.1.3 Plastic particles and concentrations) was added to the donor chamber (the "mucosa side") with the same amount of Ringer added to the receiver chamber (the "serosa side") to avoid differences in hydrostatic pressure between the chamber – halves. A total of six mid and hindguts were exposed to the FluoSpheres (PS) particle solution, while the rest (n = 6) were exposed to PET particles. The experiment lasted for one hour while temperature, PD and R values were monitored continuously (see appendix S3). After 10 min, 200 μl Ringer solution was removed form the donor and receiver chamber and transferred to Eppendorf-tubes for microassay analysis. At termination of the incubation (1 h), all remaining Ringer solution was transferred to Eppendorf 1,5 ml tubes for further analysis. All tissue

segments were at the same time transferred to separate cassettes, placed in 4% formaldehyde (volume fixative ratio approximately 1:20 (tissue:fixative)) and kept dark and cold in a fridge overnight (approximately 24 hours) before paraffin infiltration and histological investigations. The Ussing chambers and electrodes were carefully cleaned in three separate baths of soapy water and flushed in tap water between every trial to avoid contamination.

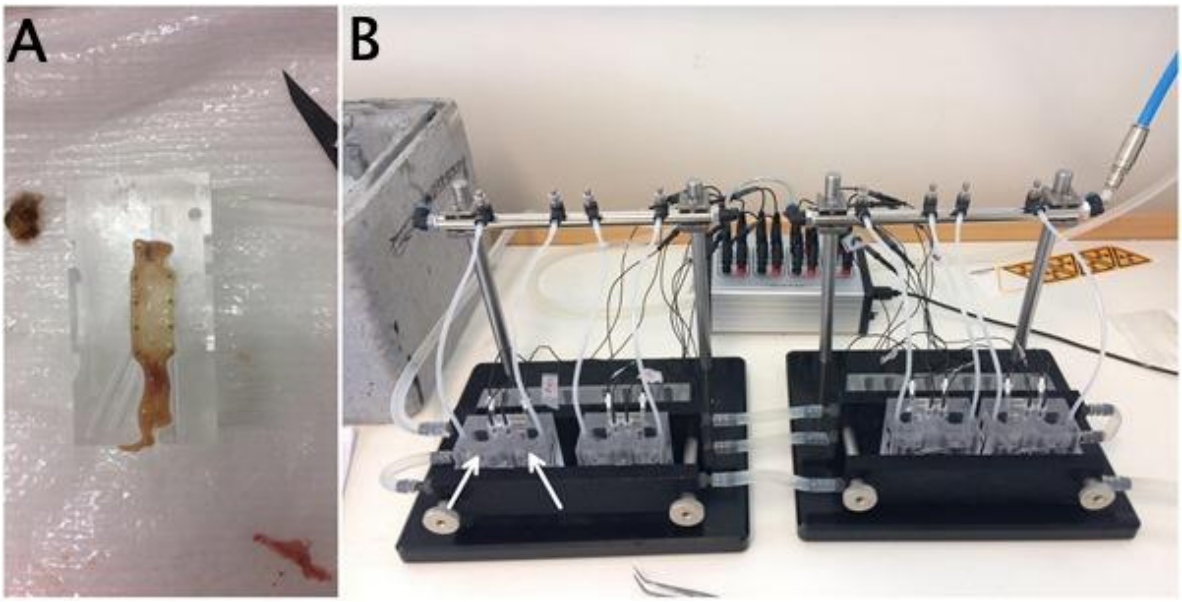

Figure 4. Illustration of the Ussing chamber experiment. The gut segment cut longitudinally, was placed on pins on the donor chamber half (A). The donor and receiver chamber-halves (B, white arrows to the left and right, respectively) were put together with the tissue segment in between. Illustration: Gina Almås Gundersen.

3.1.5 Microassay

A Cary Eclipse Fluorescent plate reader (Holger Teknologi, Holmlia, Oslo) was used to measure the concentration of plastic particles in the Ringer solution collected after 10 minutes in the Ussing chamber. A series of dilutions with particles (40 nm PS, 0.5 μm PS and PET) were made in Ringer solution and added in triplicates to a 96-well plate for preparation of a standard curve (See appendix S4). All samples were analyzed with Advanced Reads (data program). Ex.580 / Em.600 was used for red 0.5 μm PS particles, while Ex.505 / Em.515 was used for green 40 nm PS and PET particles (ThermoFisher, ThermoFisher).

3.2 Feeding experiment

A feeding experiment was conducted on parr to study the potential transport of PET particles over the intestinal epithelium *in vivo*, and the potential distribution to other tissues (blood, liver, spleen and head kidney).

3.2.1 Parr care and husbandry

Parr (n = 61) were transported from Salmar Settefisk, Kjørsvikbugen in April 2018 and kept at the fish holding facilities at NTNU SeaLab during the whole feeding period. The fish (weight 100.4 $\pm$ 26.7 g.; length 18.8 $\pm$1.8 cm) were divided into two tanks (control (n = 30) and experimental (n = 30)) supplied with aerated flow-through freshwater at 8.8 $\pm$ 0.0℃ and O_2 – concentration 96.0 $\pm$ 0.8% (See appendix S5). Light regime was set to 24:0h. Commercial (control) feed (Sparos, Portugal) were given using Arvo – Tec T Drum 2000 (Arvo – Tec Oy, Huutokoski, Finland) automatic feeders twice a day from the day of arrival at SeaLab. After appetite had recovered (3 days), the fish were fed the PET-feed (Sparos, Portugal) for 39 days and had daily supervision with monitoring of appetite and health status (e.g. swimming activity). The experiment was approved by the Norwegian Food Safety Authority (FODS-ID: 15252).

3.2.2 Feed manufactory and PET particles

The PET particles used in the experiment were made as described in Weber *et al*., (2018) from two green Mountain Dew soft drink bottles with excitation at 465 – 495 nm. Bottle material was frozen in liquid nitrogen (2 min) and crushed in a swing mill (Retsch, MM400, Haan, Germany) for 5 – 24 minutes at 30 Hz with a Ø 25 mm stainless steel ball. The particles were expected to be in the size range ≤ 150 µm (Weber *et al*., 2018).

Experimental and control feed were manufactured by Sparos LDA, Portugal with nutritional composition recommended for parr. 0.10% PET particles (1g/kg) were incorporated into the experimental feed by the manufacturer.

3.2.3 Size distribution

The size distribution of the PET particles was determined with a Beckman Coulter ™ Multisizer 4e Coulter counter (Beckman Coulter ™ , Indianapolis, US) at NTNU Gløshaugen. PET (0.0997 g) was filtered through 90 µm and 45 µm sieves (Retsch®). The sieves were rinsed and sonicated (VWR Ultrasonic Cleaner USC – TH) for 2 x 2 min to remove potential contamination. The PET particles were sifted on a Retsch AS 200 Basic vibratory sieve shaker for 40 min. The particles filtered through the 45 µm sieve were added 0.9% filtrated saltwater (Coulter Isoton^{R} II Diluent) and measured through a 30 µm aperture tube (Part nr. A36391, Florida, USA) until 10 000 particles were counted. Several measurements were made to get the distribution as exact as possible. All the equipment was iso-certificated, i.e. approved in accordance to the Iso 3310-1 standard.

3.2.4 Dissection

The five (n = 5) fish used in the experiment were gently hauled into a 20L bucket and euthanized with an overdose Metacain (FINQUREL vet. 1000 mg/g. Scannvac, Norway, Årnes). The procedure was gently conducted to avoid damage to or stress in the fish.

Blood samples were taken immediately from the caudal part of the dorsal vein using 4 ml vacuutainers (VACUTEST KIMA srl – Vacuum tubes, Italy) after the fish were euthanized and kept on ice. Blood smears were made on VWR microscope slides, air-dried and dipped in 100% methanol for dehydration. These were, after examination in the fluorescence microscope, stained with Hemacolor in accordance to Hemacolor blood smear straining protocol (See appendix S6).

The digestive tracts of all fish were checked for luminal content to ensure the fish had been eating. The liver, head kidney and spleen were carefully dissected out with scalpels and forceps. The rostral part of the liver and head kidney, and all of the spleen, were cut out and put into tissue processing cassettes covered with 4% formaldehyde. The mid part of the midgut and the hindgut were separated from the rest of the intestine and placed in cassettes. All cassettes were immediately transferred to a bottle of 4% formaldehyde (volume fixative ratio approximately 1:20 (tissue:fixative) and kept dark in a fridge overnight (approximately 24 hours) for fixation.

3.3 Preparation of tissue

The following preparation of tissues (processing, paraffin infiltration, microscopy and Hematoxylin & Eosin (H&E) staining) was conducted in the same way for tissue samples from the two experiments (Ussing experiment and feeding experiment).

3.3.1 Processing and paraffin infiltration

All tissue samples were dehydrated through a series of graded ethanol baths and infiltrated with paraffin wax before sectioning. The processing was conducted automatically with a tissue processor (Leica TP1020, Leica Microsystems Nussloch GmbH, Germany) overnight. The infiltration included series of dehydration using various concentrations of ethanol and xylene (clearing agent) and final embedding in paraffin wax (See appendix S7). After infiltration, tissues were cut in smaller samples and embedded in paraffin blocks with a Leica EG1120 (Leica Microsystems, Nussloch GmbH, Germany). Four μm sections were made with a microtome (Leica RM2255, Leica Biosystems, Nussloch GmbH, Germany) and picked up on VWR microscope slides. Knives where changed between different tissue types to avoid contamination. All slides were dried in room temperature (RT) for >30 minutes and kept in a 37℃ incubator over night before storage at RT.

3.3.2 Fluorescence microscopy

Blood smears and slides with sections of the mid- and hindgut, liver, spleen and head kidney were examined under a Nikon fluorescence microscope (Nikon eclipse 90i with Digital Imaging Head, Nikon Corp. Tokyo, JP) and analyzed with Nikon NIS-element viewer software (NIS-element Documentation, v. 3.22.15). Pictures were taken with a Nikon DS-Fi1 camera connected to DS-U2 controller (Nikon Corp. Tokyo, JP). Tissues exposed to 40 nm PS particles and PET particles, respectively, were examined with the three fluorescent filter types DFR (Ex. 385 – 400 nm/475 – 490 nm/545 – 565 nm, Em. 450 – 465 nm/505 – 535 nm/580 – 620 nm), B2A (Ex. 450 – 490 nm, Em. 515 nm) and B2E (Ex. 465 – 495 nm, Em. 515 – 555 nm). Tissues exposed to red 0.5 μm PS particles were examined with DFR, B2A and YFP (Ex. 575 – 595 nm, Em. 603 – 617 nm). All sections were then stained with Hematoxylin & Eosin (H&E) (see section 3.3.3 Hematoxylin & Eosin staining) and new pictures were taken in the light microscope with DIC ("Differential interference contrast") for overlay. Overlays were made by

using the same coordinates in the microscope as for pictures taken with the fluorescence filters. Extended information about the microscope, filter types and fluorescence lamp are given in appendix S8.

3.3.2.1 Characterization of the PET and PS polymers

To make sure that PS and PET particles were detected, a test of the particular polymers were conducted under the fluorescent microscope before examination of the tissues. PET and 0.5 μm PS particles were processed and embedded in paraffin blocks similarly to the tissue samples. Sections were made on the same microtome (Leica RM2255, Leica Biosystems, Nussloch GmbH, Germany) and picked up on VWR microscope slides. A drop of the 40 nm PS particle stock solution diluted in deionized water was placed on a microscope slide. Both types of polymers were examined with various fluorescence filters and exposed to continuous fluorescent light over an extended period (5 – 30 min) to investigate a potential bleaching, documented through a time-laps function. PET fluorescence was detected only with the filters DFR, B2A and B2E, while red 0.5 μm PS-particles were detected with DFR, B2A and YFR. The individual 40 nm PS-particles were too small to be detected, but the fluorescence could be seen with B2A and B2E. None of the particular polymers bleached following long exposure (unlike auto fluorescence from tissue that bleached rapidly). See appendix S9 for pictures of time-laps and fluorescence on various filters.

3.3.3 Hematoxylin & Eosin (H&E) staining

Histology and fluorescent microscopy is a qualitative approach for the investigation of fluorescent plastic particles, a powerful method when used the proper way (Delie, 1998). H&E staining is a method used to examine the morphology of different cells and tissues. Hematoxylin gives basophile or positively charged substances, such as DNA and RNA a blue color, while eosin dyes acidophilic substances (e.g. collagen and cytoplasm) red (Junqueira & Carneiro, 2005). Sections of mid- and hindguts and liver were stained manually with H&E after examination in the fluorescence microscope in accordance to a standardized procedure. Slides with tissue samples were placed in Tissue clear for 3 x 5 min, before embedded in graded baths of ethanol (from 100 % to 70%) for 4 x 2 min. The slides were further placed in distilled water (dist H_2O) for 5 min before staining with Mayers Hematoxylin for 3 min. Slides were washed in tap water for 3 min, dipped fast 5x in 1% HCl in 70% ethanol before stained with eosin (2

min). All samples were dipped in tap water and dist. H_2O before dehydration. Dehydration were conducted in 70% ethanol (dip), 100% ethanol (30 sec) and 100% ethanol (2 x 2 min). The procedure was finalized by placing the slides in Tissue clear (3 x 5 min) and attaching coverslip slides to the microscope slides using NeoMout.

3.3.4 Picture modifications

The pictures taken in the fluorescent microscope, both on the fluorescence filters (DFR, B2A, B2E and YFP) and with DIC after straining, were modified in photoshop (Adobe Photoshop CS3 Extended, v. 10.0) and ImageJ (Image Processing and Analysis in Java 1.52a, USA). Scale bars and arrows were added in ImageJ, while Photoshop were used to change the contrast and make overlays. The contrast of the pictures was enhanced by using a curve-function, not expected to alter the characteristics of the fluorescent plastic particles. An overlay was made between a picture taken on fluorescence filter DFR or YFP (after curve was changed) and the same H&E stained section. A new filter (termed e.g. “Exclusion,” “Lighter color” or “Linear dodge”) were added to enhance the contrast between the tissue/background and the particle, and to make the small particles more viable in the stained sections.

3.4 Control groups

Nanoplastic particles have good capacity to disperse in water and are, due to the small size, hard to detect when spread. Unfortunately, the control fish in the feeding experiment became contaminated. To avoid further contamination between experimental and control groups, the “new” fish used as control were separated from the experimental group in time and space. These control fish were used in other non-related trials not expected to affect the particular experiment in this thesis. All tissue segments and blood smears from the control fish were prepared in the same way as for the experimental group.

3 Results

3.1 *Ex vivo* exposure to PS and PET nanoplastic particles (Ussing experiment)

The Ussing chamber was used as an *ex vivo* technique to measure the epithelial barrier function of the intestine exposed to fluorescent PS and PET particles for one hour.

All the n = 12 post-smolts (n = 12 midguts and n = 12 hindguts) were used in the experiment.

3.1.1 Morphology of the salmonid intestine

The general organization of the salmonid midgut is presented in Figure 5 (A and B) stained with H&E. The numerous mucosal folds project deep into the lumen. The apical part of the folds show some signs of physical damage which is assumed to be caused by the combined feed and muscle contraction, and do not represent dietary influence. The mucus layer is covering the microvilli at the folds apical end, and goblet cells are evenly spread along the length of the folds. Interepithelial leucocytes are scattered along the base of the enterocytes. The lamina propria make up the middle and basal part of the folds. Underneath the lamina propria is the stratum compactum, stratum granulosum and the circular muscle layer. The serosa constitutes the outermost layer facing the circulatory system.

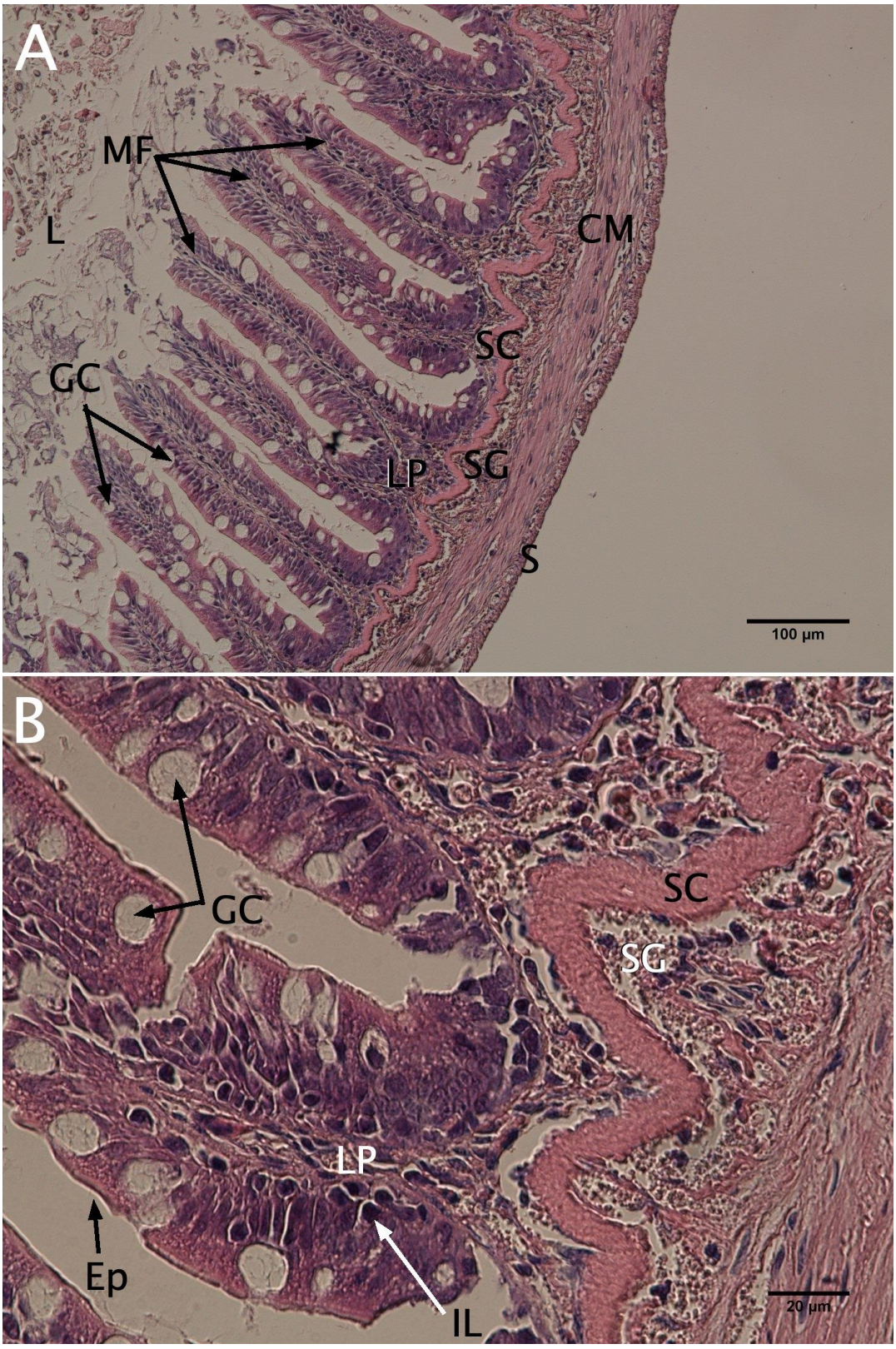

Figure 5. Hematoxylin & Eosin (H&E) stained cross section of the midgut from the Atlantic salmon (*Salmo salar*) at 10x magnification (A) and 40x magnification (B), respectively. Mucus secreting goblet cells (GC) are located on the epithelium (Ep) of the numerous mucosal folds (MF), facing the lumen (L). The lamina propria (LP) makes up the middle and basal end of the fold. IL: intraepithelial lymphocyte SC: stratum compactum, SG: stratum granulosum, CM: circular muscle, S: serosa.

3.2.1 Intestinal exposure and uptake of PS and PET nanoparticles

Fluorescence microscopy and H&E staining made it possible to detect the fluorescent PS (0.5 µm) and PET particles. The slides were first examined under the fluorescence microscope. Image and position were recorded before the slides were stained with H&E. The images were then overlaid in photoshop to enhance the particles location in the tissue or luminal mucus layer. Nevertheless, the 40 nm PS particles were not detected in the luminal mucus layer nor in the intestinal tissue in the present study, using fluorescence microscopy and histology. Original pictures and modifications for all results are presented in appendix S10.

Numerous 0.5 µm PS particles were observed in the luminal mucus layer of the midgut segments (Figure 6A and B). Some particles appeared to have translocated or passed the mucus layer. Most of these were found in the intersection of the basal part of the enterocytes and in the lamina propria (Figure 7A and B). A few particles were also found at the basal part of the mucosal fold close to the stratum granulosum (Figure 8A and B). It was not possible to relate this staining to any cellular population of leucocytes or other cell types. Some detached and injured tissue can also be observed in relation to the tissue segments, both in the folds and by the stratum granulosum.

In the hindgut, relatively high numbers of PS particles were observed in the luminal mucus layer of all fish examined (Figure 9A and B). However, no particles were found either inside enterocytes, or passed into inner cellular structures of intact tissue.

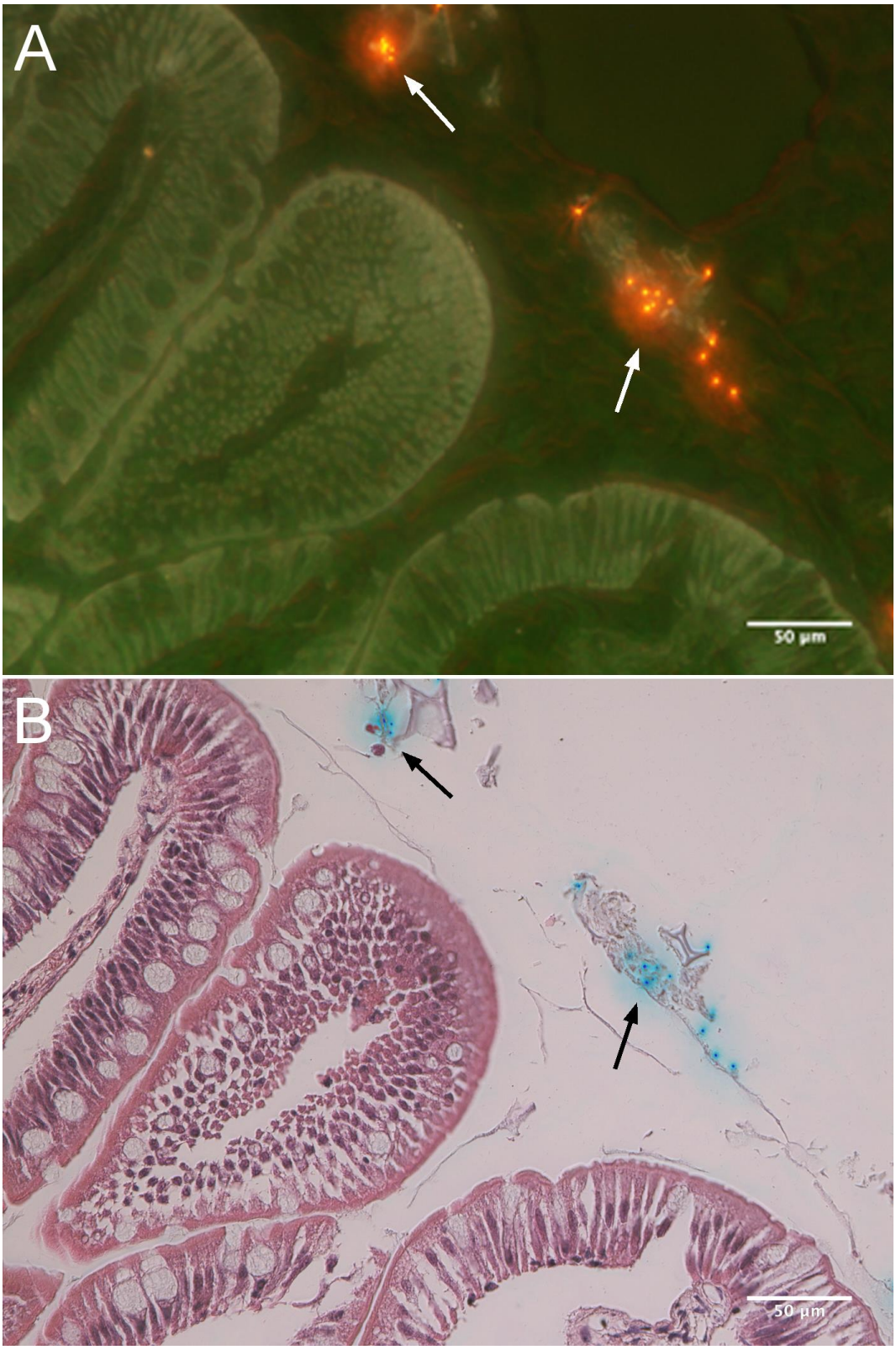

Figure 6: Fluorescent FluoSphere polystyrene (PS) particles (0.5 µm) in luminal mucus (white and black arrows) in the midgut of the Atlantic salmon (*Salmo salar*) after one-hour exposure in the Ussing chamber. Fluorescence on filter type A: DFR. A curve-function (Photoshop) was used to enhance the contrast between the background/tissue and the particles. B: Overlay between Hematoxylin & Eosin (H&E) stained section and picture taken with filter type DFR. The particles in B are blue due to the filter "Exclusion" (Photoshop) used to enhance the contrast between the tissue/background and the particles. Both pictures: 20x magnification. See appendix S10, figure S10.A for original images and modifications.

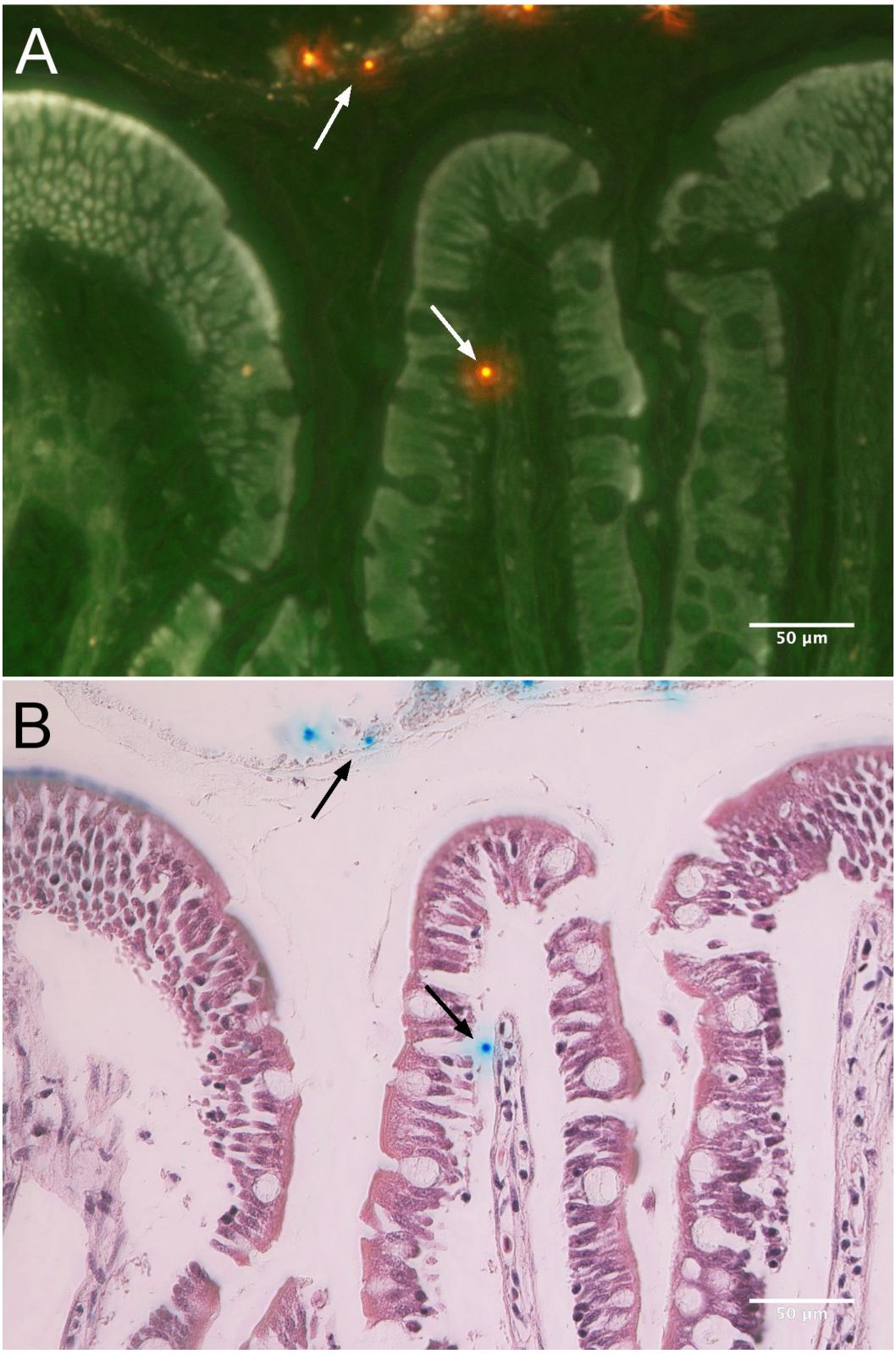

Figure 7. Fluorescent FluoSphere Polystyrene (PS) particle (0.5 µm) in a mucosal fold (white and black arrows) of the midgut from the Atlantic salmon (*Salmo salar*) after one-hour exposure in the Ussing chamber. Particles can also be observed in the luminal mucus layer (top of the pictures). Fluorescence with filter type A: DFR. A curve-function (Photoshop) was used to enhance the contrast. B: Overlay between Hematoxylin & Eosin (H&E) stained section and picture taken with filter type DFR. The particles in B are blue due to the filter "Exclusion" (Photoshop) used to enhance the contrast between the tissue/background and the particles. 20x magnification. See appendix S10, figure S10.B for original images and modifications.

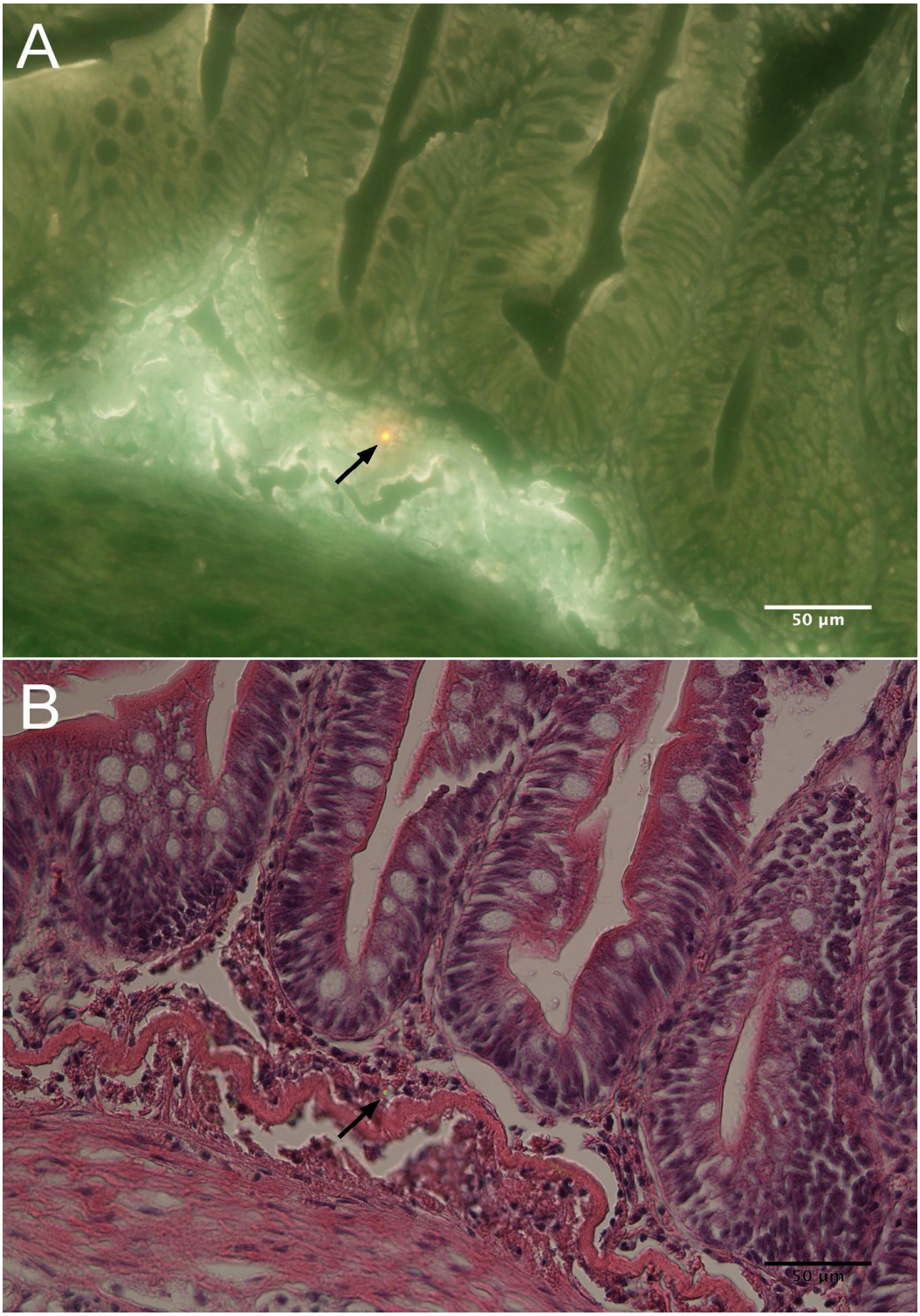

Figure 8. Fluorescent FluoSphere Polystyrene (PS) particle (0.5 µm) in the stratum granulosum (white and black arrows) of the mid-gut from the Atlantic salmon (*Salmo salar*) after one-hour exposure in the Ussing chamber. Fluorescens on filter A: DFR. A curve-function (Photoshop) was used to enhance the contrast. B: Overlay between Hematoxylin & Eosin (H&E) stained section and picture taken with filter type DFR. Filter "Lighter Color" (Photoshop) was used to enhance the contrast between the tissue/background and the particle. Both pictures: 20x magnification. See appendix S10, figure S10.C for original images and modifications.

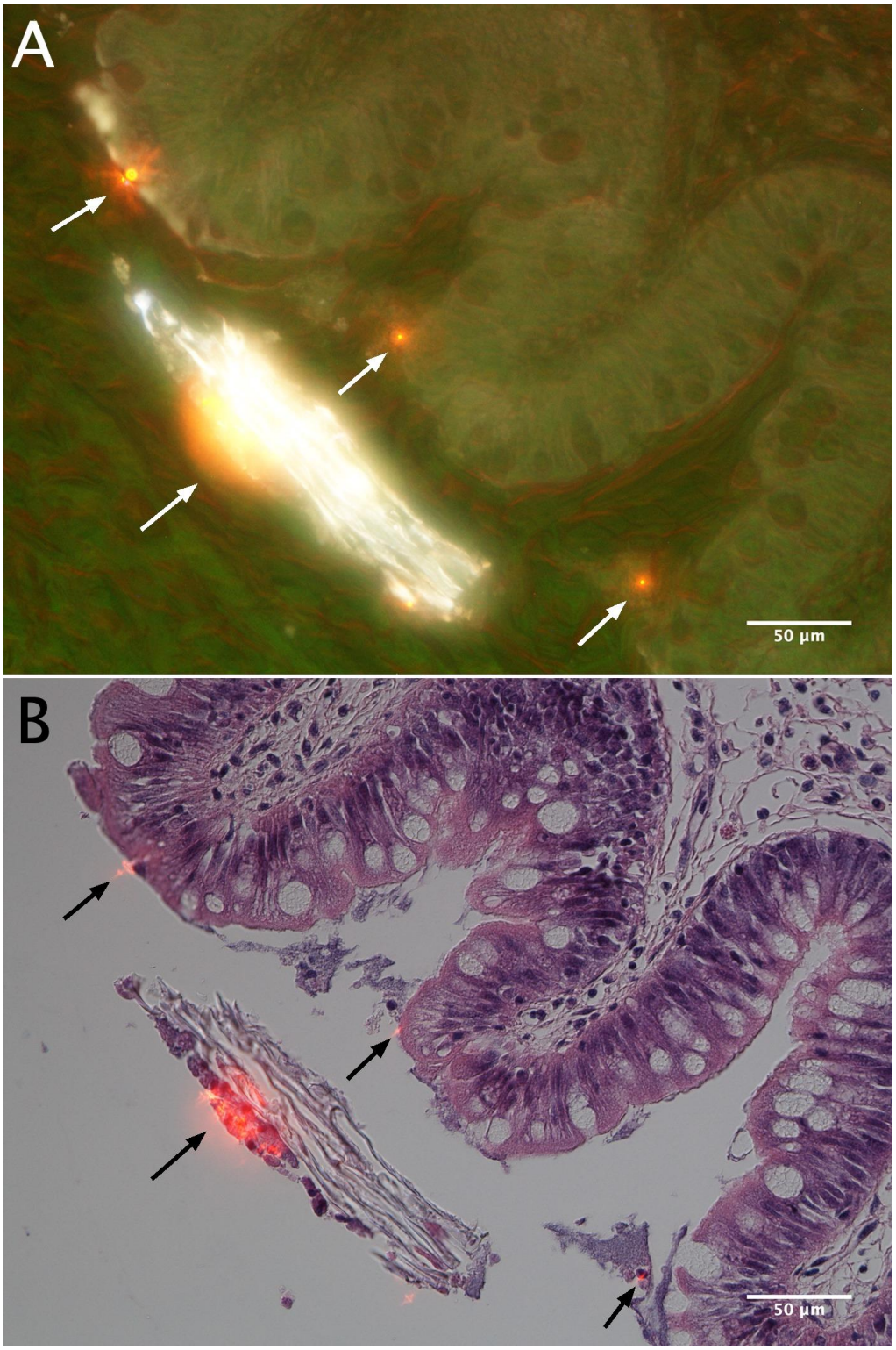

Figure 9. Fluorescent FluoSphere Polystyrene (PS) particle (0.5 µm) in the luminal mucus layer (white and black arrows) in the hindgut of the Atlantic salmon (*Salmo salar*) after one-hour exposure in the Ussing chamber. Fluorescence on filter A: DFR. A curve-function (Photoshop) was used to enhance the contrast. B: Overlay between Hematoxylin & Eosin (H&E) stained section and picture taken with filter type DFR. Filter "Lighter Color" (Photoshop) was used to enhance the contrast between the tissue/background and the particle. Both pictures: 20x magnification. See appendix S10, figure S10.E for original images and modifications.

The prevalence of fluorescent PET particles from the Mountain Dew bottles were considerably lower than PS both in luminal space (Figure 10A and B) and in the intestinal tissue. Only one particle was observed in the stratum compactum of the hindgut (Figure 11A and B). Some physical injury was observed in tissues exposed to PET particles, especially at the basal end of the folds.

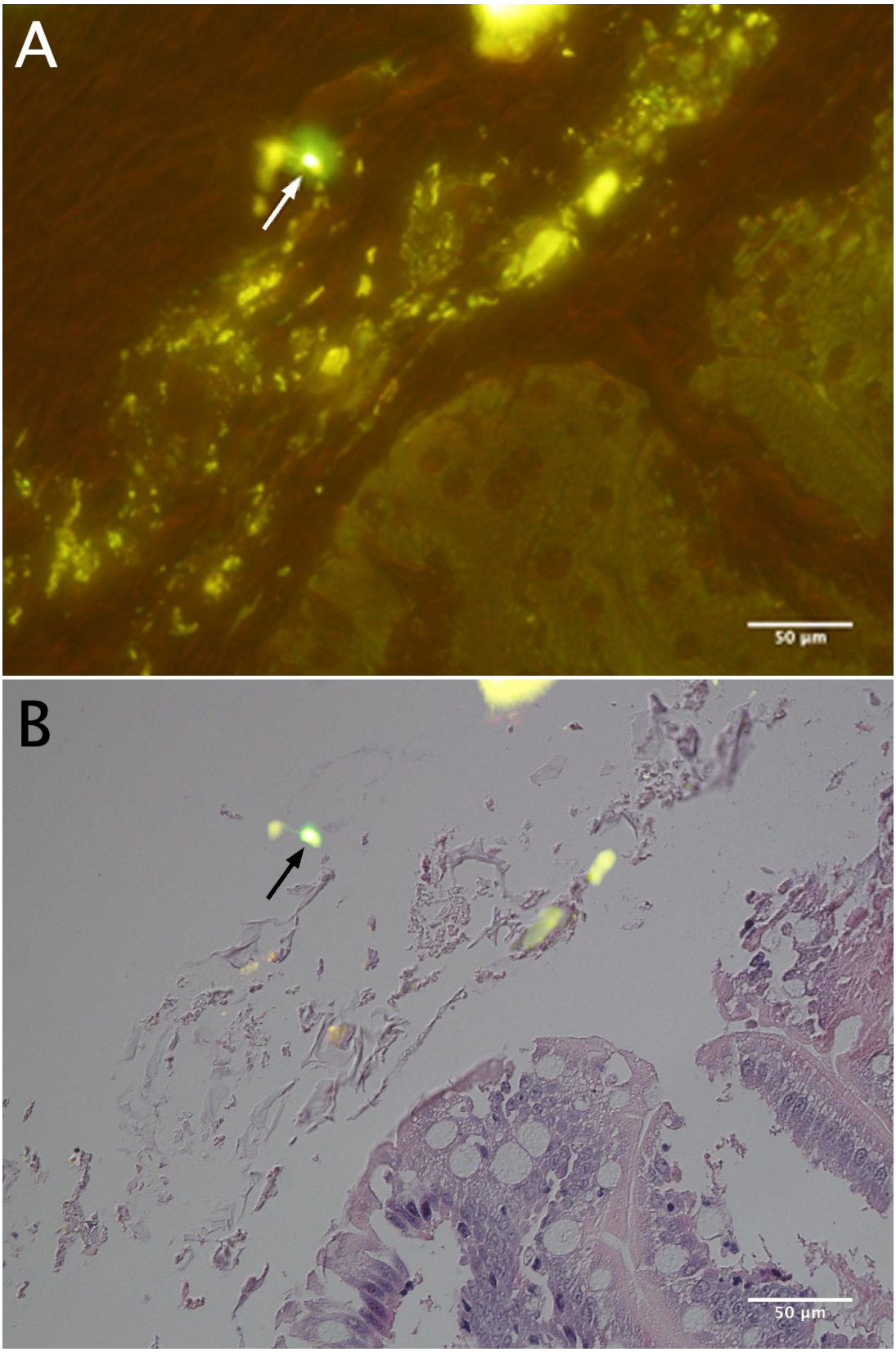

Figure 10. Fluorescent Polyethylene terephthalate (PET) particle(s) in the luminal mucus layer in the midgut of the Atlantic salmon (*Salmo salar*) after one-hour exposure in the Ussing chamber. Fluorescence with filter type A: B2A. A curve-function (Photoshop) was used to enhance the contrast. B: Overlay between Hematoxylin & Eosin (H&E) stained section and picture taken with filter type DFR. Filter "Screen" (Photoshop) was used to enhance the contrast between the tissue/background and the particle in D. 20x magnification. See appendix S10, figure S10.F for original images and modifications.

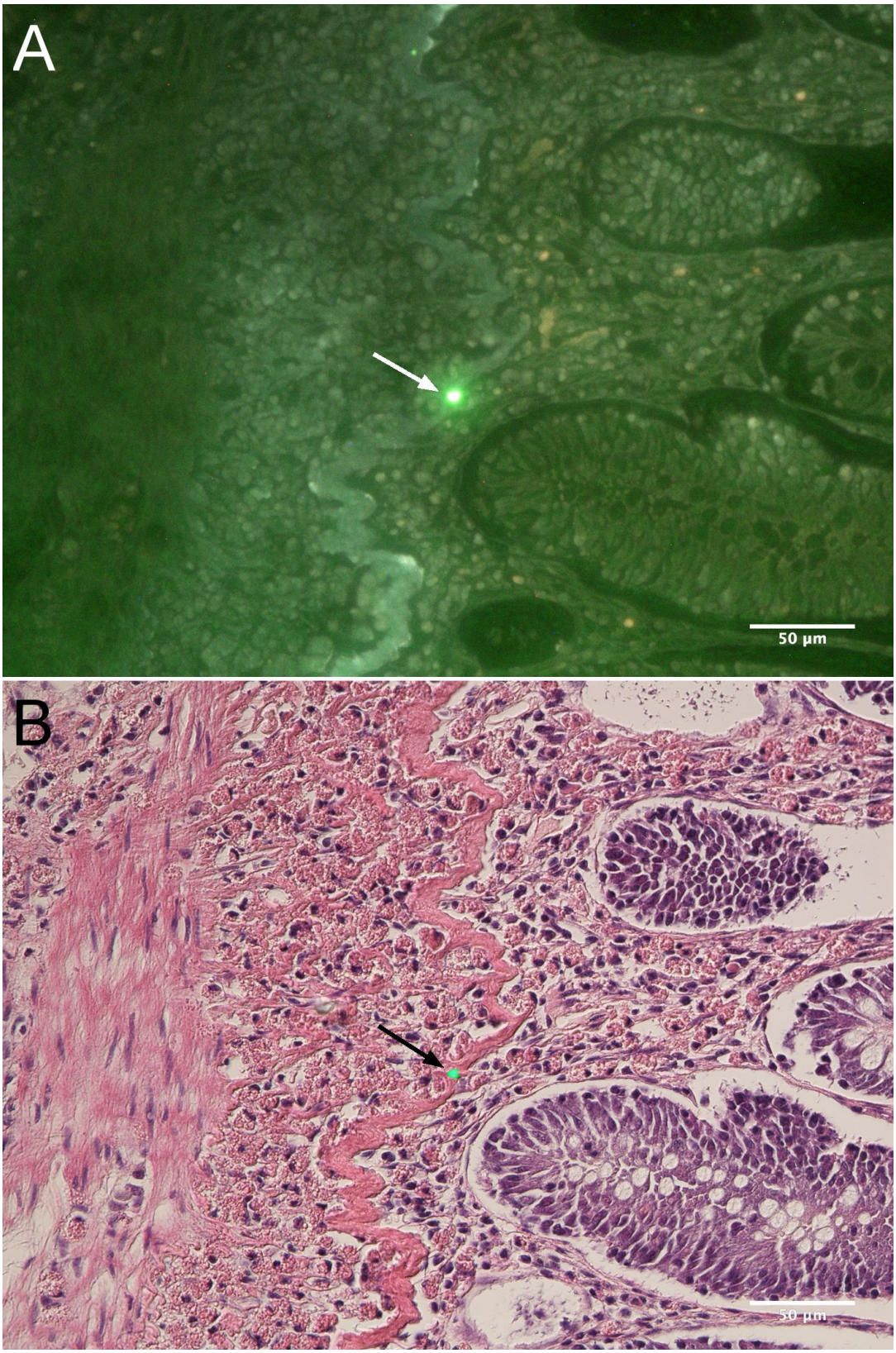

Figure 11. Fluorescent Polyethylene terephthalate (PET) particle in the stratus compactum of the hindgut from the Atlantic salmon (*Salmo salar*) after one-hour exposure in the Ussing chamber. Fluorescence with filter type A: DFR. A curve-function (Photoshop) was used to enhance the contrast. B: Overlay between Hematoxylin & Eosin (HE) stained section and picture taken with filter type DFR. Filter "Lighter Color" (Photoshop) was used to enhance the contrast between the tissue/background and the particle in D. 20x magnification. See appendix S10, figure S10.D for original images and modifications.

3.3 *In vivo* exposure to PET nanoplastic particles (Feeding experiment)

For long intestinal exposure, PET plastic particles (≤ 150 µm) were embedded into fish diets and fed to Atlantic salmon parr for 39 days. Mid-and hind-gut segments, blood samples, liver, spleen and head kidney segments from n = 5 individuals were examined using a fluorescence microscope and histology.

3.3.1 Size distribution of PET particles

The PET particles were expected to be of various sizes ≤ 150 µm (Weber et al., 2014 – supplement data). Figure 12 shows the size distribution of particles 0.6 µm ≥ 18 µm after particle filtration and measurements in the coulter counter. The sample also contained particles < 2 µm, which were harder to quantify due to background noise in the measurements. A size distribution for all particles ≤ 18 µm are presented in appendix S11.

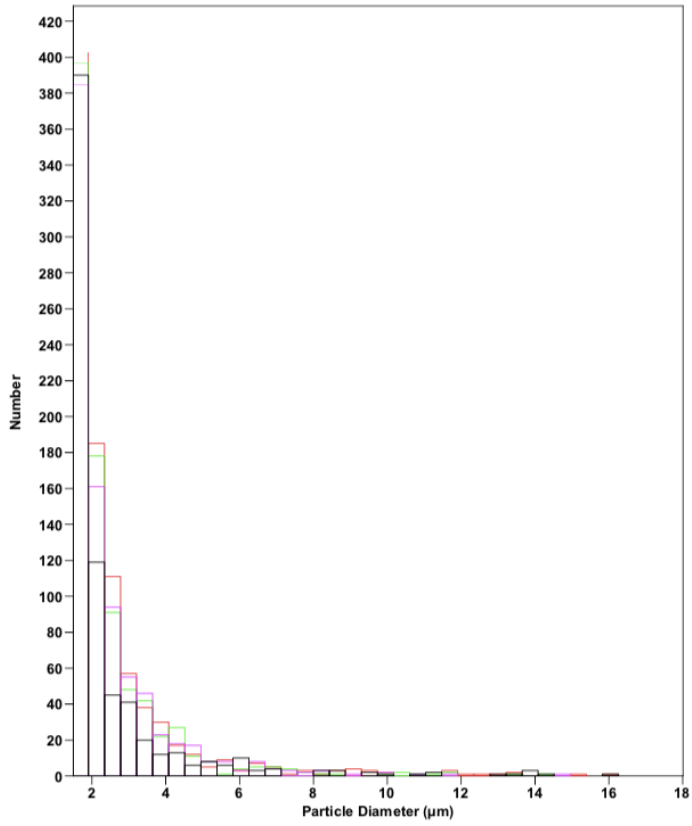

Figure 12. Size distribution of Polyethylene terephthalate (PET) particles (0.6 ≥ 18 µm) in the sample made from two fluorescent Mountain Dew bottles used in the experimental feed. Several measurements were conducted and ~10 000 particles were counted. Particles where filtered through a 45 µm sieve and measured through a 30 µm aperture in the Coulter counter (appendix).

3.3.2 Experimental feed and PET particles

All the 5 experimental fish had PET supplemented feed in the intestine and thus verified as being under influence of plastics exposure. Consequently, all fish had significant fluorescence in the luminal content in both mid- and hindgut histological preparations. Figure 13 (A and B) show luminal content with fluorescent PET particles from the feed in the midgut. Most of the fluorescence was located in the feed matrix. Some particles can also be observed translocated to the tissue, in association to the lamina propria, an enterocyte and at the basal end of the mucosal fold. Figure 14 (A – C) confirm presence of fluorescent PET particles in the experimental feed. The size of the particles observed in the feed/luminal content may indicate that aggregations of particles have occurred. Control diets without PET particles did not contain any fluorescent material interfering with the distinctive pattern of PET (Figure 14D - F).

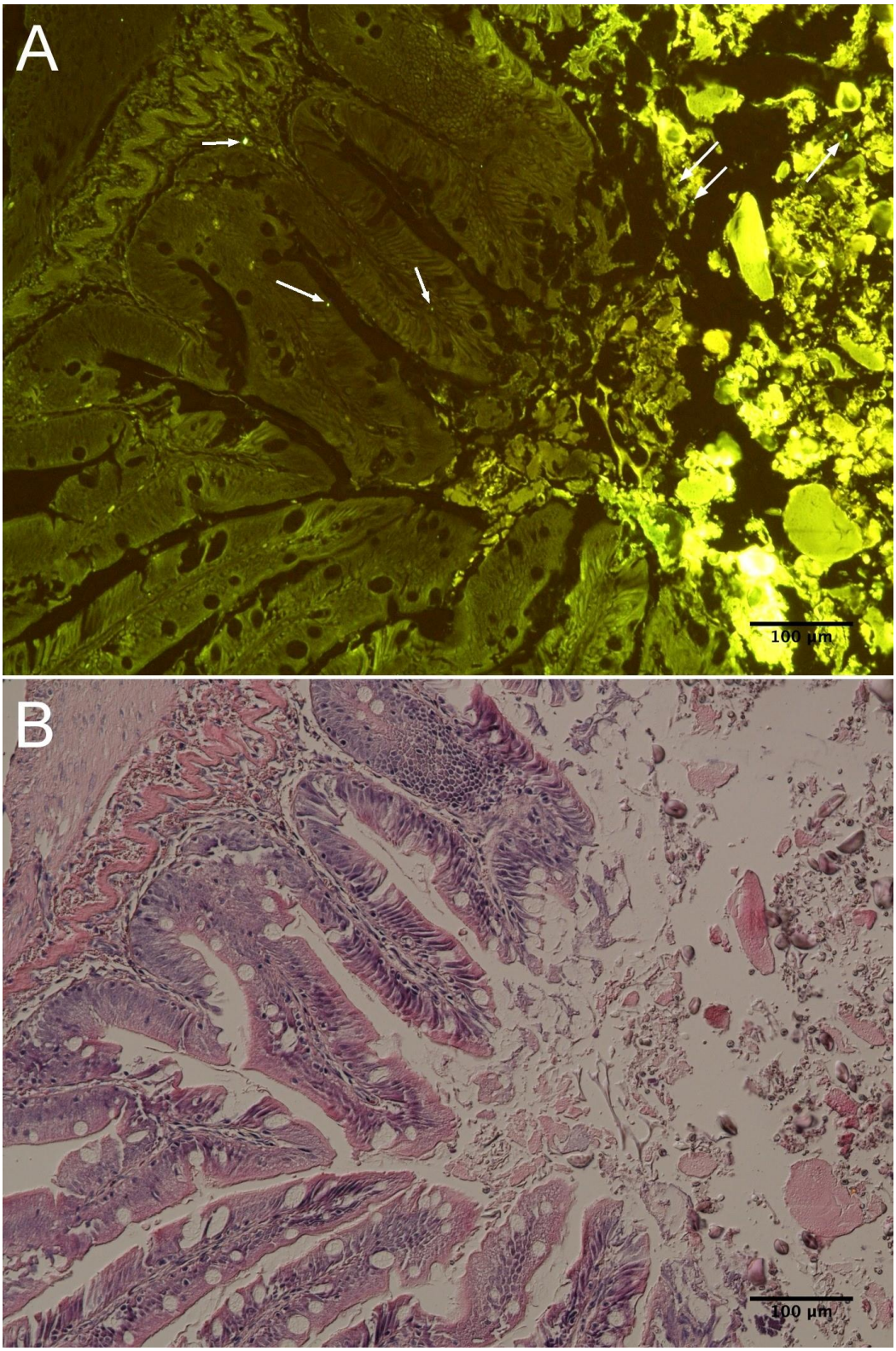

Figure 13. Cross section of the midgut from the Atlantic salmon (*Salmo salar*) with green fluorescent Polyethylene terephthalate (PET) particles in the luminal content (A, white arrows). Particles can also be observed in the intestinal tissue (white arrows). Pictures with filter type A: B2A. A curve-function (Photoshop) is used to enhance the contrast. B: illustrates the same cross section stained with Hematoxylin & Eosin (H&E). Both pictures: 10x magnification.

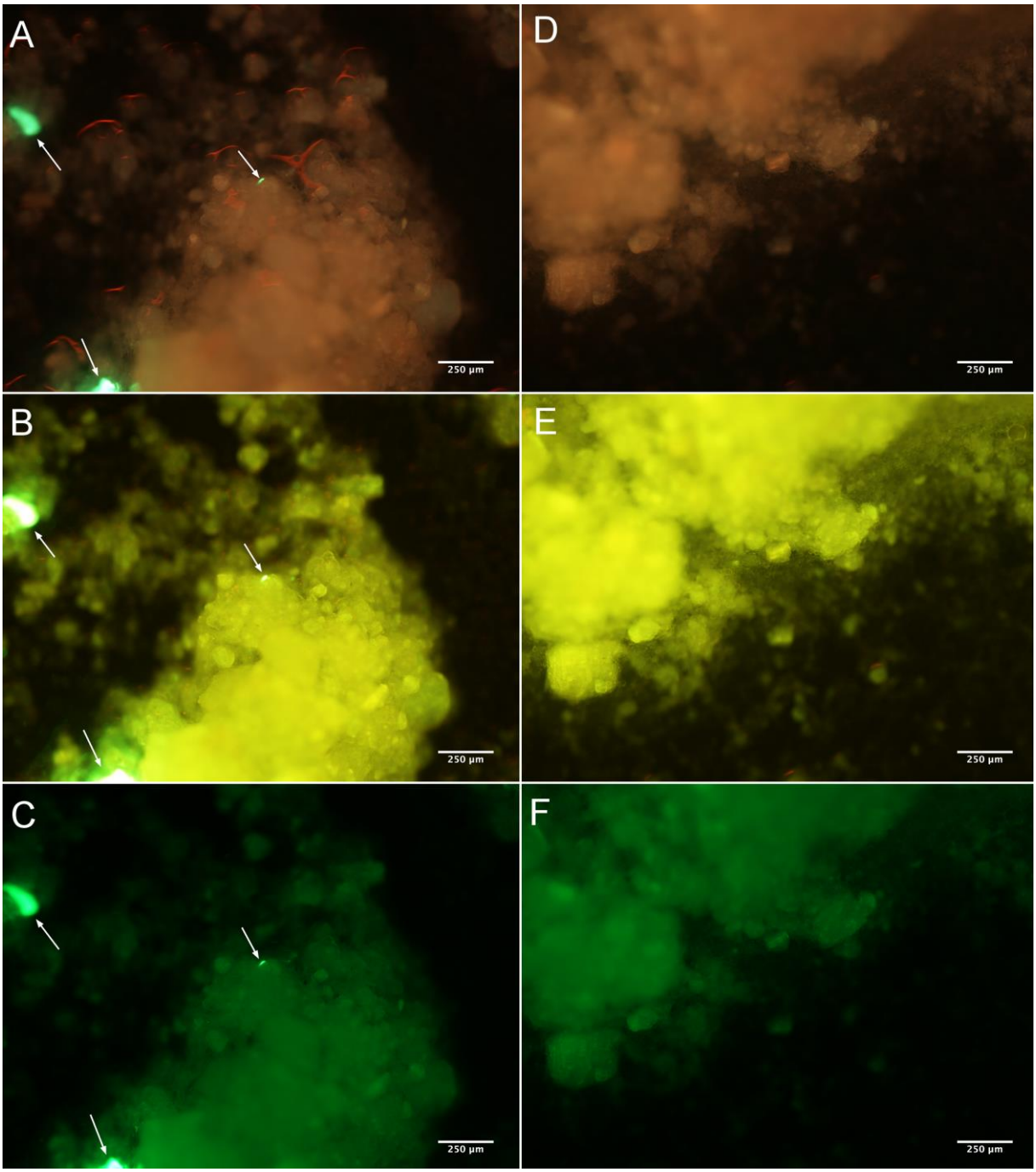

Figure 14. Fluorescent Polyethylene terephthalate (PET) particles (white arrows) in the experimental salmon (parr) feed with fluorescence on filter type A) DFR, B) B2A and C) B2E. D, E and F illustrate PET free control feed on fluorescence filters DFR, B2A and B2E, respectively. The fluorescence observed in the background of all pictures is auto fluorescence. All pictures: 4x magnification.

3.2.3 Intestinal uptake of PET particles and translocation to blood and liver

Fluorescent PET particles were observed in mid- and hindgut tissues, blood samples and the anterior part of the liver from all the n = 5 experimental individuals. Most particles (per slide examined) was observed in the midgut and in blood samples. No particles were observed in samples examined from the spleen or the head kidney. In general, midgut sections had a high

level of translocated PET particles. Figure 15 (A and B) shows fluorescent PET particles in two midgut folds, presented in the lamina propria and in association to an enterocyte (arrow to the left). Particles translocated to the basal end of the folds can also be observed in association with intraepithelial leucocytes (Figure 16A and B).

Translocation of PET particles were to a lesser extent observed in the hindgut samples examined. Figure 17 (A and B) show one PET particle translocated to the basal end of an enterocyte, in close proximity to the lamina propria. See appendix S12 for original images and modifications

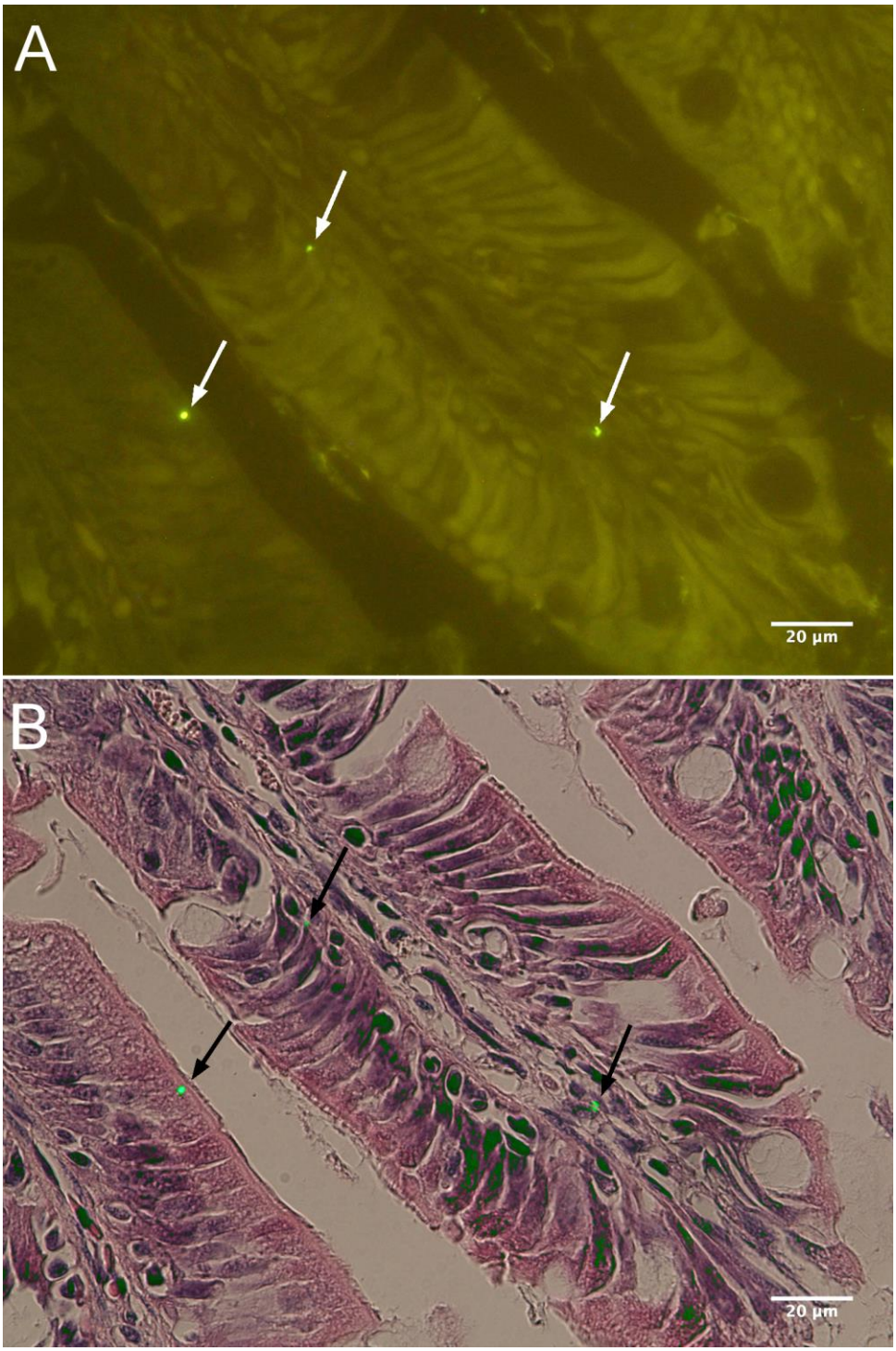

Figure 15. Fluorescent Polyethylene terephthalate (PET) particles in two mucosal folds (white and black arrows) in the midgut of the Atlantic salmon (*Salmo salar*) parr. Fluorescence on filter type A: B2A. A curve-function (Photoshop) was used to enhance the contrast. B) Overlay between Hematoxylin & Eosin (H&E) stained section and picture taken with filter DFR. The filter "Lighter color" (Photoshop) is used to enhance the contrast between the tissue/background and the particles in B. 40x magnification. See appendix S12, figure S12.B for original images and modifications.

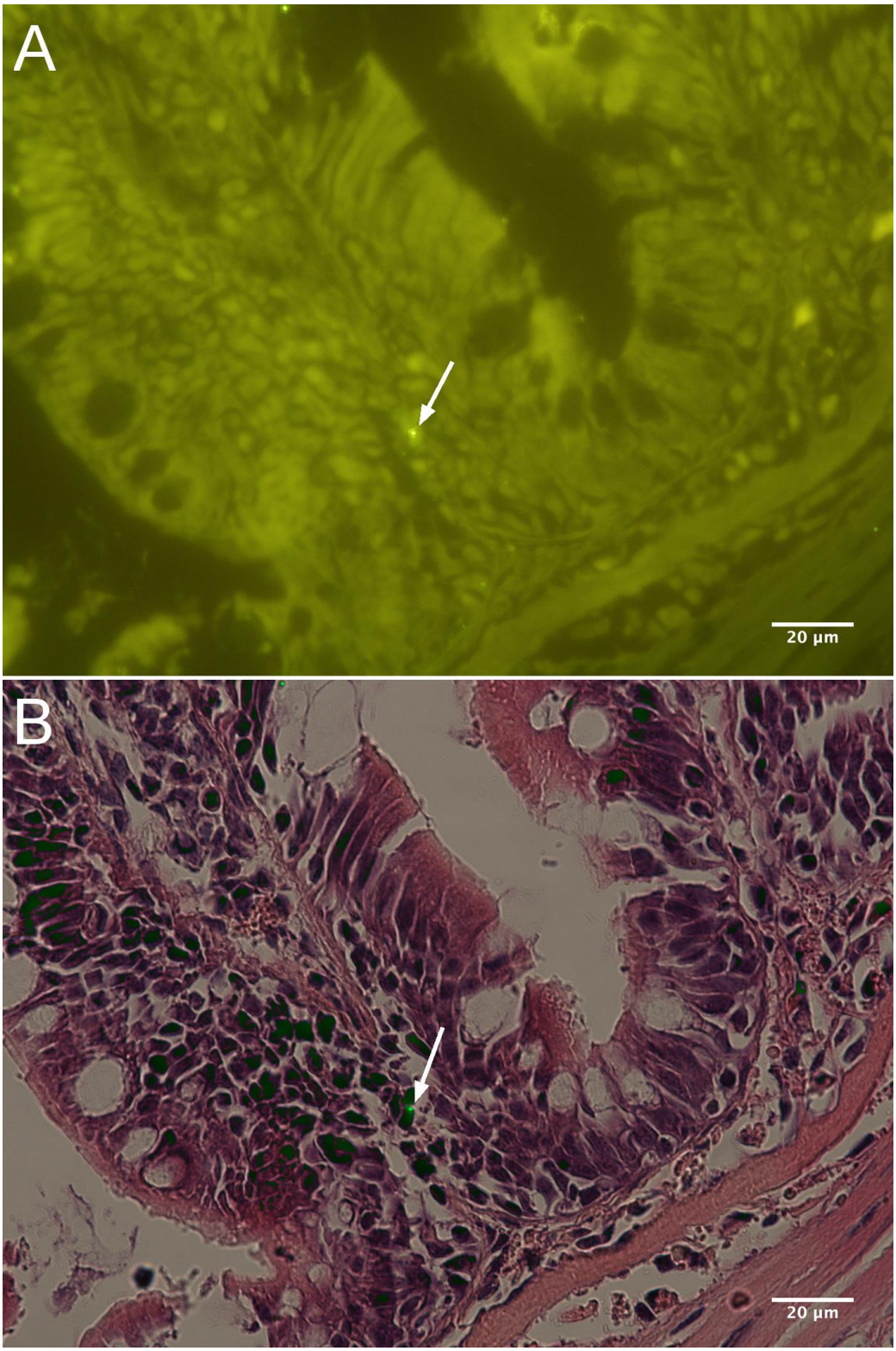

Figure 16. Fluorescent Polyethylene terephthalate (PET) particle in association to an intraepithelial leucocyte (white arrow) in the lamina propria in the midgut of the Atlantic salmon (*Salmo salar*) parr. Fluorescence on filter type A: B2A. A curve-function (Photoshop) was used to enhance the contrast. B) Overlay between Hematoxylin & Eosin (H&E)-stained section and picture taken with filter DFR. The filter "Lighter Color" (Photoshop) was used to enhance the contrast between the tissue/background and the particles in B. 40x magnification. See appendix S12, figure S12.C for original images and modifications.

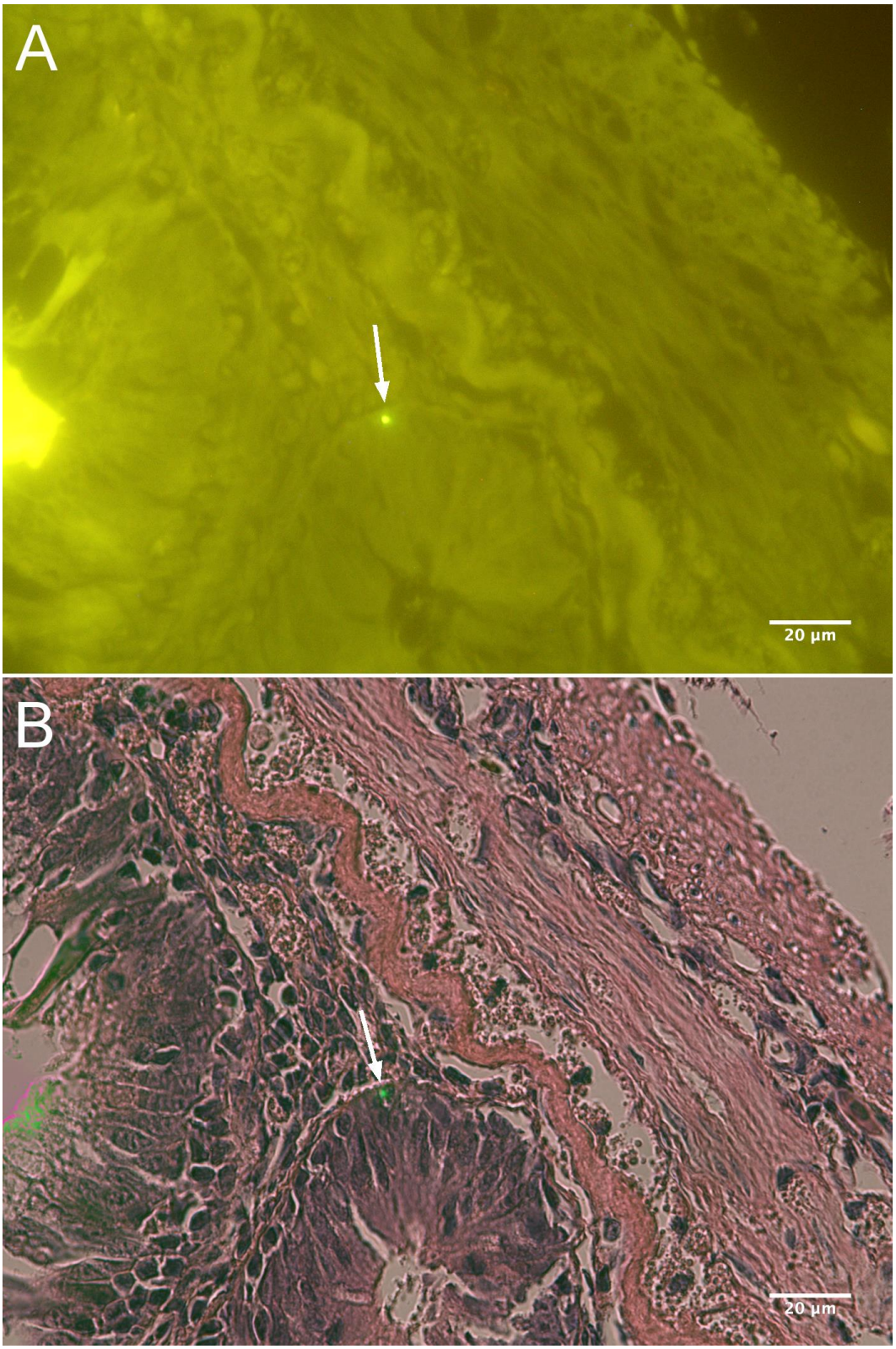

Figure 17. Fluorescent Polyethylene terephthalate (PET) particle at the basal part of a mucosal fold in the hindgut of the Atlantic salmon (*Salmo salar*) parr. Fluorescence on filter A: B2A. A curve-function (Photoshop) was used to enhance the contrast. B) Overlay between Hematoxylin & Eosin (H&E) stained section and picture taken with filter DFR. The filter "Exclusion" (Photoshop) was used to enhance the contrast between the tissue/background and the particles in D. 40x magnification. See appendix S12, figure S12.D for picture modifications.

Fluorescent PET particles were also present in caudal blood samples of parr. Most of the observations showed a close association to erythrocytes (Figure 18A and B). PET particles were also found in association with leucocytes (Figure 19 A and B). In these cases, cells contained typically one particle.

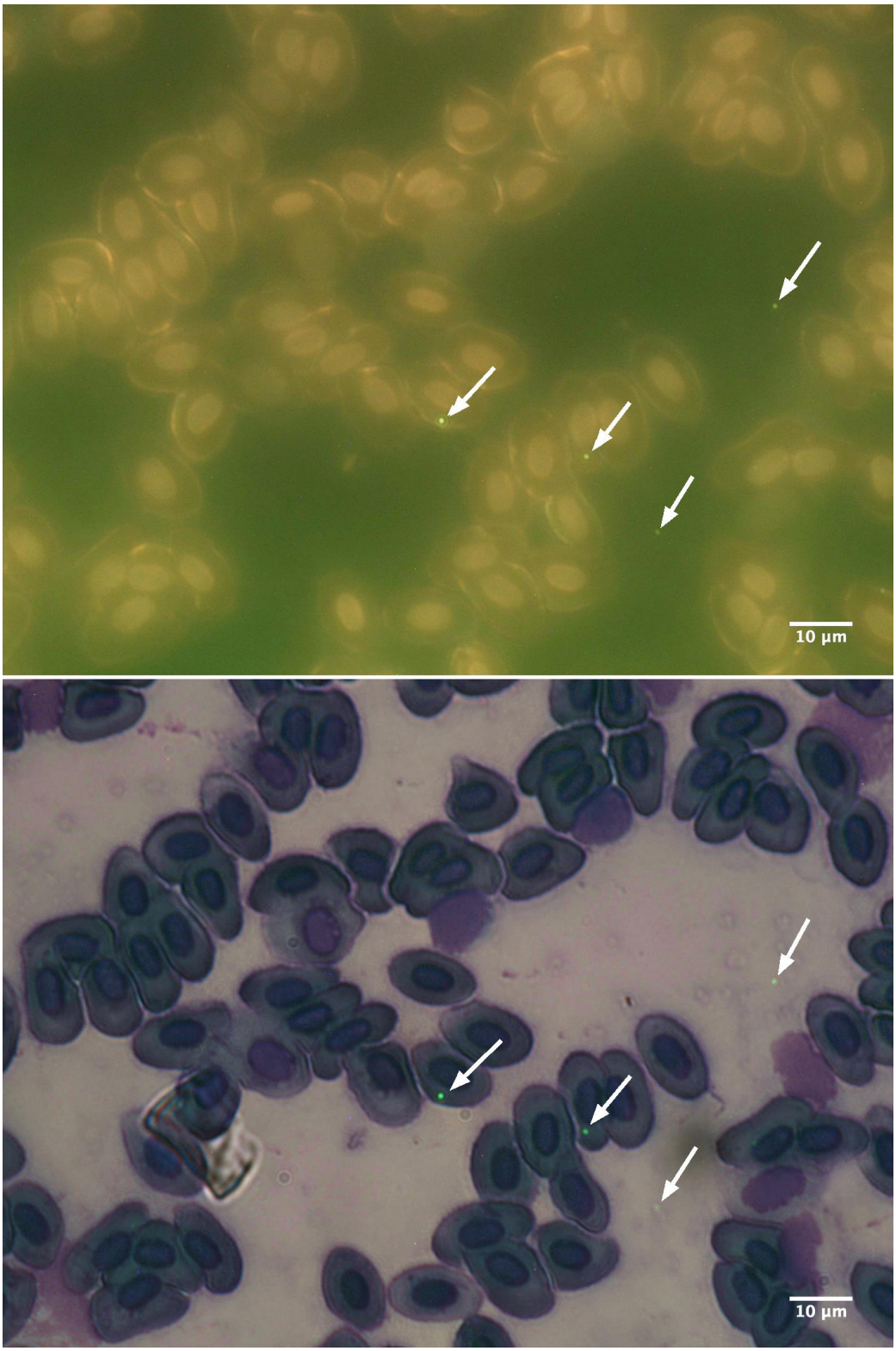

Figure 18. Polyethylene terephthalate (PET) particles in association to blood erythrocytes in a blood sample from the Atlantic salmon (*Salmo salar*) parr. Fluorescence on filter type A: DFR. A curve-function (Photoshop) was used to enhance the contrast. B: Overlay between Hemacolor stained section and picture taken with filter DFR. The filter "Linear Dodge" (Photoshop) was used to enhance the contrast between the blood cells and the particles. 60x magnification. See appendix S12, figure S12.A for original images and modifications.

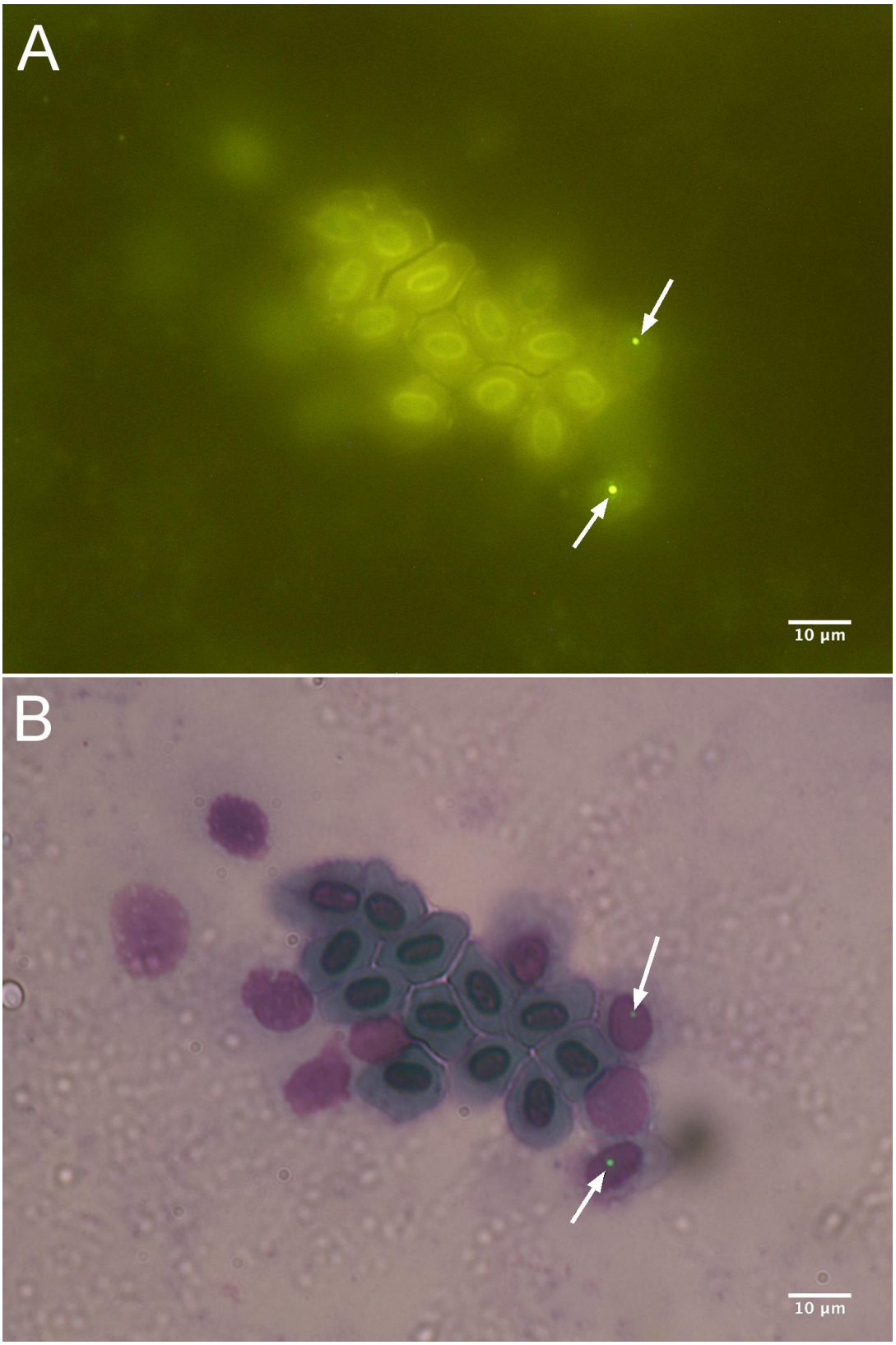

Figure 19. Polyethylene terephthalate (PET) particles in association to blood leucocytes (white arrows) in a blood sample from the Atlantic salmon (*Salmo salar*). A: Picture of the particles taken with filter type B2A. A curve-function (Photoshop) was used to enhance the contrast. B: Overlay between Hematoxylin & Eosin (H&E) stained section and picture taken with filter type DFR. The filter "Exclusion" (Photoshop) was used to enhance the contrast between the particles and the blood cells. 60x magnification. See appendix 12, figure S12.F for original images and modifications.

PET particles were also observed in the anterior part of the liver (Figure 20A and B). All particles found were associated with hepatocytes and appeared to be randomly distributed in the hepatic tissue. No particles were observed in or close to sinusoids, biliary channels, the central or portal vein in the samples examined.

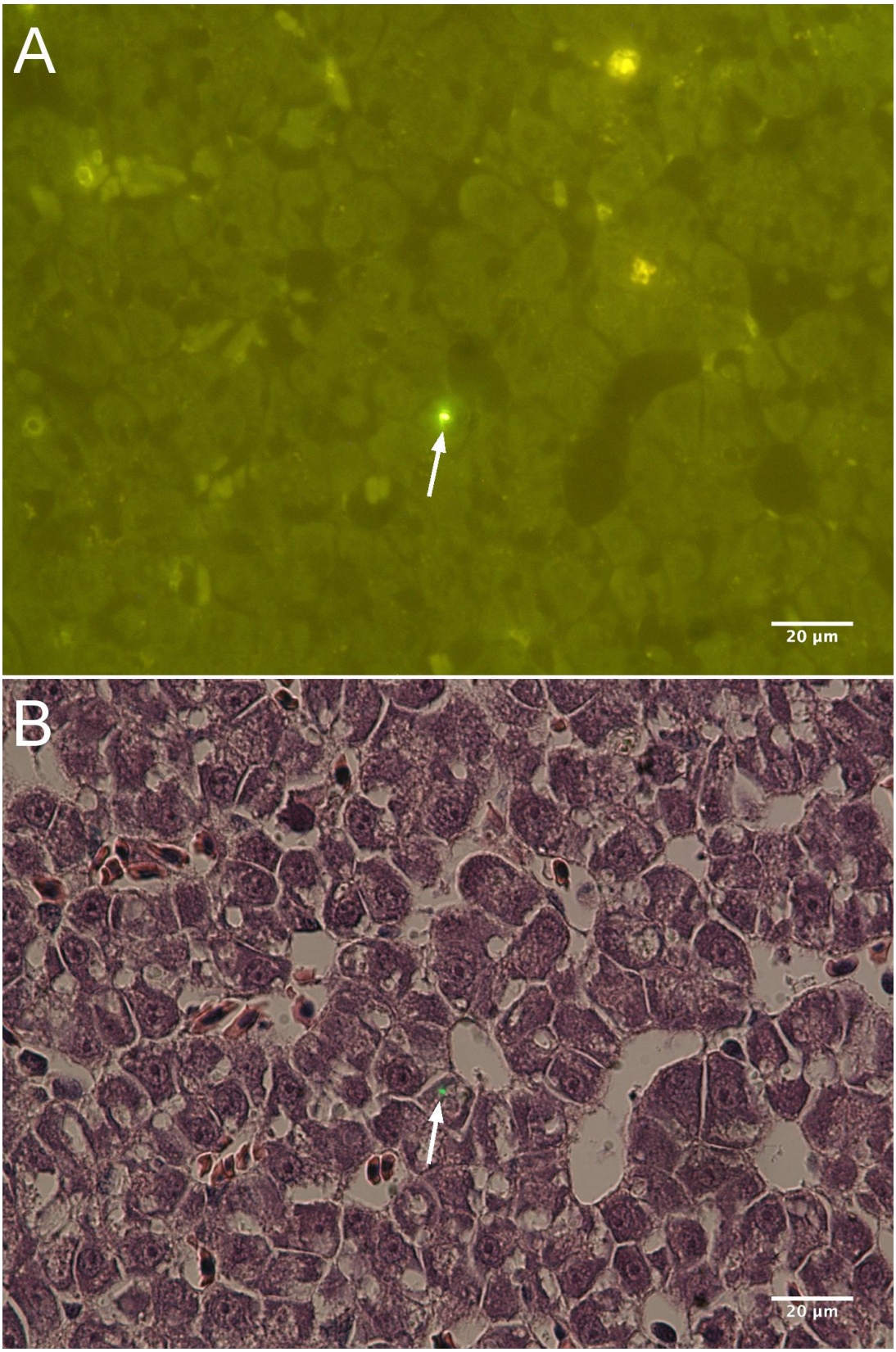

Figure 20. Fluorescent Polyethylene terephthalate (PET) particle in association to a hepatocyte in the liver of the Atlantic salmon (*Salmo salar*) parr. Fluorescence on filter A) B2A. A curve-function (Photoshop) was used to enhance the contrast B: Overlay between Hematoxylin & Eosin (H&E) stained section and picture taken with filter DFR. The filter "Exclusion" (Photoshop) was used to enhance the contrast between the tissue and the particle. 40x magnification. See appendix for picture modifications.

5. Discussion

The present study aimed to examine the uptake of nanoplastic particles in the intestine of the Atlantic salmon and to characterize translocation to other organs via the circulatory system. A pilot study was conducted to investigate the intestinal permeability and uptake of polystyrene (PS) and polyethylene terephthalate (PET) particles explicitly over the fish intestinal epithelium using the Ussing chamber. The Ussing chamber represents a well established technique for studies of the transepithelial transport of water, ions and molecules over epithelial tissues, and have been used in numerous permeability, pathogenesis and particle uptake studies (Delie, 1998). Nevertheless, only one study have used the Ussing chamber to investigate the intestinal barrier function when exposed to PS microplastic particles in salmonids (Ašmonaitė *et al*., 2018). The second study aimed to investigate the intestinal uptake and translocation of PET particles (≤ 150 µm), using an *in vivo* feeding experiment. Oral administration of particles is considered a powerful experimental approach as it represents a near physiological system and provide overall information about uptake and translocation (Delie, 1998). PS and PET are two of the most common plastic polymers produced and are therefore expected to be well distributed in the marine environment. The concentrations used were not considered environmentally relevant, but necessary for proper exposure of the tissue, also suggested by van Moos *et al*., (2012). Both experimental methods indicate uptake of PS and PET nanoplastic particles through the intestinal route in Atlantic salmon with translocation of the latter to the circulatory system and liver.

5.1 The Ussing chamber

5.1.1 Intestinal uptake of 0.5 µm PS nanoplastic particles

The majority of uptake studies have used particles in the nanometer range, because smaller particles are expected to cross epithelial barriers easier than larger particles. Nevertheless, the present study indicates that 0.5 µm PS plastic particles have the potential to cross intestinal epithelia. In correspondence with earlier studies in Sprague-Dawley rats and marine jacopever (*Sebastes schlegelii*), particles were observed within the mucosal folds, especially in the lamina propria (Hodges *et al*., 1995, Yin *et al*., 2018). Few uptake studies mentions possible cellular uptake routes, but trans- and paracellular transport have been suggested (Hodges *et al*., 1995). However, according to paracellular transport studies, the tight junction pores in healthy, intact

epithelium have permeability for particles in the size range of 0.6 – 6 nm (Fihn *et al*., 2000). The 0.5 µm particles in this study are therefore too large for such transport to occur, unless other factors have affected the barrier integrity. Many factors are known to increase the rate of translocation of macromolecules and even bacteria. These include oxygen deficiency, water temperatures, salinity and stress (Sundh et al., 2010, Sundh and Sundell, 2015). The post-smolt used in the present study had been fed experimental feed with high amounts of soya, leading to a slight inflammation in the intestine. This has probably caused increased permeability which may have led to increased particle uptake.

Endocytosis and phagocytosis have been suggested as other reasonable uptake routs in an invertebrate species. Blue mussels (*Mytulis edulis)* exposed to high density polyethylene (HDPE) particles of > 0 – 80 µm showed translocation into intestinal vacuoles and fusion with lysosomes. Particles were also observed in relation to eosinophilic granulocytes through formation of granulocytomas in the intestinal tissue (von Moos *et al*., 2012), strongly indicating initiation of the immune system. Such formation and indications of immunological reactions in the intestinal tissue is beyond the scope of this study, nor could it be detected with fluorescent microscopy. Furthermore, inter-species differences make it difficult to extrapolate these uptake results to the Atlantic salmon and do not necessarily be equally applicable in fish or other vertebrate species (Delie, 1998).

Some seromuscular detachment can be observed after the *ex vivo* exposure, suggesting that the particles may have entered through damaged tissue. Physical injury due to plastic polymer exposure have been proposed from several studies. Lei *et al*., (2018) recently discovered injured intestinal tissue in zebrafish after 10 days exposure to various 70 nm microplastic polymers. Exposure to polyethylene (PE), polypropylene (PP) and polyvinylchloride (PVC) in particular, caused injury to mucosal folds and the enterocytes. Nevertheless, no injury was associated with exposure to 0.1, 1.0 and 5.0 µm PS plastic particles in this study, indicating different effects of various polymer types. The observations were in agreement with findings from Pèda *et al*., (2016) who noticed severe histological alterations of the intestinal tissue in PVC exposed seabass (*Dicentrarchus labrax*). Moderate alterations, including vacuolation of the enterocytes and increased number of goblet cells were observed in fish exposed for 30 days, while the 60- and 90-days exposure groups showed more severe alterations. The 90 days exposed group

showed loss of structural integrity, seromuscular edema and detachment of the mucosal epithelium. A recent Ussing study detected slight, but insignificant increase in the number of goblet cells, and no other physiological alterations or injury in intestinal segments of rainbow trout exposed to PS microplastics for 28 days (Ašmonaitė *et al*., 2018). The latter indicates that time of exposure is a critical factor regarding hazardous effects. These results taken into consideration, there are no basis to claim that the one hour exposure in the present study would cause such significant injury and enhanced particle uptake. The tissue may also have been damaged due to unproper treatment, during preparation and/or sectioning, as mentioned by Delie (1998). Sectioning in particular may cause ruptures, and the knife may drag particles and cause "artificial" particle translocation into the tissue (Delie, 1998). Indications of particles dragged into the tissue was observed in some of the sections examined.

5.1.2 Intestinal exposure to 40 nm PS particles

The 40 nm fluorescent PS particles were neither observed in the luminal mucus layer nor in the epithelial tissue in the *ex vivo* study. This was mainly due to instrumental limitations and does not necessarily correspondent to lack of exposure or uptake. Due to their small sizes, these particles were expected to readily cross the epithelia. They were also expected to aggregate with accumulations in e.g. intestinal vacuoles, as the case for HDPE particles in blue mussels (*M. edulis)* (von Moos *et al*., 2012). Individual particles were impossible to detect in the fluorescence microscope, even without the tissue on the 10x – 60x magnification used in this study. This was particularly challenging since the green autofluorescence of the tissue was impossible to separate from the same fluorescence of the 40 nm PS particles.

Bleaching, the exposure of the slides to light, removed some of the background fluorescence. However, with the time and resources available to this study, such methodology was considered to time-consuming.

Parts of the Ringer solutions from the luminal and serosal side of the Ussing chambers were collected to estimate tissue translocation. Unfortunately, the microassay method used was unable to record any fluorescence on either side of the intestinal preparations. The reason for this is yet unknown. The fluorescence could have been to low or there may have been some errors in settings or electrical circuits.

5.1.3 Intestinal uptake of PET nanoplastic particles

Few studies have used PET particles in relation to intestinal uptake studies (Weber *et al*., 2018). A pilot study using the Ussing chamber would therefore give good indications of a potential uptake over the salmonid intestinal epithelium. The PET particles were to a lesser extent found in the luminal mucus or intestinal tissue than PS particles. The few particles that were found translocated may have entered through ruptures or damaged tissue. The PET bottle material was manufactured by "crushing", producing particles that would be of different size and shapes. Infinitive structure and potentially sharp edges in these particles may have caused physical injury, as mentioned above. The particles also have been too large for uptake to occur. The coulter counter data showed presence of small sized particles (≤ 2 µm) in the PET sample, but particles up to ≤ 150 µm were also present, as informed by the manufacturer (Weber *et al*., 2018). However, lack of observations of several particles may also be a result of improper exposure in the Ussing chamber. It was observed that many of the particles stacked to the Ussing chamber walls or sank to the bottom of the chambers. PET have a specific gravity of 1.29 – 1.40 g/cm^3, which is higher than water (approx. 1 g/cm^3). Challenges with keeping the particles in suspension may have resulted in lack of contact with the tissue. Such observations strongly suggest that the particle polymer in use should be carefully considered before such studies.

5.1.4 Accumulation of 0.5 µm PS and PET particles in the luminal mucus-layer

The luminal mucus layer traps PS and PET plastic particles, as in agreement with similar studies (Pedà *et al*., 2016). Mucus is produced by the goblet cells partly to lubricate the intestinal epithelium and ease the transport of luminal content down the intestine, but also to protect the epithelia against bacteria and other foreign and potentially harmful agents present (Jutfelt, 2011). An increase in mucus producing goblet cells has been observed following stress and inflammatory stimuli, but also in association to plastic polymer exposure. 30 days exposure to PVC microplastics increased the number of goblet cells in seabass (*D. labrax*), indicating a first line defense system against this type of polymer (Pedà *et al*., 2016). On the contrary, the 2018 Ussing study indicated only a slight, but insignificant ($p > 0,05$) increase in goblet cells in the intestinal tissues of rainbow trout orally exposed to PS microplastics for 28 days (Ašmonaitė *et al*., 2018). This may indicate that different polymers cause different affects as discussed by Lei *et al*., (2018). Some increased mucus production will also occur due to physical stress in the

Ussing chamber. The number and potential increase in goblet cells during exposure were not examined or compared to any control group in the present study. Such observations and further examination are nevertheless interesting regarding the protective function of the mucus layer in relation to nano- and microplastic exposure, and the ability to prevent small plastic particles from reaching the epithelium.

5.1.5 Limitations to the ex vivo Ussing chamber approach

The Ussing chamber provides information about permeability and transport activity of the epithelium in study over a limited time span. The intestinal integrity and transport may be affected by unproper treatment by the tissue before the experiment. The seromuscular layer must also be stripped from the epithelium to obtain meaningful data, as the serosa can hinder the particles from penetrating all layers of the intestine. Edelblum and Turner, (2015) specify that tissues becomes anoxic immediately after removal from the fish. Oxygen depletion and exposure to high (room) temperatures, may reduce the tissue`s metabolic rate and thus affect transport mechanisms. The tissue may also go into shock and die. The exposure time in the Ussing chamber should therefore be carefully considered (Delie, 1998).

5.2 *In vivo* exposure and uptake of PET nanoplastic particles and translocation to the circulatory system and liver.

5.2.1 Intestinal uptake of PET nanoplastic particles

The *in vivo* feeding experiment strongly indicates translocation of PET nanoplastics over the entire intestinal epithelium of Atlantic salmon parr. Translocation to the mucosal folds and, in particular, the lamina propria agrees with results from the *ex vivo* Ussing chamber experiment and other uptake studies (Hodges *et al*., 1995, Yin *et al*., 2018). The particles in the tissue was in the size range of < 2 µm (measured in ImageJ, not illustrated), demonstrating that only the smallest particles from the feed had been translocated. Hodges *et al*., (1995) observed translocation of 2 µm PS particles particles to various intestinal structures in rats only 0.5 hours after oral administration, while even larger 15 µm PS microparticles were observed in the mucosal folds of the marine jacopever after 14-days exposure (Yin *et al*., 2018). As in the case for the 0.5 µm PS microplastics in the *ex vivo* experiment discussed above, transport of such large particles through the tight junction complexes seems quite unlikely based on the 0.6 nm

– 6 nm junction pores, unless other factors have affected the barrier integrity. Translocation due to damaged tissue may be a potential cause also for these PET nanoparticles, but signs of intestinal damage was not observed or compared to any control group in this case.

The proximal midgut segment of the intestine is the main uptake rout for nutrients, and the permeability is therefor expected to be higher in this proximal part, compared to the distal hindgut segment where nutrient uptake plays a minor part (Jutfelt, 2011). This may be some of the explanation for the higher uptake of PET particles observed in the midgut compared to the hindgut segments examined. This further agrees with observations of the translocated 2 µm PS particles in rat intestines, in which most particles were observed in the proximal intestine compared to the distal intestine (Hodges *et al*., 1995). However, such differences in intestinal segments have not been mentioned in the previous uptake studies on fish (Yin et al., 2018).

5.2.2 Translocation of PET particles to the circulatory system

The circulatory system is important for transportation and distribution of nutrients from the intestine. In fish, blood erythrocytes also take up and transport oxygen from the gills to cells and tissues (Kryvi and Poppe, 2016). Micro- and nanoplastic particles have been reported translocated to the circulatory system in vertebrate and invertebrate species, respectively (Veneman et al., 2017, Browne et al., 2008) and have shown to alter blood chemistry. In particular, PS nanoparticles have been shown bound to apolipoproteins in zebrafish serum (Cedervall et al., 2012), while PS microparticles were shown to affect blood coagulation in human plasma (Oslakovic et al., 2012). The current study shows PET particles in association with both erythrocytes and blood leucocytes, verifying both translocation and transport in Atlantic salmon. Few studies have reported the presence of plastic particles in the circulatory system, or shown how they get transported. A 2005 *in vitro* study using confocal microscopy confirmed intracellular translocation of 0.2 µm PS particles into human erythrocytes suggesting they were transported inside the blood cells and not as membrane bound particles (Geiser et al., 2005). Larger 1 µm PS-particles did not translocate into the erythrocytes. Fluorescence microscopy do not confirm if the particles are transported through uptake in the red blood cells or are membrane bond in the present study. Furthermore, lack of information on the zeta potential (charge) of the PET particles makes it impossible to confirm attraction to the negatively charged erythrocytes (Fernandes et al., 2011). However, based on Geiser et al`s.,

(2005) observations and the size of the PET particles in this study, it's indicative that the particles are membrane bond rather than translocated.

Blood leucocytes are important components of the immune system, as they defense the organism against foreign agents, bacteria and viruses (Janqueira and Carneiro, 2005). Veneman et al., (2017) discovered neutrophils and macrophages co-located with 700 nm PS particles in injected zebrafish larvae using imaging and transcriptomics. Interactions between PS particles and neutrophils were also reported from studies on Fathead minnow (*Pimephales promelas*) (Greven et al., 2016). Nevertheless, attraction and activation of blood immune cells in relation to plastic polymer exposure is to a less extant reported from the literature, nor is it well understood. Based on the observations in the present study, more research should be conducted to gain knowledge of the potential immunological reactions due to PET polymer exposure.

5.2.3 Translocation of PET nanoplastic particles to the liver

Translocation of PET nanoplastic particles into liver tissue of the Atlantic salmon agrees with other, similar uptake and translocation studies in fish. Kashiwada (2006) observed 39,4 nm PS particles in the liver of Medaka (*O. latipes*), and larger 70 nm and 5 µm PS particles were translocated to hepatic tissue in zebrafish (Lu *et al*., 2016). Nevertheless, none of these studies indicates the main routes of entrance into the tissue, nor exactly where the particles are located. The size of the particles observed in the hepatic tissue of the present study, corresponds with the same sizes detected in the intestinal tissue and the circulatory system, further indicating that particles < 2 µm have the highest possibility to be translocated into organs of the Atlantic salmon. However, even bigger particles of 124 – 600 nm have been reported in wild caught species, such as European anchovies and mullets (Avio *et al.*, 2015, Collard *et al*., 2017). The liver is an important filtration organ in vertebrates that eliminates toxic substance before entering the circulatory system. Approximately 70 – 80% of the blood entering the liver, enter through the portal vein and all blood with nutrients and other substances from the intestine, enters through this route before distribution to the circulatory system (Janqueira and Carneiro, 2005). Translocation of PET nanoplastic particles may therefore be consistent with the expectations that also nanoplastic particles enters through the portal vein after uptake through the intestine. Nevertheless, particles in the tissue samples examined was only detected randomly located in the hepatic tissue, and not observed in relation to e.g. blood vessels or sinusoids.

Since samples only from the anterior part of the liver were examined, there are no further indications of translocation or observations in the portal vein.

6. Conclusions

The current study shows that 0.5 µm PS and ≤ 2 µm PET nanoplastic particles are translocated through the intestinal epithelium in Atlantic salmon parr and post-smolt. It also confirms translocation of ≤ 2 µm PET particles to the circulatory system and liver of parr. However, cellular uptake mechanisms could not be confirmed with fluorescence microscopy and histology. The histological examinations indicate that the highest number of particles appeared to cross the intestinal epithelium through the midgut segment. The translocated particles also seem to be associated with intraepithelial leucocytes, which may indicate recognition by the immune system. Particles are also associated with erythrocytes and blood leucocytes in the circulatory system, but any uptake by these cells or immunological responses could not be confirmed in this study.

7. Future perspectives

7.1 Uptake of nanoplastics in the Atlantic salmon

The present study highly confirms the extended need for scientific knowledge regarding uptake mechanisms and potentially harmful effects in the Atlantic salmon. Increased knowledge is considered important regarding fish health and welfare, especially in relation to the aquaculture industry where fish may be prone to plastic particle exposure. Furthermore, most uptake studies have used other vertebrate or invertebrate species (Hodges *et al*., 1995, Browne *et al*., 2008, Pitt *et al*., 2018), which may have other intestinal uptake characteristics non-comparable to salmonids. Inter-species differences may therefore limit extrapolation to other species (Delie, 1998), including the Atlantic salmon . The present study did not aim to investigate the potential uptake of PET nanoplastic particles over the gill epithelium, nor can it be rejected (Kashiwada, 2006). Despite strong indications of translocation due to intestinal uptake, some particles may have leaked from the feed in the fish holding tanks and exposed the gill epithelium. No water samples were collected and analyzed for fluorescence during the 39 days feeding period but is to a great extant recommended for future uptake studies in fish. Other organs (like the kidneys, muscles and gallbladder) should also be examined, since the fate of ingested and translocated plastic particles remains unknown.

7.2 Experimental methods

The present study used a qualitative approach through fluorescence microscopy and histology to investigate translocation into tissues. Despite a much-used methodological approach, histology does not confirm particle translocation into individual cells (Delie, 1998). Confocal microscopy should therefore be conducted to gain more knowledge about particle localization. This would in particular be interesting in examination of erythrocyte – associated particles, based on current results that indicate intracellular localization (Geiser et al., 2005). Particles associated with immune cells, as indicated in the present study, should be investigated with immunohistochemical approaches.

Furthermore, fluorescence microscopy and histology are not suitable for particle quantification, and the method unable examination of whole organs. A quantitative analysis should therefore be conducted to confirm the number of particles translocated into different organ systems.

Hypochlorite digestion of organs have proved to be a powerful method for extraction and isolation of microplastic particles. Raman spectroscopy can further identify different polymers in the extracted sample (Collard et al., 2017). The properties of the PET polymer were not well established in head of the study. Characterization of the PET particles using SEM (scanning electron microscopy) should be done to determine the shape of the particles. The zeta potential should also be established to determine the electrical charge of the PET polymer.

References:

ANDRADY, A. L. 2003a. Common plastics materials *In:* ANDRADY, A. L. (ed.) *Plastics and the Environment* Hoboken, New Jersey: John Wiley & Sons, Inc.

ANDRADY, A. L. 2003b. An Environmental Primer *In:* ANDRADY, A. L. (ed.) *Plastics and the Environment* Hoboken, New Jersey John Wiley & Sons, Inc

ANDRADY, A. L. 2011. Microplastics in the marine environment. *Marine Pollution Bulletin,* 62**,** 1596-1605.

ANDRADY, A. L. 2017. The plastic in microplastics: A review. *Marine Pollution Bulletin,* 119**,** 12-22.

ANDRADY, A. L. & NEAL, M. A. 2009. Applications and societal benefits of plastics. *Philos Trans R Soc Lond B Biol Sci,* 364**,** 1977-84.

AŠMONAITĖ, G., SUNDH, H., ASKER, N. & CARNEY ALMROTH, B. 2018. Rainbow Trout Maintain Intestinal Transport and Barrier Functions Following Exposure to Polystyrene Microplastics. *Environmental Science & Technology,* 52**,** 14392-14401.

AVIO, C. G., GORBI, S. & REGOLI, F. 2015. Experimental development of a new protocol for extraction and characterization of microplastics in fish tissues: First observations in commercial species from Adriatic Sea. *Marine Environmental Research,* 111**,** 18-26.

BELLAS, J., MARTÍNEZ-ARMENTAL, J., MARTÍNEZ-CÁMARA, A., BESADA, V. & MARTÍNEZ-GÓMEZ, C. 2016. Ingestion of microplastics by demersal fish from the Spanish Atlantic and Mediterranean coasts. *Marine Pollution Bulletin,* 109**,** 55-60.

BOERGER, C. M., LATTIN, G. L., MOORE, S. L. & MOORE, C. J. 2010. Plastic ingestion by planktivorous fishes in the North Pacific Central Gyre. *Marine Pollution Bulletin,* 60**,** 2275-2278.

BONE, Q. M., RICHARD H. 2008. *Biology og Fishes,* U. K, Tylor & Francis Group.

BRENNECKE, D., FERREIRA, E. C., COSTA, T. M. M., APPEL, D., DA GAMA, B. A. P. & LENZ, M. 2015. Ingested microplastics (>100µm) are translocated to organs of the tropical fiddler crab Uca rapax. *Marine Pollution Bulletin,* 96**,** 491-495.

BROWNE, M. A., CRUMP, P., NIVEN, S. J., TEUTEN, E., TONKIN, A., GALLOWAY, T. & THOMPSON, R. 2011. Accumulation of Microplastic on Shorelines Woldwide: Sources and Sinks. *Environmental Science & Technology,* 45**,** 9175-9179.

BROWNE, M. A., DISSANAYAKE, A., GALLOWAY, T. S., LOWE, D. M. & THOMPSON, R. C. 2008. Ingested Microscopic Plastic Translocates to the Circulatory System of the Mussel, Mytilus edulis (L.). *Environmental Science & Technology,* 42**,** 5026-5031.

CEDERVALL, T., HANSSON, L.-A., LARD, M., FROHM, B. & LINSE, S. 2012. Food Chain Transport of Nanoparticles Affects Behaviour and Fat Metabolism in Fish. *PLOS ONE,* 7**,** e32254.

CLARKE, L. L. 2009. A guide to Ussing chamber studies of mouse intestine. *American Journal of Physiology-Gastrointestinal and Liver Physiology,* 296**,** G1151-G1166.

COLLARD, F., GILBERT, B., COMPÈRE, P., EPPE, G., DAS, K., JAUNIAUX, T. & PARMENTIER, E. 2017. Microplastics in livers of European anchovies (Engraulis encrasicolus, L.). *Environmental Pollution,* 229**,** 1000-1005.

CÓZAR, A., MARTÍ, E., DUARTE, C. M., GARCÍA-DE-LOMAS, J., VAN SEBILLE, E., BALLATORE, T. J., EGUÍLUZ, V. M., GONZÁLEZ-GORDILLO, J. I., PEDROTTI, M. L., ECHEVARRÍA, F., TROUBLÈ, R. & IRIGOIEN, X. 2017. The Arctic Ocean as a dead end for floating plastics in the North Atlantic branch of the Thermohaline Circulation. *Science Advances,* 3**,** e1600582.

DAVISON, P. & ASCH, R. G. 2011. Plastic ingestion by mesopelagic fishes in the North Pacific Subtropical Gyre. *Marine Ecology Progress Series,* 432**,** 173-180.

DELIE, F. 1998. Evaluation of nano- and microparticle uptake by the gastrointestinal tract. *Advanced Drug Delivery Reviews,* 34**,** 221-233.

DOYLE-MCCULLOUGH, M., SMYTH, S. H., MOYES, S. M. & CARR, K. E. 2007. Factors influencing intestinal microparticle uptake in vivo. *International Journal of Pharmaceutics,* 335**,** 79-89.

EDELBLUM, K. L. & TURNER, J. R. 2015. Chapter 12 - Epithelial Cells: Structure, Transport, and Barrier Function. *In:* MESTECKY, J., STROBER, W., RUSSELL, M. W., KELSALL, B. L., CHEROUTRE, H. & LAMBRECHT, B. N. (eds.) *Mucosal Immunology (Fourth Edition).* Boston: Academic Press.

EERKES-MEDRANO, D., THOMPSON, R. C. & ALDRIDGE, D. C. 2015. Microplastics in freshwater systems: A review of the emerging threats, identification of knowledge gaps and prioritisation of research needs. *Water Research,* 75**,** 63-82.

ERIKSEN, M., LEBRETON, L. C., CARSON, H. S., THIEL, M., MOORE, C. J., BORERRO, J. C., GALGANI, F., RYAN, P. G. & REISSER, J. 2014. Plastic Pollution in the World's Oceans: More than 5 Trillion Plastic Pieces Weighing over 250,000 Tons Afloat at Sea. *PLoS One,* 9**,** e111913.

FENDALL, L. S. & SEWELL, M. A. 2009. Contributing to marine pollution by washing your face: Microplastics in facial cleansers. *Marine Pollution Bulletin,* 58**,** 1225-1228.

FERNANDES, H. P., CESAR, C. L. & BARJAS-CASTRO, M. D. L. 2011. Electrical properties of the red blood cell membrane and immunohematological investigation. *Revista brasileira de hematologia e hemoterapia,* 33**,** 297-301.

FIHN, B. M., SJÖQVIST, A. & JODAL, M. 2000. Permeability of the rat small intestinal epithelium along the villus-crypt axis: Effects of glucose transport. *Gastroenterology,* 119**,** 1029-1036.

FOEKEMA, E. M., DE GRUIJTER, C., MERGIA, M. T., VAN FRANEKER, J. A., MURK, A. J. & KOELMANS, A. A. 2013. Plastic in North Sea Fish. *Environmental Science & Technology,* 47**,** 8818-8824.

GEISER, M., ROTHEN-RUTISHAUSER, B., KAPP, N., SCHÜRCH, S., KREYLING, W., SCHULZ, H., SEMMLER, M., HOF, V. I., HEYDER, J. & GEHR, P. 2005. Ultrafine Particles Cross Cellular Membranes by Nonphagocytic Mechanisms in Lungs and in Cultured Cells. *Environmental Health Perspectives,* 113**,** 1555-1560.

GREVEN, A.-C., MERK, T., KARAGÖZ, F., MOHR, K., KLAPPER, M., JOVANOVIĆ, B. & PALIĆ, D. 2016. Polycarbonate and polystyrene nanoplastic particles act as stressors to the innate immune system of fathead minnow (Pimephales promelas). *Environmental Toxicology and Chemistry,* 35**,** 3093-3100.

HODGES, G. M., CARR, E. A., HAZZARD, R. A. & CARR, K. E. 1995. Uptake and translocation of microparticles in small intestine. *Digestive Diseases and Sciences,* 40**,** 967-975.

JAMBECK, J. R., GEYER, R., WILCOX, C., SIEGLER, T. R., PERRYMAN, M., ANDRADY, A., NARAYAN, R. & LAW, K. L. 2015. Marine pollution. Plastic waste inputs from land into the ocean. *Science,* 347**,** 768-71.

JANQUEIRA, L. C. & CARNEIRO, J. 2005. *Basic histology - text and atlas* USA, The McGraw Hill Companies

JOVANOVIĆ, B. 2017. Ingestion of microplastics by fish and its potential consequences from a physical perspective. *Integrated Environmental Assessment and Management,* 13**,** 510-515.

JUTFELT, F. 2011. Barrier function of the gut. *In:* FARRELL, A. P. (ed.) *Encyclopedia of Fish Physiology From Genom to Environment* San Diego: Elsevier

KASHIWADA, S. 2006. Distribution of Nanoparticles in the See-through Medaka (Oryzias latipes). *Environmental Health Perspectives,* 114**,** 1697-1702.

KRYVI, H. & POPPE, T. 2016. *Fiskeanatomi* Bergen, Fagbokforlaget

LEI, L., WU, S., LU, S., LIU, M., SONG, Y., FU, Z., SHI, H., RALEY-SUSMAN, K. M. & HE, D. 2018. Microplastic particles cause intestinal damage and other adverse effects in zebrafish Danio rerio and nematode Caenorhabditis elegans. *Science of The Total Environment,* 619-620**,** 1-8.

LU, Y., ZHANG, Y., DENG, Y., JIANG, W., ZHAO, Y., GENG, J., DING, L. & REN, H. 2016. Uptake and Accumulation of Polystyrene Microplastics in Zebrafish (Danio rerio) and Toxic Effects in Liver. *Environmental Science & Technology,* 50**,** 4054-4060.

LUSHER, A. L., MCHUGH, M. & THOMPSON, R. C. 2013. Occurrence of microplastics in the gastrointestinal tract of pelagic and demersal fish from the English Channel. *Marine Pollution Bulletin,* 67**,** 94-99.

MARIEB, E. N. A. H., KATJA 2016. *Human Anatomy and Physiology,* Essex, England Pearson Education Limited

MATTSSON, K., JOHNSON, E. V., MALMENDAL, A., LINSE, S., HANSSON, L.-A. & CEDERVALL, T. 2017. Brain damage and behavioural disorders in fish induced by plastic nanoparticles delivered through the food chain. *Scientific Reports,* 7**,** 11452.

MOORE, C. J. 2008. Synthetic polymers in the marine environment: A rapidly increasing, long-term threat. *Environmental Research,* 108**,** 131-139.

MOORE, C. J., MOORE, S. L., LEECASTER, M. K. & WEISBERG, S. B. 2001. A Comparison of Plastic and Plankton in the North Pacific Central Gyre. *Marine Pollution Bulletin,* 42**,** 1297-1300.

MURALISRINIVASAN, N. S. 2016. Plastics - applications *Plastic Waste Management: Processing and Disposal.* Shawbury, Shrewsbury, Shropshire, U.K: Smithers Rapra Technology Ltd.

NAPPER, I. E., BAKIR, A., ROWLAND, S. J. & THOMPSON, R. C. 2015. Characterisation, quantity and sorptive properties of microplastics extracted from cosmetics. *Marine Pollution Bulletin,* 99**,** 178-185.

NAPPER, I. E. & THOMPSON, R. C. 2016. Release of synthetic microplastic plastic fibres from domestic washing machines: Effects of fabric type and washing conditions. *Marine Pollution Bulletin,* 112**,** 39-45.

OLIVIER, V., MEISEN, I., MECKELEIN, B., HIRST, T. R., PETER-KATALINIC, J., SCHMIDT, M. A. & FREY, A. 2003. Influence of Targeting Ligand Flexibility on Receptor Binding of Particulate Drug Delivery Systems. *Bioconjugate Chemistry,* 14**,** 1203-1208.

OPENSTAX, A. P. 2016. The Digestive system *Anatomy and Physiology.* OpenStrax

OSLAKOVIC, C., CEDERVALL, T., LINSE, S. & DAHLBÄCK, B. 2012. Polystyrene nanoparticles affecting blood coagulation. *Nanomedicine: Nanotechnology, Biology and Medicine,* 8**,** 981-986.

PEDÀ, C., CACCAMO, L., FOSSI, M. C., GAI, F., ANDALORO, F., GENOVESE, L., PERDICHIZZI, A., ROMEO, T. & MARICCHIOLO, G. 2016. Intestinal alterations in European sea bass Dicentrarchus labrax (Linnaeus, 1758) exposed to microplastics: Preliminary results. *Environmental Pollution,* 212**,** 251-256.

PEEKEN, I., PRIMPKE, S., BEYER, B., GÜTERMANN, J., KATLEIN, C., KRUMPEN, T., BERGMANN, M., HEHEMANN, L. & GERDTS, G. 2018. Arctic sea ice is an important temporal sink and means of transport for microplastic. *Nature Communications,* 9**,** 1505.

PITT, J. A., KOZAL, J. S., JAYASUNDARA, N., MASSARSKY, A., TREVISAN, R., GEITNER, N., WIESNER, M., LEVIN, E. D. & DI GIULIO, R. T. 2018. Uptake, tissue distribution, and toxicity of polystyrene nanoparticles in developing zebrafish (Danio rerio). *Aquatic Toxicology,* 194**,** 185-194.

PLASTICSEUROPE. 2017. *Plastics - the Facts 2017* [Online]. Brussel, Belgium PlasticsEurope Available: https://www.plasticseurope.org/application/files/5715/1717/4180/Plastics_the_facts_2017_

FINAL_for_website_one_page.pdf?fbclid=IwAR3rgZDigH9ewN5dR3j_4FvDxDisQPNOAeBxQdKbWCV6UBpPX28DJGuddhs [Accessed 04.02 2019].

PLASTICSEUROPE. 2018. *Plastics - the Facts 2018. An analysis of European plastics production, demand and waste data* [Online]. Brussel, Belgium PlasticsEurope Available: https://www.plasticseurope.org/application/files/6315/4510/9658/Plastics_the_facts_2018_AF_web.pdf?fbclid=IwAR3FEWvdgiXUMhNWNUptQjtBfy3A_t0IQCwOOEpNy0pZ6Qc3LH9he41IXsI [Accessed 07.5 2019].

REISSER, J., SLAT, B., NOBLE, K., DU PLESSIS, K., EPP, M., PROIETTI, M., DE SONNEVILLE, J., BECKER, T. & PATTIARATCHI, C. 2015. The vertical distribution of buoyant plastics at sea: an observational study in the North Atlantic Gyre. *Biogeosciences,* 12**,** 1249-1256.

ROCHMAN, C. M., KUROBE, T., FLORES, I. & TEH, S. J. 2014. Early warning signs of endocrine disruption in adult fish from the ingestion of polyethylene with and without sorbed chemical pollutants from the marine environment. *Science of The Total Environment,* 493**,** 656-661.

SHAH, A. A., HASAN, F., HAMEED, A. & AHMED, S. 2008. Biological degradation of plastics: A comprehensive review. *Biotechnology Advances,* 26**,** 246-265.

SUNDH, H., KVAMME, B. O., FRIDELL, F., OLSEN, R. E., ELLIS, T., TARANGER, G. L. & SUNDELL, K. 2010. Intestinal barrier function of Atlantic salmon (Salmo salar L.) post smolts is reduced by common sea cage environments and suggested as a possible physiological welfare indicator. *BMC Physiology,* 10**,** 22.

SUNDH, H. & SUNDELL, K. S. 2015. 7 - Environmental impacts on fish mucosa. *In:* BECK, B. H. & PEATMAN, E. (eds.) *Mucosal Health in Aquaculture.* San Diego: Academic Press.

THERMOFISHER, S. *FluoSphare Carboxylate-Modified Microspheres, 0.04 um, yellow-green fluorescent (505/515), 5% solids, azide free* [Online]. thermofisher.com: Thermo Fisher Scientific Available: https://www.thermofisher.com/order/catalog/product/F8795?fbclid=IwAR1S3_iogXbkz2UiJe-QuneTNtVu-Qu4olvmF2O3p8vxjp4SB5guBJSjyHs [Accessed 22.04 2019].

THERMOFISHER, S. *FluoSpheres Carboxylate-Modified Microspheres, 0.5 um, red fluorescent (580/605), 2% solids* [Online]. thermofisher.com: Thermo Fisher Scientific Available: https://www.thermofisher.com/order/catalog/product/F8812?fbclid=IwAR285sinW6JHeUo_-iHpmSmBIxf_IBR3ClWiJH1drw3U0lgpSobO-GRShFg [Accessed 22.04 2019].

THIEL, M., HINOJOSA, I. A., MIRANDA, L., PANTOJA, J. F., RIVADENEIRA, M. M. & VÁSQUEZ, N. 2013. Anthropogenic marine debris in the coastal environment: A multi-year comparison between coastal waters and local shores. *Marine Pollution Bulletin,* 71**,** 307-316.

THOMPSON, R. C. 2006. *Plastic debris in the marine environment:Consequences and solutions*.

TOPÇU, E. N., TONAY, A. M., DEDE, A., ÖZTÜRK, A. A. & ÖZTÜRK, B. 2013. Origin and abundance of marine litter along sandy beaches of the Turkish Western Black Sea Coast. *Marine Environmental Research,* 85**,** 21-28.

VAN POMEREN, M., BRUN, N. R., PEIJNENBURG, W. J. G. M. & VIJVER, M. G. 2017. Exploring uptake and biodistribution of polystyrene (nano)particles in zebrafish embryos at different developmental stages. *Aquatic Toxicology,* 190**,** 40-45.

VENEMAN, W. J., SPAINK, H. P., BRUN, N. R., BOSKER, T. & VIJVER, M. G. 2017. Pathway analysis of systemic transcriptome responses to injected polystyrene particles in zebrafish larvae. *Aquatic Toxicology,* 190**,** 112-120.

VON MOOS, N., BURKHARDT-HOLM, P. & KÖHLER, A. 2012. Uptake and Effects of Microplastics on Cells and Tissue of the Blue Mussel Mytilus edulis L. after an Experimental Exposure. *Environmental Science & Technology,* 46**,** 11327-11335.

WAGNER, M., SCHERER, C., ALVAREZ-MUÑOZ, D., BRENNHOLT, N., BOURRAIN, X., BUCHINGER, S., FRIES, E., GROSBOIS, C., KLASMEIER, J., MARTI, T., RODRIGUEZ-MOZAZ, S., URBATZKA, R., VETHAAK, A. D., WINTHER-NIELSEN, M. & REIFFERSCHEID, G. 2014. Microplastics in freshwater ecosystems: what we know and what we need to know. *Environmental Sciences Europe,* 26**,** 12.

WEBER, A., SCHERER, C., BRENNHOLT, N., REIFFERSCHEID, G. & WAGNER, M. 2018. PET microplastics do not negatively affect the survival, development, metabolism and feeding activity of the freshwater invertebrate Gammarus pulex. *Environmental Pollution,* 234**,** 181-189.

YIN, L., CHEN, B., XIA, B., SHI, X. & QU, K. 2018. Polystyrene microplastics alter the behavior, energy reserve and nutritional composition of marine jacopever (Sebastes schlegelii). *Journal of Hazardous Materials,* 360**,** 97-105.

ZIHNI, C., MILLS, C., MATTER, K. & BALDA, M. S. 2016. Tight junctions: from simple barriers to multifunctional molecular gates. *Nature Reviews Molecular Cell Biology,* 17**,** 564.

Appendix

Appendix S1 Experimental feed (Biomar)

The fish used in the Ussing-experiment were fed salmon (smolt) feed with composition described in table S1.

Table S1. Feed composition of the salmon (smolt) feed (Biomar).

Recipe No:		**A: Cont**
Raw Material Name (Allix)	%	%
Butyrat A	%	
Butyrat B	%	
Glutamat	%	
Succinat	%	
Myhra	%	
Fish Meal LT	%	10
Fish Meal SA Superprime	%	15
Fish Meal SA Krill	%	
Soya HP48, Non Gmo	%	15,015
Soya SPC	%	11,8
Sunflower Expeller, low fiber	%	0
Wheat Gluten	%	5,7
Maize Gluten	%	5
Pea Protein	%	5
Wheat	%	11,3
Fish Oil, 18 EPA+DHA	%	8,03
Rapeseed Oil, Crude	%	11,73
Vitamines, minerals and additives	%	1,864
Crystaline amino acids	%	1,159
YTTRIUM	%	0,05
Lucantin Pink, BASF	%	0,055
Water change	%	-1,703

Total		100
Analysis (Teoretisk)		
MOISTURE (%)	%	6
ENERGY - crude (MJ/kg)	MJ/kg	23,13
ENERGY - DE Salmon Std (MJ/kg)	MJ/kg	19,2
PROTEIN - crude (%)	%	45,11
Protein - DP Salmon (%)	%	39,98
FAT - crude (%)	%	23,89
ASH (%)	%	7,74
PHOSPHORUS - total (%)	%	1,18
STARCH - crude (%)	%	8,22

Appendix S2 Physiological Ringer solution

The intestinal tissue samples must be provided with moisture, energy and oxygen immediately after removal from the fish, during seromuscular peeling and the experimental period in the Ussing chamber. A physiological Ringer solution with adjusted pH (7,8) and temperature (~ 4ºC) was made as described in table S2

Add to ringer:
Glucose: 1,8 g/L
Glutamine (L-glutamine): 2,9 g/L

Table S2. Stock solutions (Stock 1 and stock 2) for the physiological Ringer-solution.

Stock 1			
Salt	**Finished ringer (mM)**	**0,5 L 10 x stock (g)**	**1L 20 x stock (g)**
NaCl	150	87,8	175,6
KCl	2,5	1,9	3,8
$CaCl_2$	2,5	2,8	5,6
$MgCl_2$*6 H_2O	1,0	2,0	4,0
Stock 2			
$NaHCO_3$	7,0	5,9	11,8
NaH_2PO_4*$2H_2O$	0,7	1,1 (0,98)	2,2
Hepes	5,0	11,9	23,8

1:10 of each stock solution is added to deionized water (50 + 450 ml) and bubbled for 10 min on ice. The solutions are mixed while still on ice and added glucose and glutamine. pH is adjusted to 7,8. Osmoloarity (mOsm) = 300 ± 10.

$NaHCO_3$ and NaH_2PO_4*$2H_2O$ is added to stock 2 if oxygen with 0,3% CO_2 is used. This is not necessary if atmospheric air is conducted in the experiment.

Appendix S3 R and PD values (Ussing chamber)

The PD and R-values for the intestinal tissue samples were monitored continuously during the acclimation and experimental period in the Ussing chamber (approximately 2 hours in total); graphically illustrated in in figure S3.A – S3.10. The graphs represent 10 of the 12 fish (F1 – F2, F5 – F12) used in the experiment. Measurements from two fish (F3 – F4) exposed to PET particles are lacking due to improper measurements. Orange (light and dark) and gray/black represents mid-and hindgut segments from the same fish.

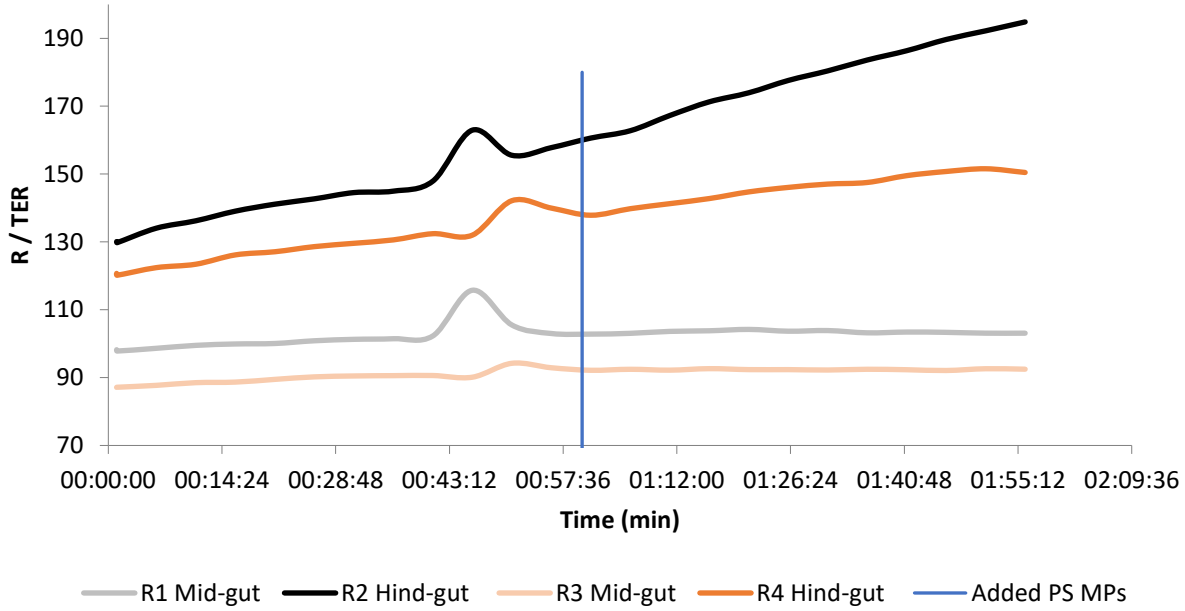

Figure S3.A. R values for mid (light orange and gray lines) and hind- (dark orange and black lines) gut segments from 2 fish (F1 and F2) exposed to 0.5 µm FluoSphere polystyrene (PS) microplastic particles in the Ussing chamber. The first hour represents the acclimation period where the intestinal segments were left in the chamber only with Ringer solution. The PS microplastic particles were added after one hour acclimation, marked with a blue, vertical line (added PS MPs). The experimental period lasted for another hour.

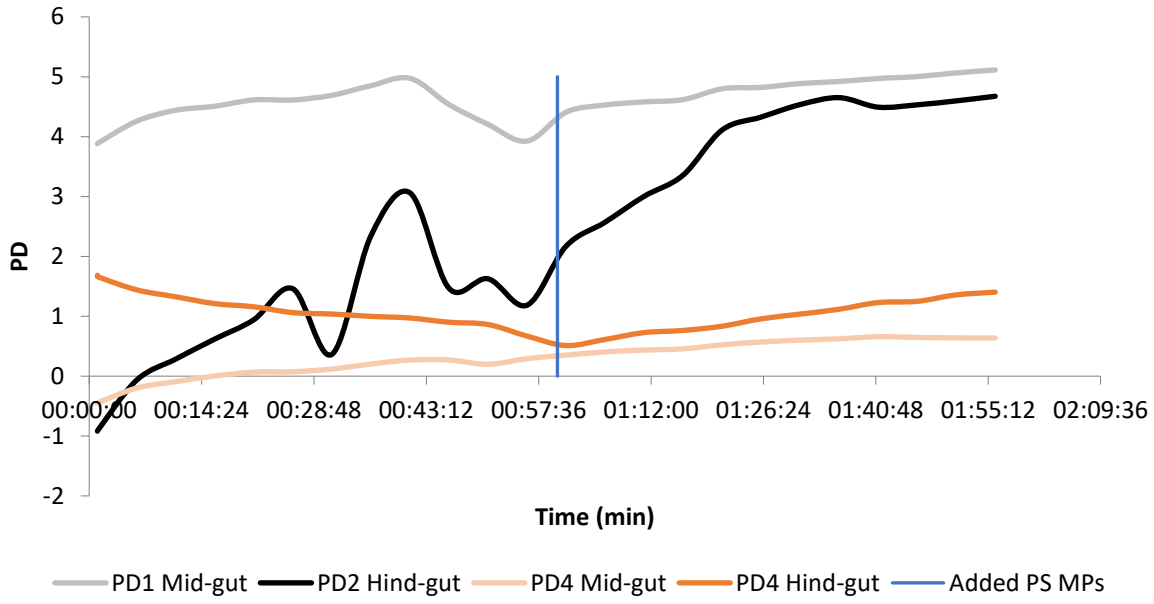

Figure S3.B. PD-values for mid (light orange and gray lines) and hind- (dark orange and black lines) gut segments from 2 fish (F1 and F2) exposed to 0.5 µm FluoSphere polystyrene (PS) microplastic particles in the Ussing chamber. The first hour represents the acclimation period where the intestinal segments were left in the chamber only with Ringer solution. The PS microplastic particles were added after one hour acclimation, marked with a blue, vertical line (added PS MPs). The experimental period lasted for another hour.

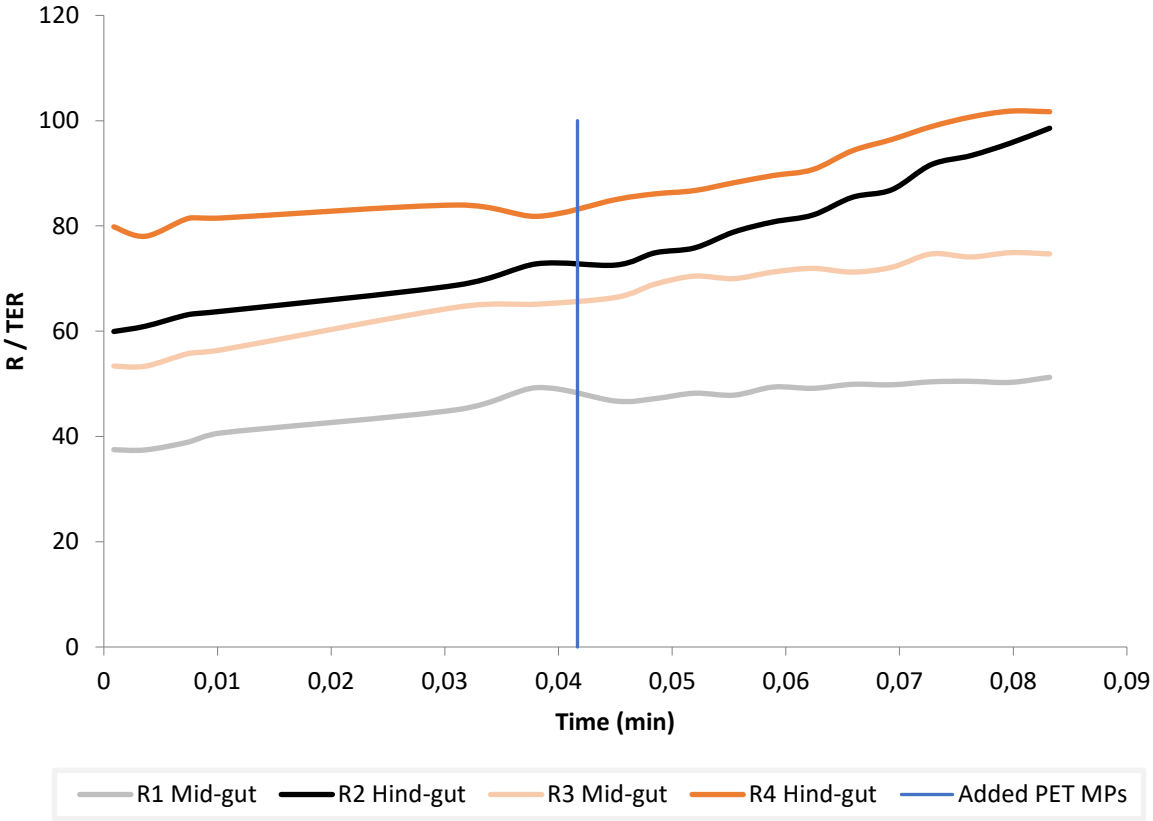

Figure S3.C. R values for mid (light orange and gray lines) and hind- (dark orange and black lines) gut segments from 2 fish (F5 and F6) exposed to Polyethylene terephthalate (PET) microplastic particles in the Ussing chamber. The first hour represents the acclimation period were the intestinal segments where left in the chamber only with Ringer solution. The PET microplastic particles were added after one hour acclimation, marked with a blue, vertical line (added PET MPs). The experimental period lasted for another hour.

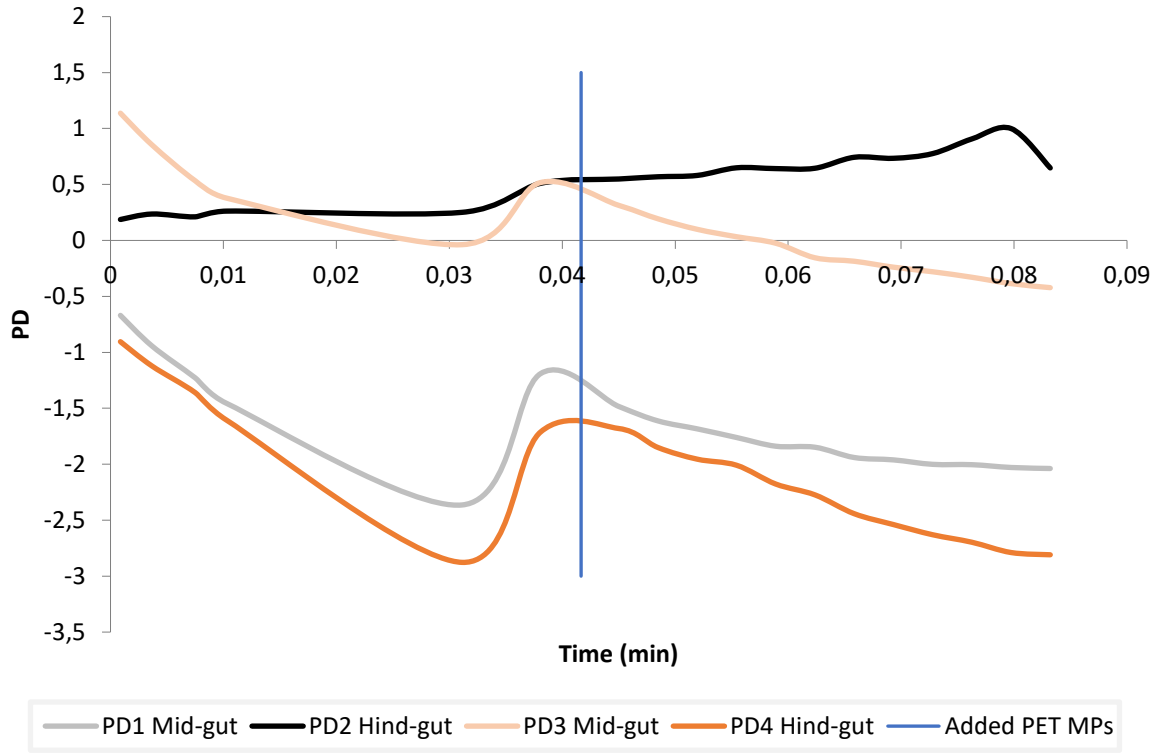

Figure S3.D. PD values for mid (light orange and gray lines) and hind- (dark orange and black lines) gut segments from 2 fish (F5 and F6) exposed to Polyethylene terephthalate (PET) microplastic particles in the Ussing chamber. The first hour represents the acclimation period where the intestinal segments were left in the chamber with Ringer solution. The PET microplastic particles were added after one hour acclimation, marked with a blue, vertical line (added PET MPs). The experimental period lasted for another hour.

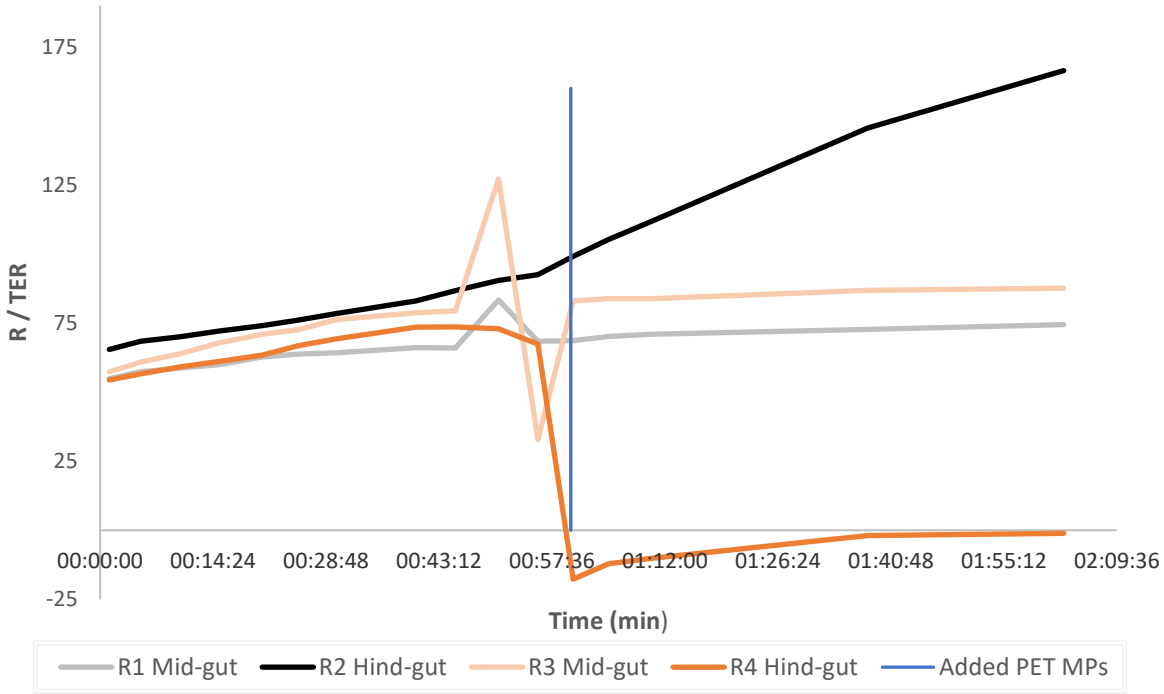

Figure S3.E. R values for mid (light orange and gray lines) and hind- (dark orange and black lines) gut segments from 2 fish (F7 and F8) exposed to Polyethylene terephthalate (PET) microplastic particles in the

Ussing chamber. The first hour represents the acclimation period where the intestinal segments were left in the chamber only with Ringer solution. The PET microplastic particles were added after one hour acclimation, marked with a blue, vertical line (added PET MPs). The experimental period lasted for another hour.

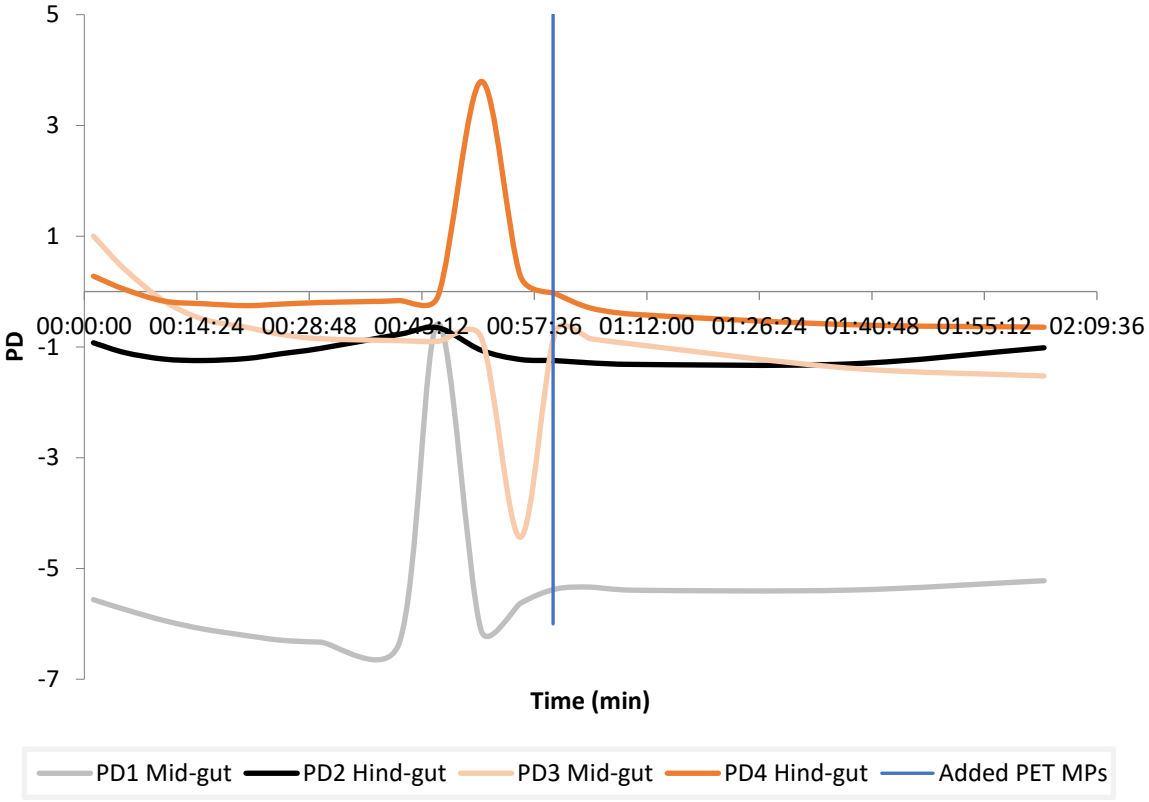

Figure S3.F. PD values for mid (light orange and gray lines) and hind- (dark orange and and black lines) gut segments from 2 fish (F7 and F8) exposed to Polyethylene terephthalate (PET) microplastic particles in the Ussing chamber. The first hour represents the acclimation period where the intestinal segments were left in the chamber only with Ringer-solution. The PET microplastic particles were added after one hour acclimation, marked with a blue, vertical line (added PET MPs). The experimental period lasted for another hour.

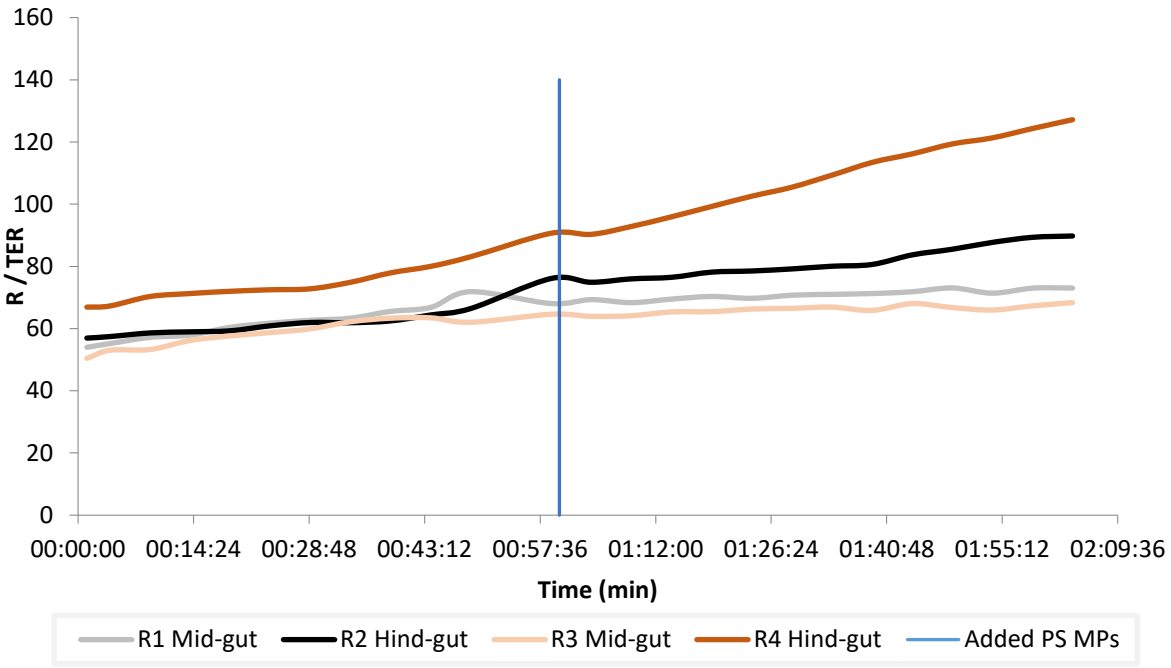

Figure S3.G. R values for mid (light orange and gray lines) and hind- (dark orange and black lines) gut segments from 2 fish (F9 and F10) exposed to 0.5 µm FluoSphere polystyrene (PS) microplastic particles in the Ussing chamber. The first hour represents the acclimation period where the intestinal segments were left in the chamber only with Ringer solution. The PS-microplastic particles were added after one hour acclimation, marked with a blue, vertical line (added PS MPs). The experimental period lasted for another hour.

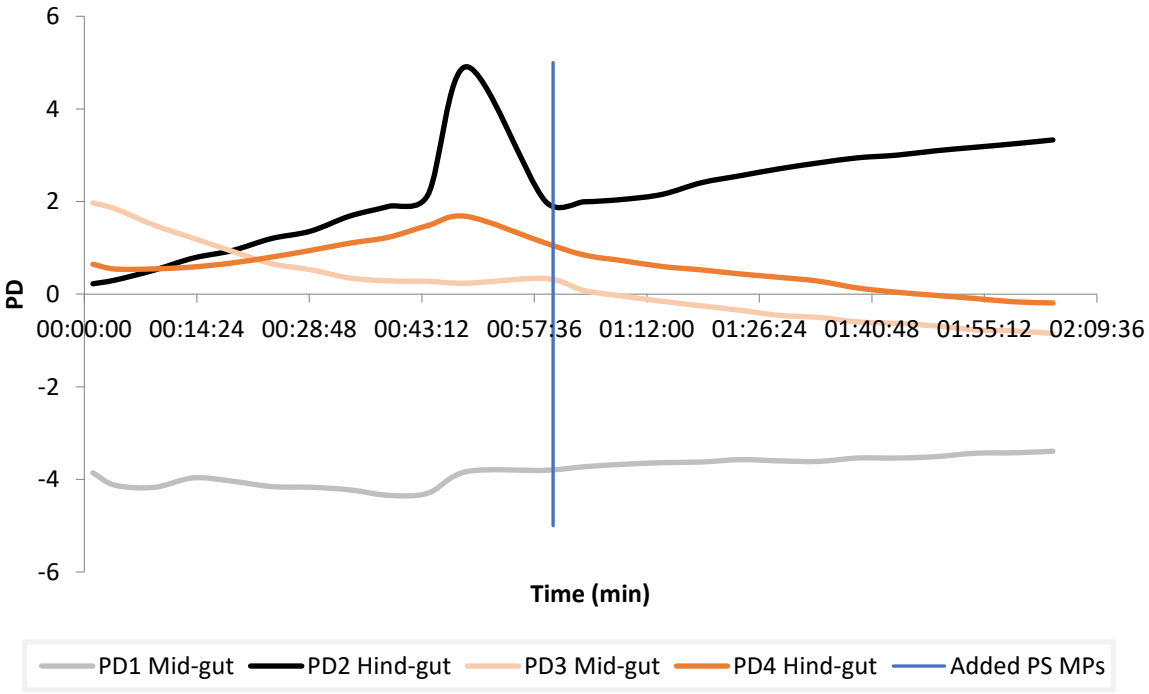

Figure S3.H. PD values for mid (light orange and gray lines) and hind- (dark orange and black lines) gut segments from 2 fish (F9 and F10) exposed to 0.5 µm FluoSphere polystyrene (PS) microplastic particles in the Ussing chamber. The first hour represents the acclimation period where the intestinal segments were left in the chamber only with Ringer solution. The PS microplastic particles were added after one hour acclimation, marked with a blue, vertical line (added PS MPs). The experimental period lasted for another hour.

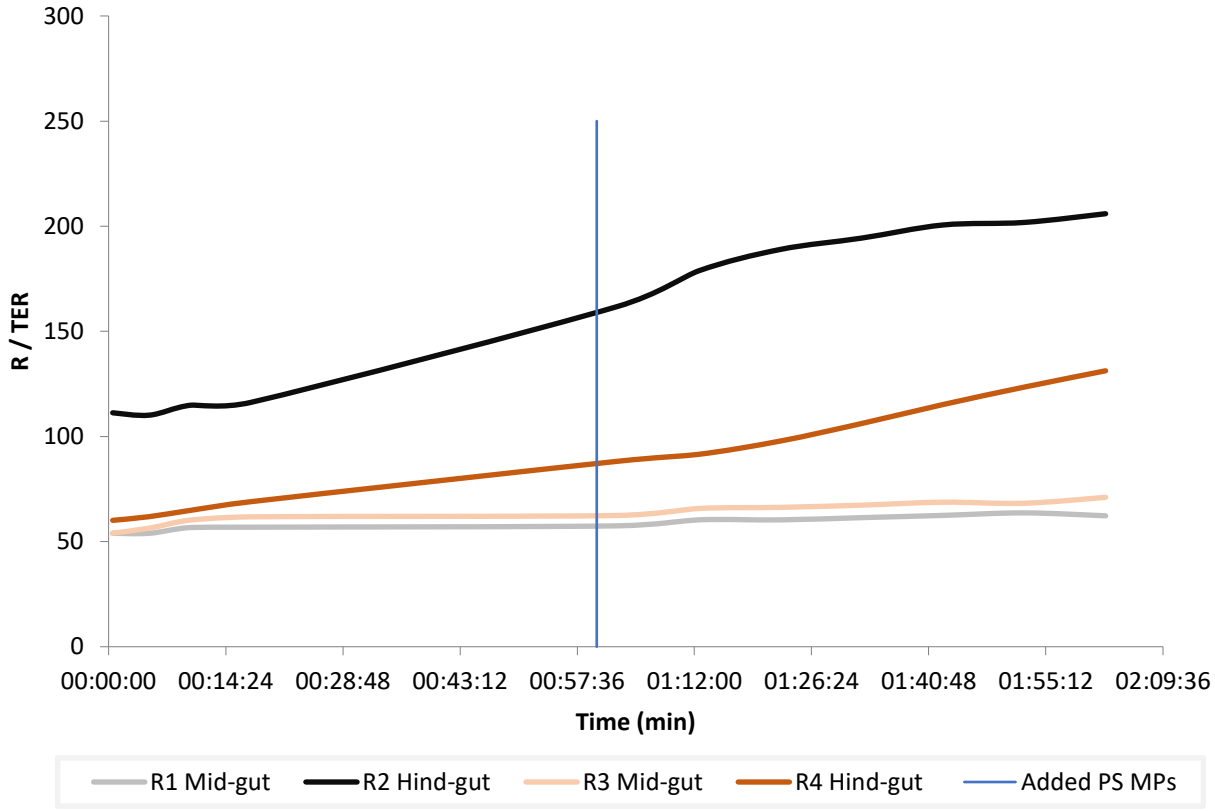

Figure S3.I. R values for mid (light orange and gray lines) and hind- (dark orange and black lines) gut segments from 2 fish (F11 and F12) exposed to 0.5 µm FluoSphere polystyrene (PS) microplastic particles in the Ussing chamber. The first hour represents the acclimation period where the intestinal segments were left in the chamber only with Ringer solution. The PS microplastic particles were added after one hour acclimation, marked with a blue, vertical line (added PS MPs). The experimental period lasted for another hour.

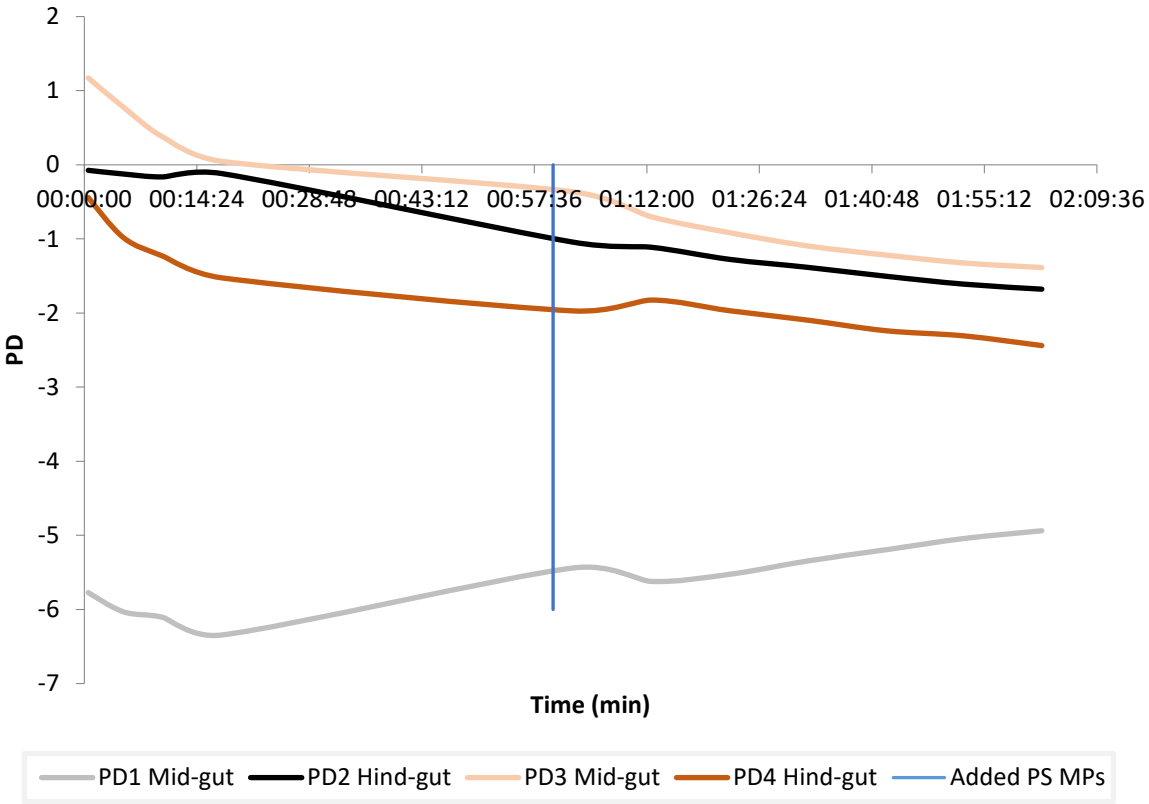

Figure S3.J. PD values for mid (light orange and gray lines) and hind- (dark orange and black lines) gut segments from 2 fish (F11 and F12) exposed to 0.5 µm FluoSphere polystyrene (PS) microplastic particles in the Ussing chamber. The first hour represents the acclimation period where the intestinal segments were left in the chamber only with Ringer solution. The PS microplastic particles were added after one-hour acclimation, marked with a blue, vertical line (added PS MPs). The experimental period lasted for another hour.

Appendix S4 Microassay

An attempted standard curve was made for the microassay analysis. Series of dilutions were made based on the concentration of 40 nm and 0.5 µm polystyrene (PS) nanoplastic particles added to the Ussing chamber (Table S4.A). The measured absorptions for the series of dilutions (Table S4.B) and standard curve (Figure S4.A) for the 0.5 µm PS particles was made to detect the concentrations of 0.5 µm PS particles in the Ussing chamber after 5 min exposure. The calculated concentrations are presented in table S4.C based on the standard curve.

Table S4.A. Series of dilutions of the concentrations (µl 0.5 µm and 40 nm FluoSphere Polystyrene (PS)-particles / 200 µl Ringer) used to make a standard curve. M (18.75) is the concentration of PS-particles used in the Ussing experiment.

Mx2	37,5	-2
M	18,75	0
M/2	9,375	2
M/4	4,69	4
M/8	2,34	8
M/16	1,17	16
M/32	0,59	32

Table S4.B. Absorption (at 580 nm) for the series of dilutions of 0.5 µm and 40 nm FluoSphere Polystyrene (PS) – particles used to make a standard curve. A1, B1 and C1, etc are triplicates.

A1	**B1**	**C1**	**Mean (absorbance)**	
988,499	988,499	988,449	988,482333	Mx2
A2	**B2**	**C2**		
33,737	51,88	44,09	43,2356667	M
A3	**B3**	**C3**		
37,58	38,135	38,227	37,9806667	M/2
A4	**B4**	**C4**		
6,984	6,071	6,448	6,501	M/4
A5	**B5**	**C5**		
1,791	1,856	2,116	1,921	M/8
A6	**B6**	**C6**		
0,599	0,597	1,087	0,761	M/16
A7	**B7**	**C7**		
0,211	0,083	0,215	0,16966667	M/32

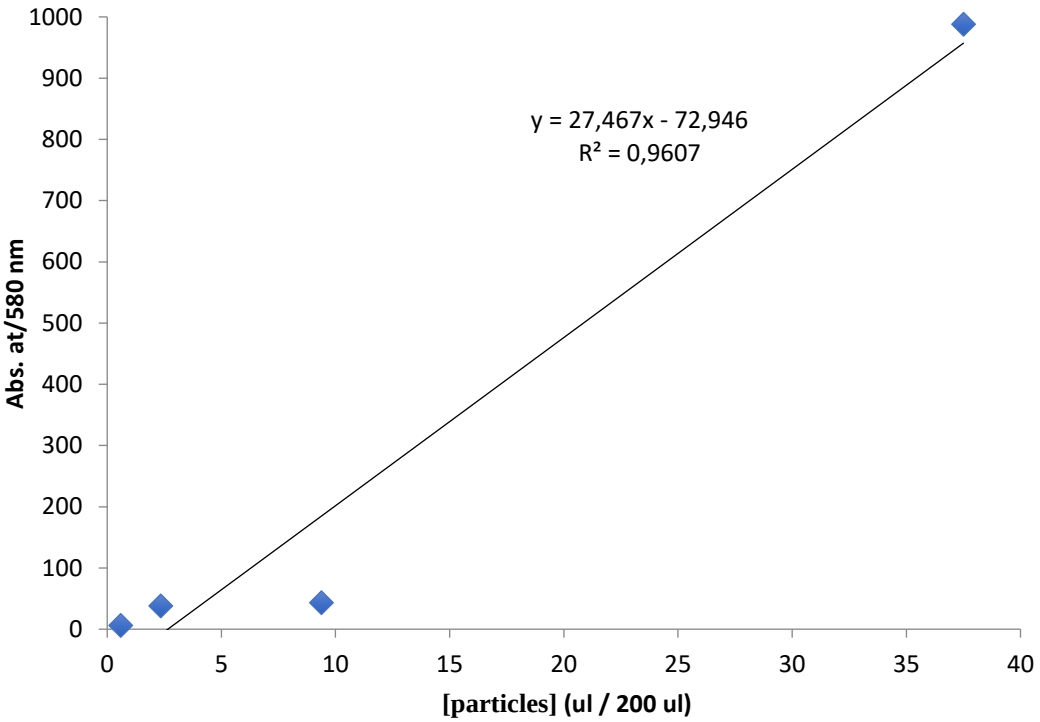

Figure S4.A. Standard curve for the concentration of 0.5 µm FluoSphere Polystyrene (PS) microplastic particles in 200 µl Ringer at abs.580 nm. The values are based on measurements form the microassay.

Table S4.C. Microassay measurements of the absorption (at 580 nm) from the Ringer solution in the Ussing chamber exposed to 0.5 µm FluoSphere Polystyrene (PS) - microplastic particles for 10 min. Two parallels were made, and the mean value were calculated. The concentrations of particles were calculated based on the equation from the standard curve (figure S4.A) MG = Midgut, HG = Hindgut. M = Mucosa-side (donor chamber), S = serosa side (receiver-chamber). F = fish number.

	Abs				**Concentrations**	
Calculations	**Parallell I**	**Parallell II**	**Mean**		**y=27,467x - 72,946**	
F1 MG M	122,211	39,042	80,6265		5,59116394	
F1 MG S	0,713	0,339	0,526		2,67491899	
F1 HG M	30,107	20,387	25,247		3,57494448	
F1 HG S	-0,21	-0,141	-0,1755		2,64937926	
F2 MG M	47,643	28,539	38,091		4,04256016	
F2 MG S	-0,501	-0,02	-0,2605		2,64628463	
F2 HG M	0,223	0,035	0,129		2,66046529	
F2 HG S	0,218	1,028	0,623		2,6784505	
F9 MG M	1,675	2,568	2,1215		2,73300688	
F9 MG S	-0,756	-1,16	-0,958		2,62089052	
F9 HG M	279,353	257,942	268,6475		12,4365056	
F9 HG S	-0,452	-0,711	-0,5815		2,63459788	
F10 MG M	4,858	4,122	4,49		2,81923763	
F10 MG S	-0,851	-0,937	-0,894		2,62322059	

F10 HG M	161,162	58,309	109,7355		6,65094477	
F10 HG S	-1,287	1,167	-0,06		2,6535843	
F11 MG M	32,241	36,175	34,208		3,90119052	
F11 MG S	-0,835	-0,134	-0,4845		1,83	
F11 HG M	29,644	34,246	31,945		3,81880074	
F11 HG S	-1,074	-1,187	-1,1305		2,61461026	
F12 MG M	58,137	64,699	61,418		4,89183384	
F12 MG S	-0,392	-0,271	-0,3315		2,64369971	
F12 HG M	15,672	18,6	17,136		2,47	
F12 HG S	-1,209	-1,075	-1,142		2,61419158	

Appendix S5 Supplementary data – experimental fish (feeding exp.)

Weight (g) and length (cm) of the experimental (n=31) and control (n=30) fish by arrival to SeaLab (before feeding) are presented in table S5.A. Temperature (T) and O_2- concentrations were continuously monitored during the whole period, from arrival of fish to SeaLab until sampling. Temperature and O_2-concentration measurements are presented in table S5.B with mean T and O2, and standard deviation.

Table S5.A. Weight (g) and length (cm) of the experimental (E, n=31, yellow) and control (n = 30, orange) fish by arrival to SeaLab before start on the feeding period. Mean weight and length (*mean)*, and standard deviation (*Std.)* are calculated for each group and in total for all fish (marked in blue).

Fish nr (E).	**Weight (g)**	**Length (cm)**	**Fish nr (control)**	**Weight (g)**	**Length (cm)**
1	115	18,9	**1**	167	23
2	65,3	16,2	**2**	106	19,5
3	119	21,2	**3**	77	16
4	133	21	**4**	119,5	20,5
5	86,2	18,9	**5**	113	19
6	144,4	22,4	**6**	174	23
7	85	18	**7**	103	19
8	75	17,5	**8**	103	19
9	67	16,5	**9**	142	22
10	89	19	**10**	73	17
11	88	18,5	**11**	114	20
12	104	19	**12**	97	18
13	73	17	**13**	119	20
14	79	17,5	**14**	68	16,5
15	75	17	**15**	112	20
16	113	19,5	**16**	102	19
17	97,4	19	**17**	110	19,5
18	61	17,5	**18**	120,8	20
19	122,4	20,5	**19**	94	18
20	116	20	**20**	91	17,5
21	99,8	19,5	**21**	88,3	18
22	82	18	**22**	70	17
23	81	18	**23**	65	16,5
24	142	22	**24**	78	17
25	118	20,5	**25**	62	15,5
26	106	19	**26**	109	19,5
27	107	20	**27**	101	18
28	109	19	**28**	176	22,5
29	93	18	**29**	77	17
30	106	19,5	**30**	81	17,5
31	63	16			
Mean	*97,2*	*18,9*		*103,8*	*18,8*
Std.	*22,9*	*1,6*		*30,2*	*2,0*
Mean total	*100,4*	*18,8*			

Std.total	*26,7*	*1,8*			

Table S5.B. Temperature (T) and O_2 – concentration (%) measurements in the fish holding tanks (experimental (yellow) and control (orange) group) from the day of arrival to SeaLab until sampling. Mean (*mean*) and standard deviation (*Std.*) are calculated for each group, and in total for all tanks (marked in blue).

Day/date	**Temp, ºC (E)**	**O_2 – cons, % (E)**	**Temp, ºC (C)**	**O_2 – cons. (C)**
20.4				
21.4				
22.4				
23.4	8,2		8,2	
24.4	8,1	96	8,1	96
25.4	8,2	96	8,2	96
26.4	8,8		8,8	
27.4	8,7	96	8,7	95
28.4	8,9		8,9	
29.4	8,9		8,8	
30.4	8,9	94	8,8	94
1.5	8,8		8,8	
2.5	8,8	94	8,7	95
3.5	8,8		8,8	
4.5	8,6		8,7	
5.5	8,8		8,8	
6.5	8,6		8,6	
7.5	8,8	90	8,8	94
8.5	8,7		8,6	
9.5	8,8	97	8,9	97
10.5	8,9		8,9	
11.5	8,8	97	8,8	96
12.5	8,9		8,8	
13.5	8,8		8,8	
14.5	8,8		8,8	
15.5	8,8		8,9	
16.5	8,8	96	8,7	97
17.5	8,9		8,9	
18.5	8,9	96	8,8	96
19.5	8,9		8,8	
20.5	8,9		8,8	
21.5	8,8	95	8,8	95
22.5	8,9		8,9	
23.5	8,9	95	8,9	95
24.5	8,7	97	8,9	95,4
25.5	8,8	98	8,8	98
26.5	8,9	100	8,9	98
27.5	-	-	-	-
28.5	8,9	99	8,8	98
29.5	-	-	-	-
Mean	*8,8*	*96,0*	*8,7*	*96,0*

Std.	*0,2*	*2,3*	*0,2*	*1,3*
Mean total	*8,8*	*96,0*		
Std. total	*0,0*	*0,8*		

Appendix S6 Hemacolor blood smear staining

The Hemacolor blood smear staining protocol (Hemacolor® Rapid staining of blood smear, Darmstadt, Germany) are presented in table S6.

Table S6. Hemacolor blood smear staining protocol.

Slide with air-dried smear	
Reagent 1 (Hemacolor® Solution 1)	5 x 1 sec
Reagent 2 (Hemacolor® Solution 2)	3 x 1 sec
Reagent 3 (Hemacolor® Solution 3)	6 x 1 sec
Reagent 4 (Buffer solution pH 7,2)	2 x 10 sec
Air-dry	
Mount with Noe-Mount® and cover glass	

Appendix S7 Tissue processing

The timed paraffin wax infiltration procedure used for all tissue samples are presented in table S7.

Table S7. Progamming worksheet for the paraffin wax timed procedure (Leica TP1020).

Station	Reagent	Vac	Duration
1	80% ethanol I	Vac	Until delayed start time, than 5 min
2	80 % II	Vac	1
3	96% I	Vac	1
4	96% II	Vac	1
5	100% I	Vac	1
6	100% II	Vac	1
7	TissueClear I	Vac	2
8	TissueClear II	Vac	2
9	Paraffin	Vac	2
10	Paraffin	Vac	2

Appendix S8 Fluorescent microscope – supplement data

Supplemented information about the fluorescent microscope, fluorescent filters, software and additional equipment

Microscope:
Nikon eclipse 90i with Digital Imaging Head (Nikon Corp. Tokyo, JP)
Camera: Nikon DS-Fi1 connected to DS-U2 controller (Nikon Corp. Tokyo, JP)
Objectives: xx with Differential Interference Contrast (DIC) (Nikon Corp. Tokyo, JP)

Fluorescent filters:
Nikon DFR (C148466) triband filter: excitation: 385-400nm/ 475-490nm/ 545-565nm; dichroic mirror: 435-470nm/ 500-540nm/ 570-645nm; emission: 450-465nm/ 505-535nm/ 580-620nm (Nikon Corp. Tokyo, JP)
B-2A (C82783): excitation: 450 – 490nm; dichroic mirror: 500nm; emission: 515nm Long Pass - (Nikon Corp. Tokyo, JP)
B-2E/C (C64763): excitation: 465-495nm; dichroic mirror: 505nm; emission: 515 – 555nm (Nikon Corp. Tokyo, JP)
'YFP'-filter: excitation: 575 – 595nm; dichroic mirror: 595nm; emission: 603 – 617nm (Omega optical, Brattleboro, VT, US).

Software:
Pictures: NIS-Elements Documentation v.3.22.15 (Build 738; 64bit; Nikon Corp. Tokyo, JP)
Control of cross board: Prior Test Control v. 2.03.10 (Prior, Cambridge, UK)
Calibration and control of fluorescent lamp: X-Cite Control Panel v.1.1.0 (Excelitas, Waltham, MA, US)
Control of microscope: iControl v. 2.0.0.3 (Nikon Corp. Tokyo, JP)

Additional equipment
Fluorescence lamp: X-cite exacte 200W Mercury lamp (Excelitas, Waltham, MA, US)
Cross board microscope: Proscan H101/2 (Prior) with Lie5 1P N2KV encoders (Numerik Jena, Jena, GE) for positioning
Controller cross board: Proscan II (Prior, Cambridge, UK)
DRO/controller cross board: CS152KB (Prior, Cambridge, UK)
Calibration of fluorescent lamp: X-cite XR2000 Radiometer with XP750 sensor (Excelitas, Waltham, MA, US)

Appendix S9 Fluorescent particles different filters and time-laps

Figure S9.A. and S9.B illustrate the fluorescing particles (40 nm and 0,5 µm FluoSphere Polystyrene (PS) particles and Polyethylene terephthalate (PET) particles) with fluorescent on various filters used to detect the particles with the fluorescent microscope. The 40 nm PS-particles (S9.A) were, because of their small size, not embedded in paraffin wax, but only examined under the fluorescent microscope. The PET and 0,5 um PS-particles (Figure S9.B) were embedded in paraffin and sectioned in a microtome in the same way as the experimental tissues. A timelaps function show bleaching of intestinal tissue with time in figure S9.C. Figure S9.D and E show fluorescent PET and PS particles, respectively, that do not bleach over time.

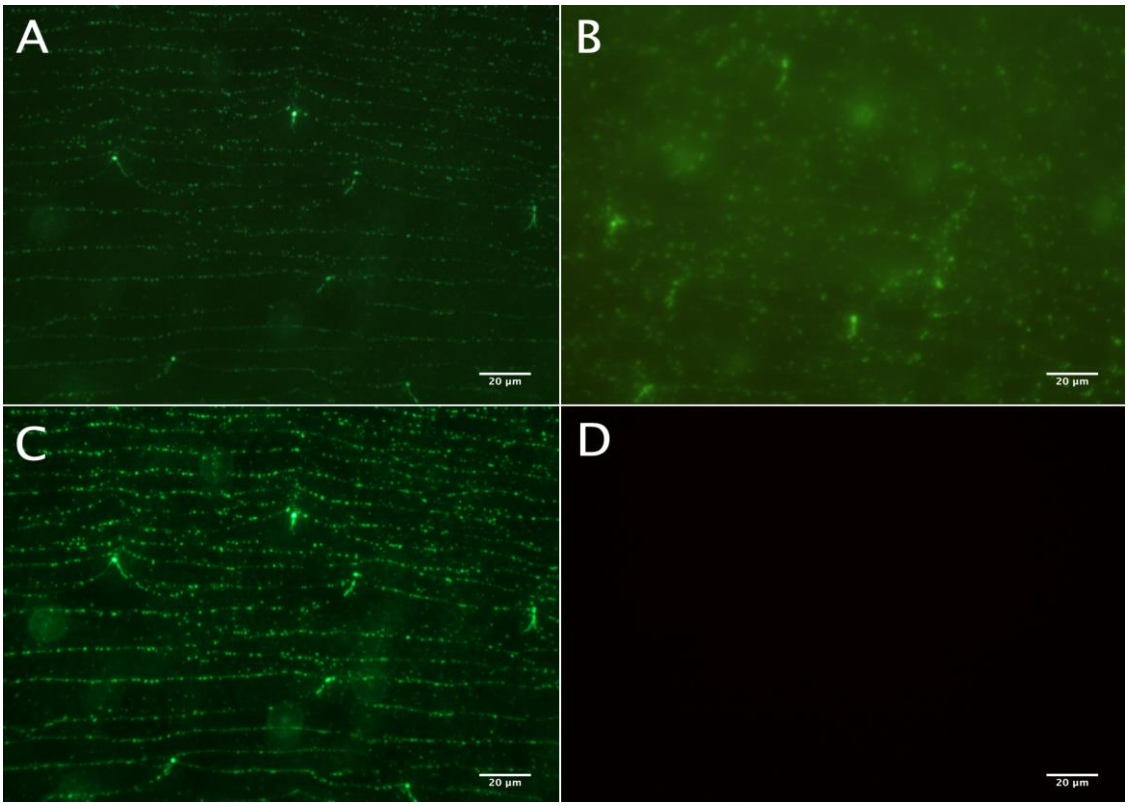

Figure S9.A. Fluorescent green FluoSphare 40 nm Polystyrene (PS) particles on different fluorescent filters: A) DFR, B) B2A and C) B2E. No fluorescence is observed on filter D) YFP. All pictures: 40x magnification

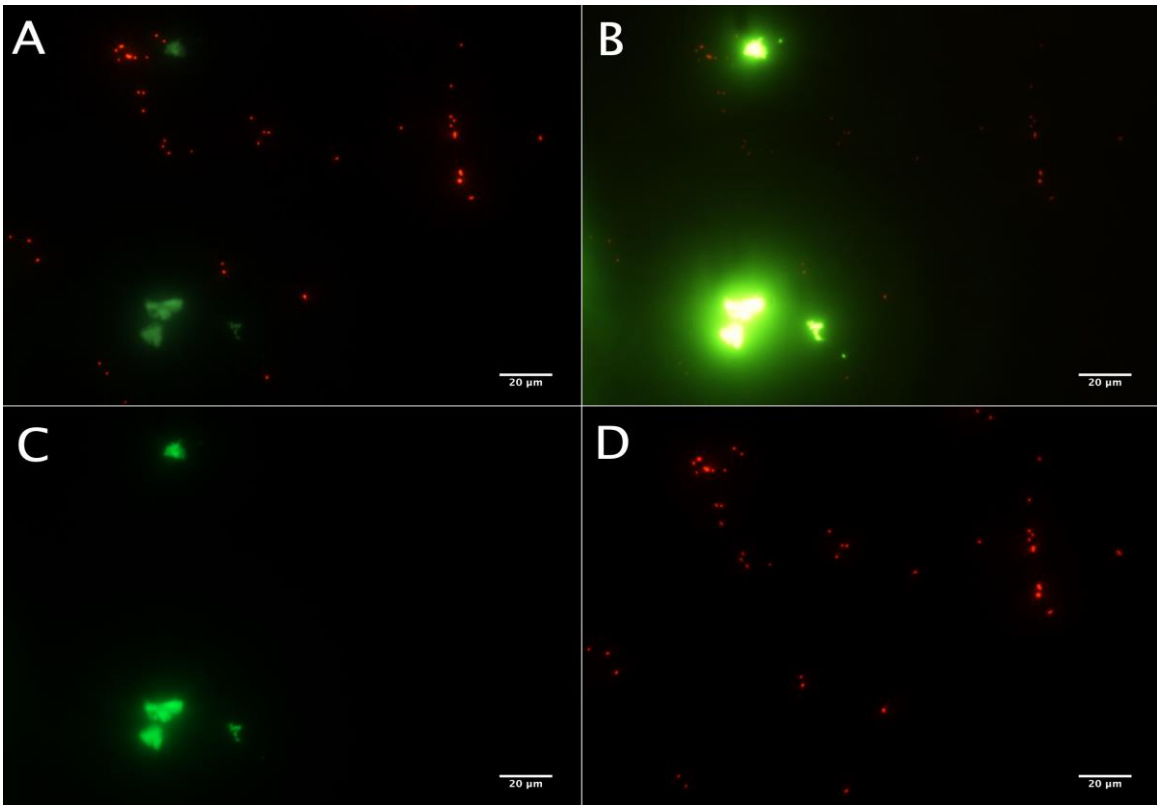

Figure S9.B. Fluorescent red 0.5 µm Polystyrene (PS) – particles fluorescing on fluorescent filters A) DFR, B) B2A and D) YFP. No fluorescence is observed on filter C) B2E. Fluorescent Polyethylene terneplate (PET) particles are visible on fluorescent filter A) DFR, B) B2A and C) B2E. No fluorescence is observed on filter D) YFP. All pictures: 40x magnification.

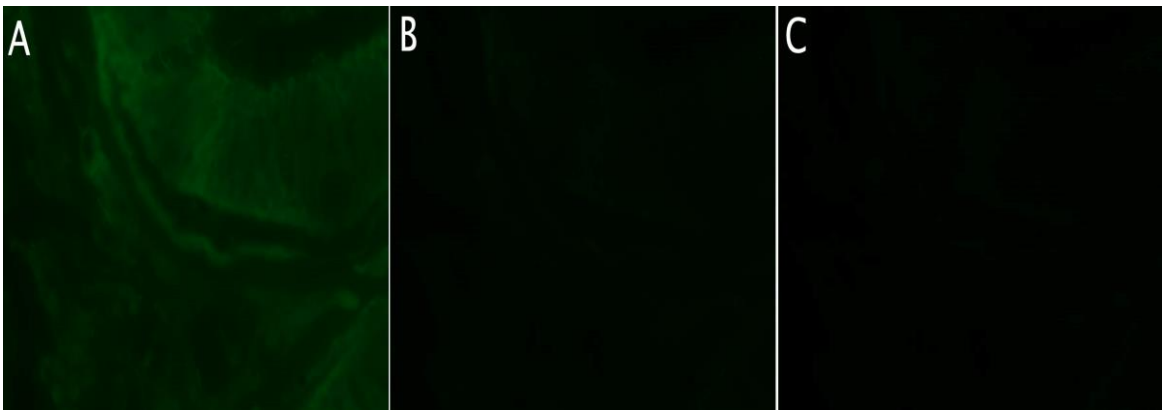

Figure S9.C. Bleaching of intestinal tissue over time using a time-laps function. Images as A: start, B: 6 min, C: 15 min. Filter B2A

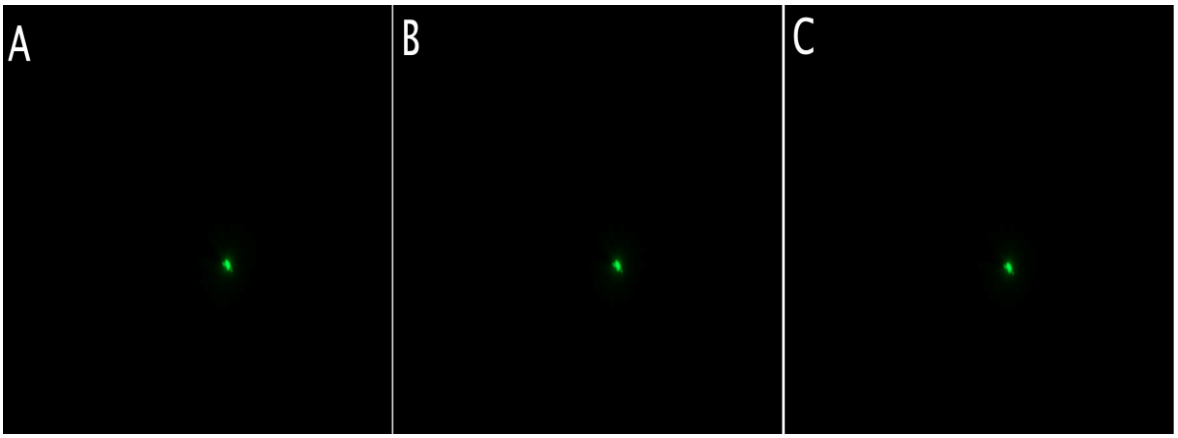

Figure S9.D. Polyethylene terephthalate (PET) particle exposed to fluorescent light over time. The particle do not bleach over time. Images at A: start, B: 6 min, C: 15 min. Filter B2A

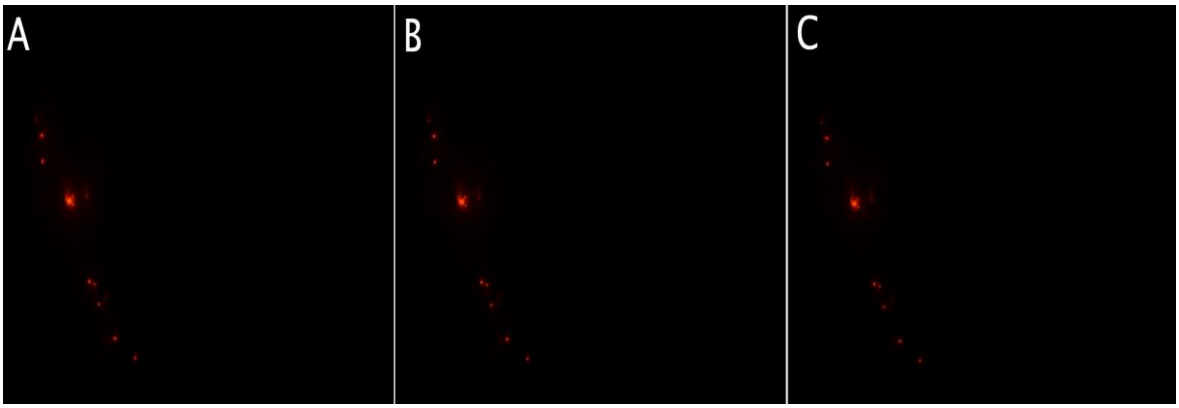

Figure S9.E. Polystyrene (PS) particles exposed to fluorescent light over time. The particles do not bleach over time. Images at A: start, B: 6 min, C: 15 min. Filter: YFP

Appendix S10 Ussing experiment – supplement data

An overview of the original and modified images of the midgut and hindgut segments exposed to polystyrene (PS) and polyethylene terephthalate (PET) particles are illustrated in figure S10.A.-E. All images contain pictures on the fluorescing filters DFR, B2A and YFP. For the modified image, a curve-function was used to enhance the contrast between the particle/background and the tissue. The change in curve is added to these images, as gray boxes in the lower left or upper right.

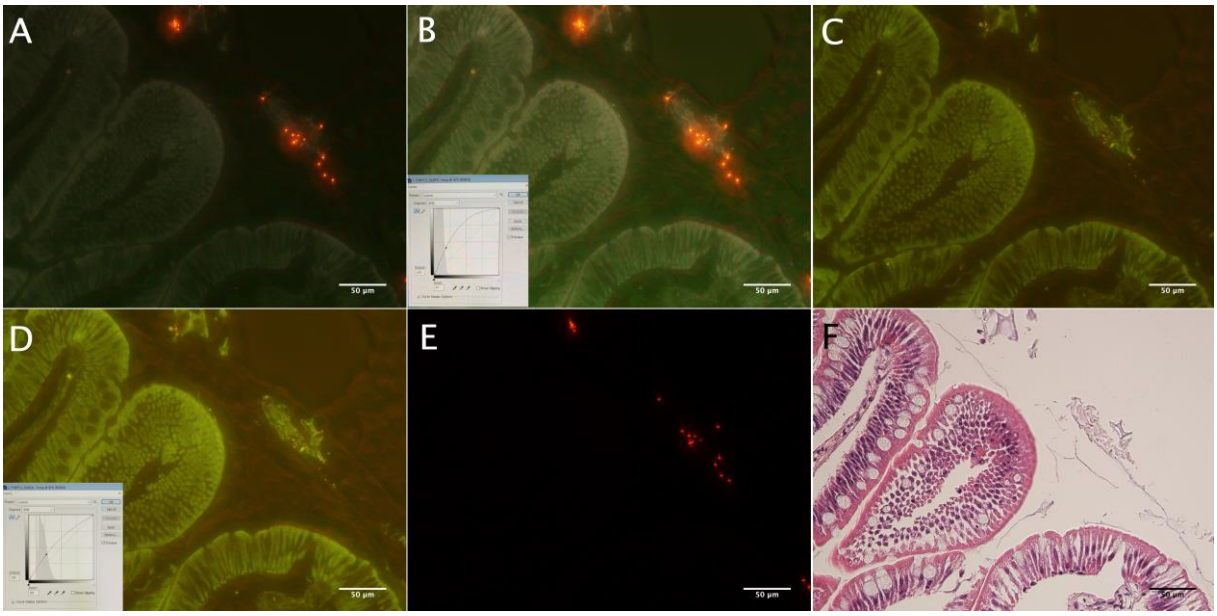

Figure S10.A. Original images of red fluorescent FluoSphere 0.5 µm Polystyrene (PS) particles in the midgut mucus layer from the Atlantic salmon (*Salmo salar*) post-smolt (A, C and E) after one hour exposure in the Ussing chamber. A curve-function (Photoshop) is used in B and D to enhance the contrast between the background/particles and the tissue. The change in curve is presented in the lower left of these pictures (gray boxes). F) The original Hematoxylin & Eosin (H&E) stained image used for overlay with YFP (E). Fluorescence filters: A - B: DFR, C - D: B2A. E: YFP. F: Light microscope (DIC). All pictures: 20x magnification.

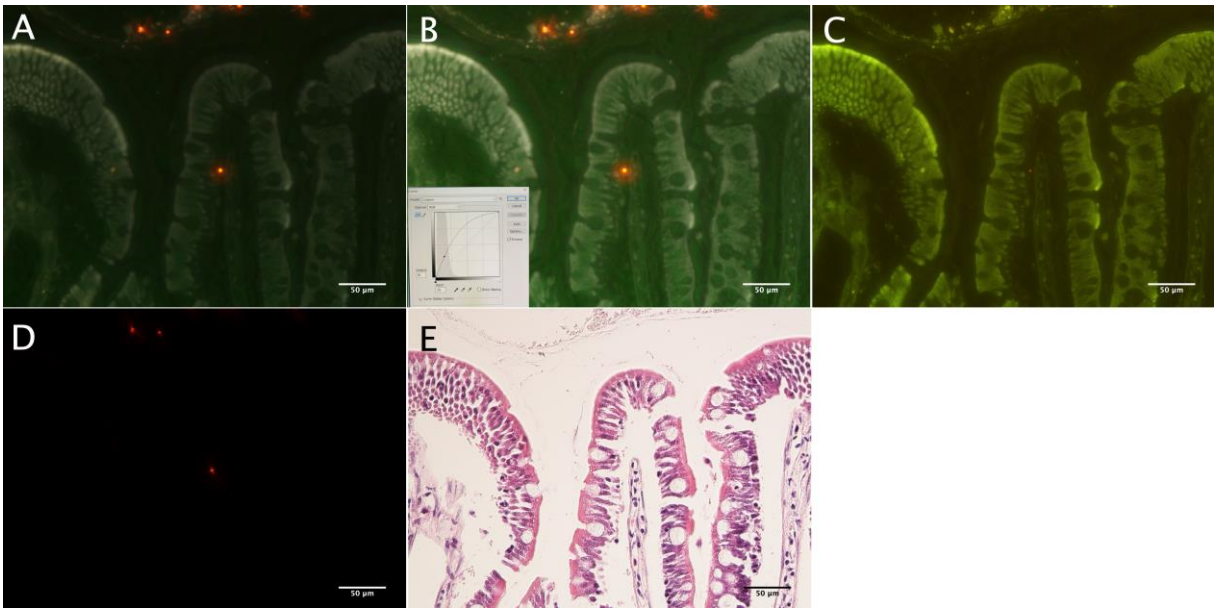

Figure S10.B. Original images of a red fluorescent FluoSphere 0.5 um Polystyrene (PS) particle in a midgut mucosal fold from the Atlantic salmon (*Salmo salar*) post-smolt after one hour exposure in the Ussing chamber (A, C and D). A curve-function (Photoshop) is used in D to enhance the contrast between the background / particle and the tissue. The change in curve is presented in the lower left of the image (gray box). E. The original Hematoxylin & Eosin (H&E) – stained picture used for overlay with YFP (D). Fluorescence filters: A - B: DFR, C: B2A, D: YFP. All pictures: 20x magnification

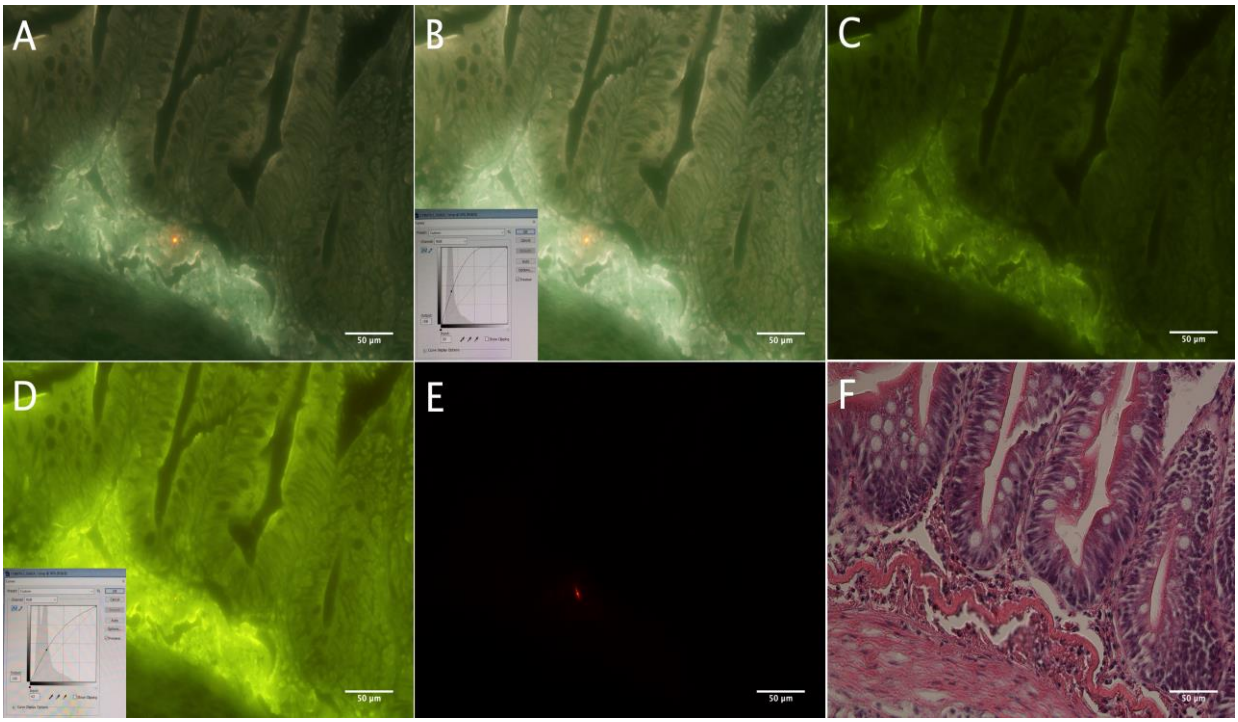

Figure S10.C. Original images of a red fluorescent FluoSphere 0.5 Polystyrene (PS) particle in lamina propria / basal end of a midgut mucosal fold in the Atlantic salmon (*Salmo salar*) post-smolt after one hour exposure in the Ussing chamber (A, C and E). A curve-function (Photoshop) is used in B and D to enhance the contrast between the background / particle and the tissue. The change in curve is presented in the lower left of these images (gray boxes). F) The original Hematoxylin & Eosin (H&E) – stained picture used for overlay with YFP (E). Fluorescence filters: A-B) DFR, C-D) B2A, E) YFP. G) Light microscope, DIC. All pictures: 20x magnification.

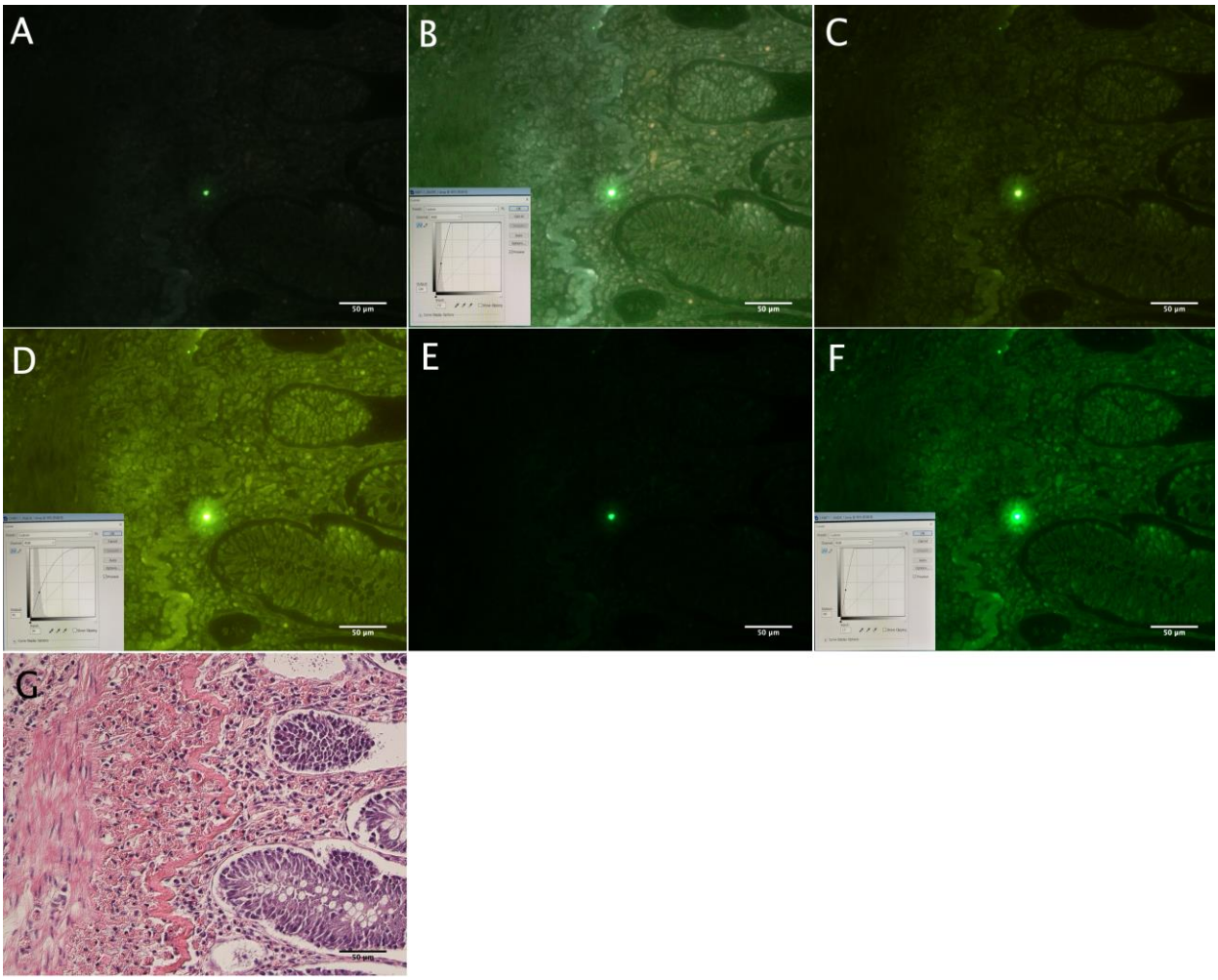

Figure S10.D. Original images of a fluorescent Polyethylene terephthalate (PET) particle stratum compactum in the hindgut of Atlantic salmon (*Salmon salar*) post-smolt after one hour exposure in the Ussing chamber (A, C, E). A curve-function (Photoshop) is used in B, D and F to enhance the contrast between the background / particle and the tissue. The change in curve is presented in the lower left of these images. G) The original Hematoxylin & Eosin (H&E) stained picture used for overlay with DFR (A). Fluorescent filters: A - B) DFR, C - D) B2A, E - F) B2E. G) Light microscope (DIC). All pictures: 20x magnification.

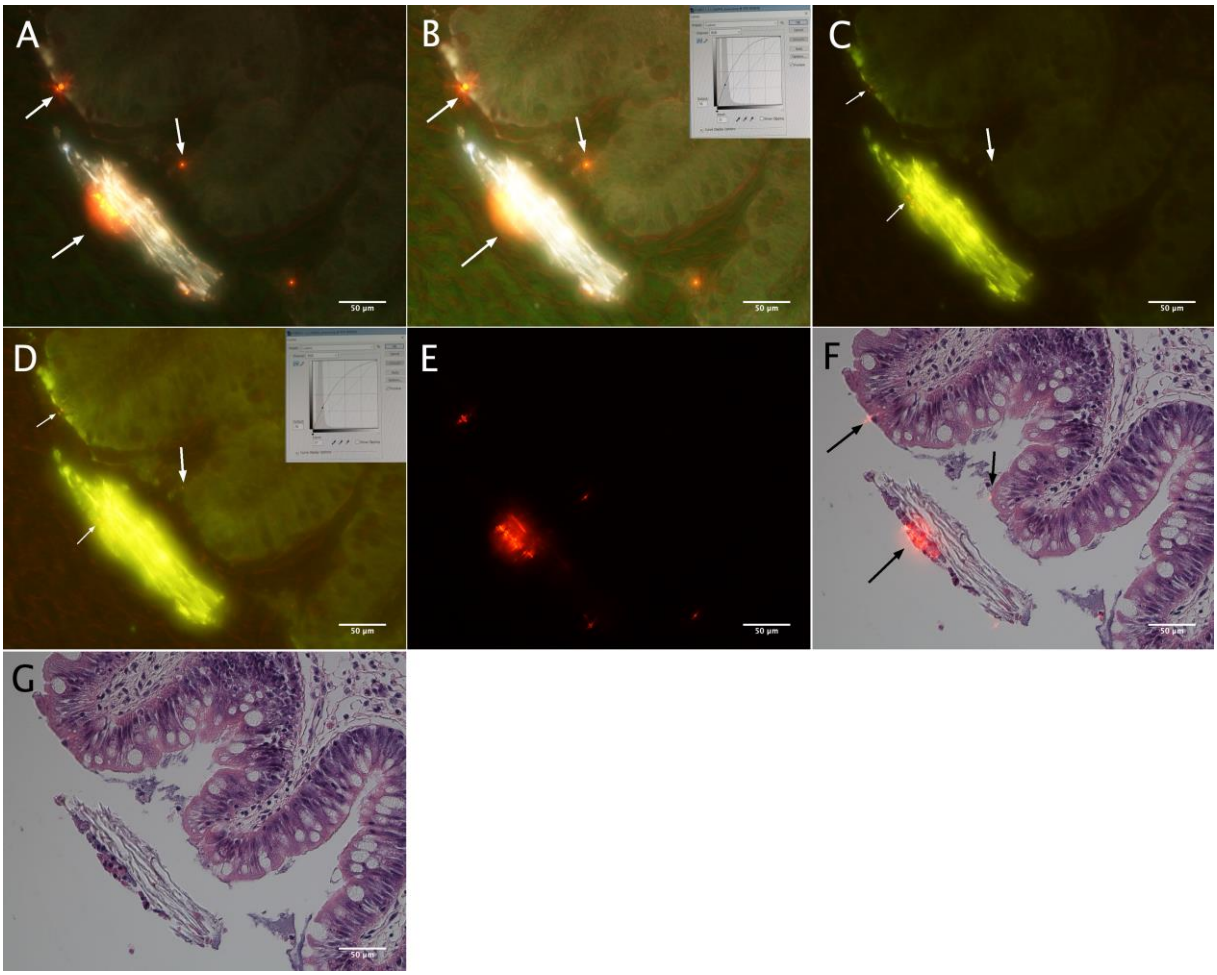

Figure S10.E. Fluorescent red 0.5 um Polystyrene (PS) particles in the hindgut luminal mucus from the Atlantic salmon (*Salmo salar*) after one hour exposure in the Ussing chamber. A, C and D are original images, while a curve-function (Photoshop) is used in B and D to enhance the contrast between the background/particles and the tissue. Changes in curve is presented in the upper right of these images (gray boxes). An overlay is made in F, by combing Hematoxylin and Eosin (H&E) stained section and picture E (YFP). The filter "Screen" (Photoshop) is used to enhance the contrast. G represents the original H&E-stained picture taken with light microscope (DIC). Fluorescent filters: A - B) DFR, C - D) B2A, E) YFP. All pictures: 20 x magnification.

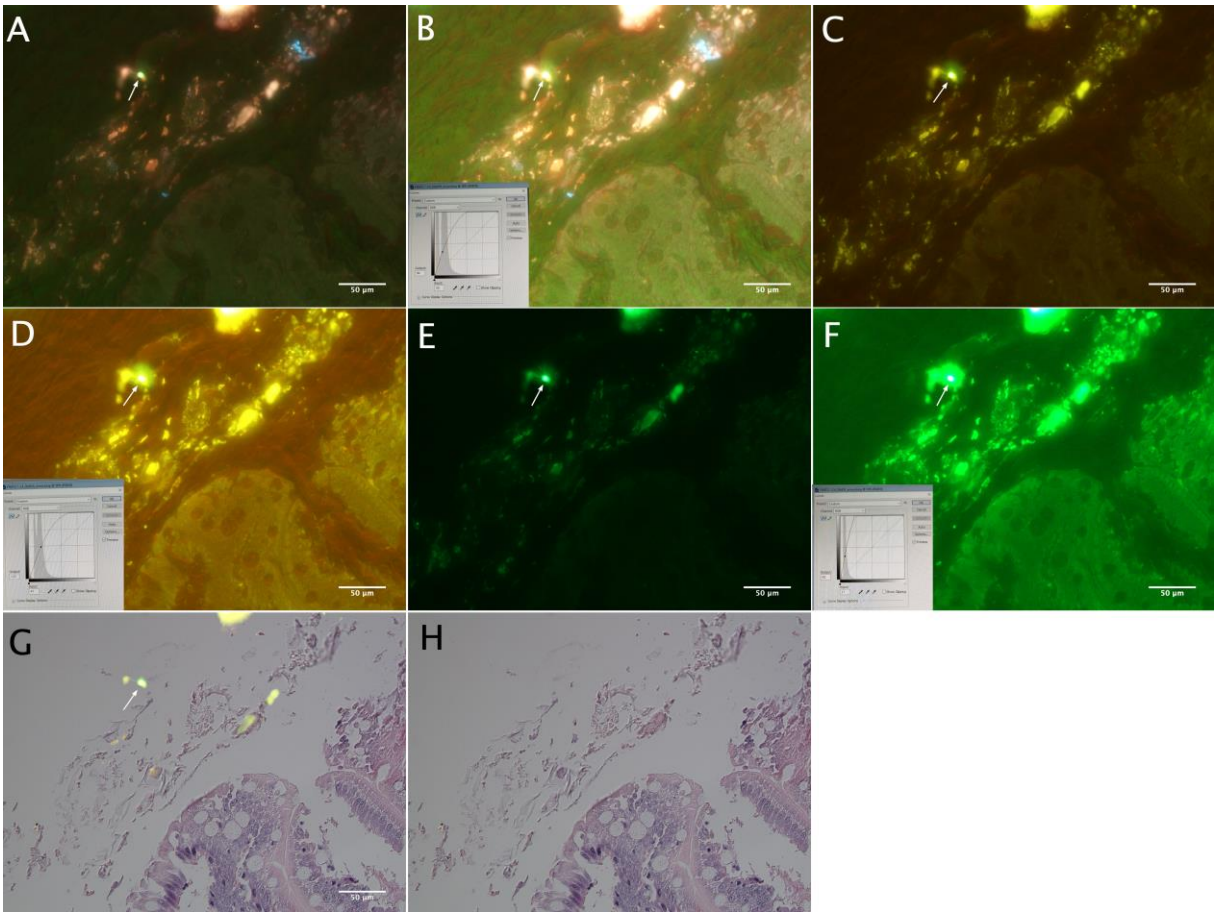

Figure S10.F. Fluorescent Polyethylene terephthalate (PET) particles in the midgut luminal mucus layer of the Atlantic salmon (*Salmo salar*) post-smolt after one hour exposure in the Ussing chamber. Original images in A, C and E, taken with fluorescence filters DFR, B2A and B2E, respectively. A curve-function (Photoshop) is used in B, D and F to enhance the contrast between the background/particles and the tissue. The change in curve is presented in the lower left of these three images (gray boxes). B, D and F are taken with fluorescent filters DFR, B2A and B2E, respectively. An overlay is made (G) between Hematoxylin & Eosin (H&E) stained section and DFR (A). The filter "Lighter" (Photoshop) is used to enhance the contrast. H) represents H&E stained section only, taken with light microscope (DIC) for overlay.

Appendix S11 Size distribution data

Size distribution data of particles 0,6 µm ≥ 18µm (not presented in results) are presented in figure S11.A.

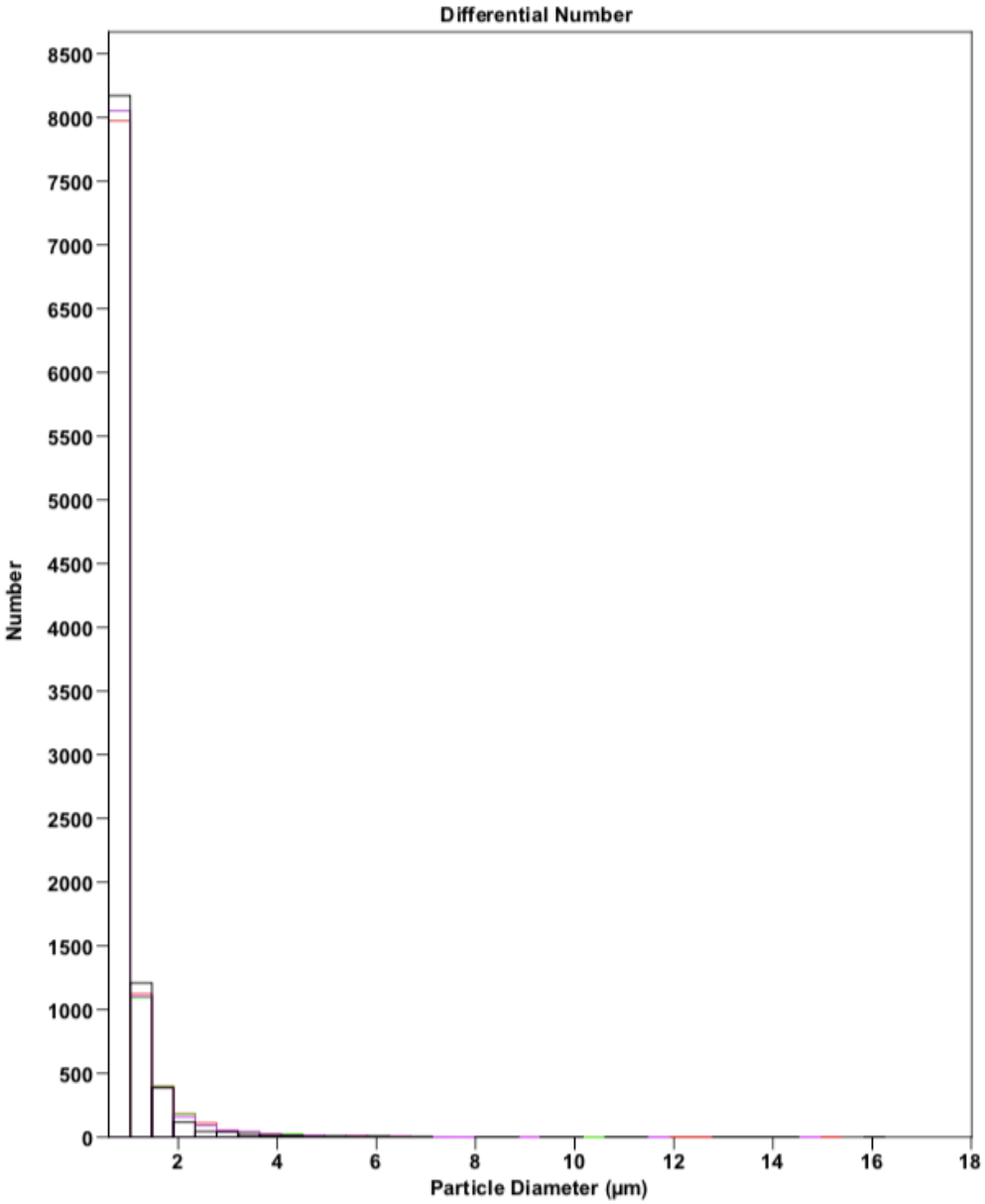

Figure S11.A. Size distribution of particles 0.6 ≥ 18 µm

Multisizer 4e data:	C:\Multisizer4e\Samples\TRUDE\Gina\siktet, un_T_ 8 Apr 2019_10-45_1.#m4		
SOM file:	C:\Multisizer4e\SOP\190408 Gina 30 µm.som (modified)		
Preference file:	C:\Multisizer4e\SOP\Default.prf		
Sample ID:	siktet, under45µm, 1µm til 18		
Operator:	TJ		
Run number:	102		
Electrolyte:	BCI ISOTON II		
Aperture:	30 µm	Kd:	44
Aperture current:	600 µA	Preamp gain:	4
Size bins:	40 from 0.6 µm to 18 µm, linear diameter		
Total count:	10081 (Coincidence corrected)		
Count > 0.6 µm:	10013	Coincidence corrected:	10095
Coincidence correction:	0.8%		
Control mode:	Total count 10000		
Elapsed time:	145.64 seconds		
Acquired:	10:40 8 Apr 2019		
Electrolyte volume:	100 mL		
Analytic volume:	2000 µL		
Sample:	1 mL		

Multisizer 4e data:	C:\Multisizer4e\Samples\TRUDE\Gina\siktet, un_T_ 8 Apr 2019_10-53_1.#m4		
SOM file:	C:\Multisizer4e\SOP\190408 Gina 30 µm.som (modified)		
Preference file:	C:\Multisizer4e\SOP\Default.prf		
Sample ID:	siktet, under45µm, 1µm til 18		
Operator:	TJ		
Run number:	103		
Electrolyte:	BCI ISOTON II		
Aperture:	30 µm	Kd:	44
Aperture current:	600 µA	Preamp gain:	4
Size bins:	40 from 0.6 µm to 18 µm, linear diameter		
Total count:	10007 (Coincidence corrected)		
Count > 0.6 µm:	10006	Coincidence corrected:	10013
Coincidence correction:	0.1%		
Control mode:	Total count 10000		
Elapsed time:	243.3 seconds		
Acquired:	10:45 8 Apr 2019		
Electrolyte volume:	100 mL		
Analytic volume:	2500 µL		
Sample:	1 mL		

Multisizer 4e data:	C:\Multisizer4e\Samples\TRUDE\Gina\siktet, un_T_ 8 Apr 2019_11-03_1.#m4		
SOM file:	C:\Multisizer4e\SOP\190408 Gina 30 µm.som (modified)		
Preference file:	C:\Multisizer4e\SOP\Default.prf		
Sample ID:	siktet, under45µm, 1µm til 18		
Operator:	TJ		
Run number:	104		
Electrolyte:	BCI ISOTON II		
Aperture:	30 µm	Kd:	44
Aperture current:	600 µA	Preamp gain:	4
Size bins:	40 from 0.6 µm to 18 µm, linear diameter		
Total count:	10006 (Coincidence corrected)		
Count > 0.6 µm:	10006	Coincidence corrected:	10012
Coincidence correction:	0.1%		
Control mode:	Total count 10000		
Elapsed time:	217.27 seconds		
Acquired:	10:54 8 Apr 2019		
Electrolyte volume:	100 mL		
Analytic volume:	3500 µL		
Sample:	1 mL		

Multisizer 4e data:	C:\Multisizer4e\Samples\TRUDE\Gina\siktet, un_T_ 8 Apr 2019_11-13_1.#m4		
SOM file:	C:\Multisizer4e\SOP\190408 Gina 30 µm.som (modified)		
Preference file:	C:\Multisizer4e\SOP\Default.prf		
Sample ID:	siktet, under45µm, 1µm til 18		
Operator:	TJ		
Run number:	105		
Electrolyte:	BCI ISOTON II		
Aperture:	30 µm	Kd:	44
Aperture current:	600 µA	Preamp gain:	4
Size bins:	40 from 0.6 µm to 18 µm, linear diameter		
Total count:	10006 (Coincidence corrected)		
Count > 0.6 µm:	10008	Coincidence corrected:	10014
Coincidence correction:	0.1%		
Control mode:	Total count 10000		
Elapsed time:	226.31 seconds		
Acquired:	11:04 8 Apr 2019		
Electrolyte volume:	100 mL		
Analytic volume:	2500 µL		
Sample:	1 mL		

Number Statistics (Arithmetic) siktet, un_T_ 8 Apr 2019_10-45_1.#m4

Calculations from 0.600 µm to 18.00 µm

Number:	10081		
Mean:	0.986 µm	95% Conf. Limits:	0.973-0.999 µm
Median:	0.868 µm	S.D.:	0.65 µm
Mode:	0.817 µm		

d_{10}: 0.654 µm d_{50}: 0.868 µm d_{90}: 1.358 µm

Number Statistics (Arithmetic) siktet, un_T_ 8 Apr 2019_10-53_1.#m4

Calculations from 0.600 µm to 18.00 µm

Number:	10007		
Mean:	1.028 µm	95% Conf. Limits:	1.013-1.042 µm
Median:	0.873 µm	S.D.:	0.73 µm
Mode:	0.817 µm		

d_{10}: 0.655 µm d_{50}: 0.873 µm d_{90}: 1.435 µm

Number Statistics (Arithmetic) siktet, un_T_ 8 Apr 2019_11-03_1.#m4

Calculations from 0.600 µm to 18.00 µm

Number:	10006		
Mean:	1.008 µm	95% Conf. Limits:	0.995-1.020 µm
Median:	0.870 µm	S.D.:	0.63 µm
Mode:	0.817 µm		

d_{10}: 0.654 µm d_{50}: 0.870 µm d_{90}: 1.413 µm

Number Statistics (Arithmetic) siktet, un_T_ 8 Apr 2019_11-13_1.#m4

Calculations from 0.600 µm to 18.00 µm

Number:	10006		
Mean:	1.008 µm	95% Conf. Limits:	0.996-1.020 µm
Median:	0.870 µm	S.D.:	0.62 µm
Mode:	0.817 µm		

d_{10}: 0.654 µm d_{50}: 0.870 µm d_{90}: 1.408 µm

Appendix S12 Feeding experiment – supplement data

An overview of the original and modified images of the midgut, hindgut, blood smears and liver section from Atlantic salmon (*Salmo salar*) parr exposed to polyethylene terephthalate (PET) particles are illustrated in figure S12.A.-F. All images contain pictures on the fluorescing filters DFR, B2A and B2E. For the modified image, a curve-function was used to enhance the contrast between the particle/background and the tissue. The change in curve is added to these images, as gray boxes in the lower left or upper right.

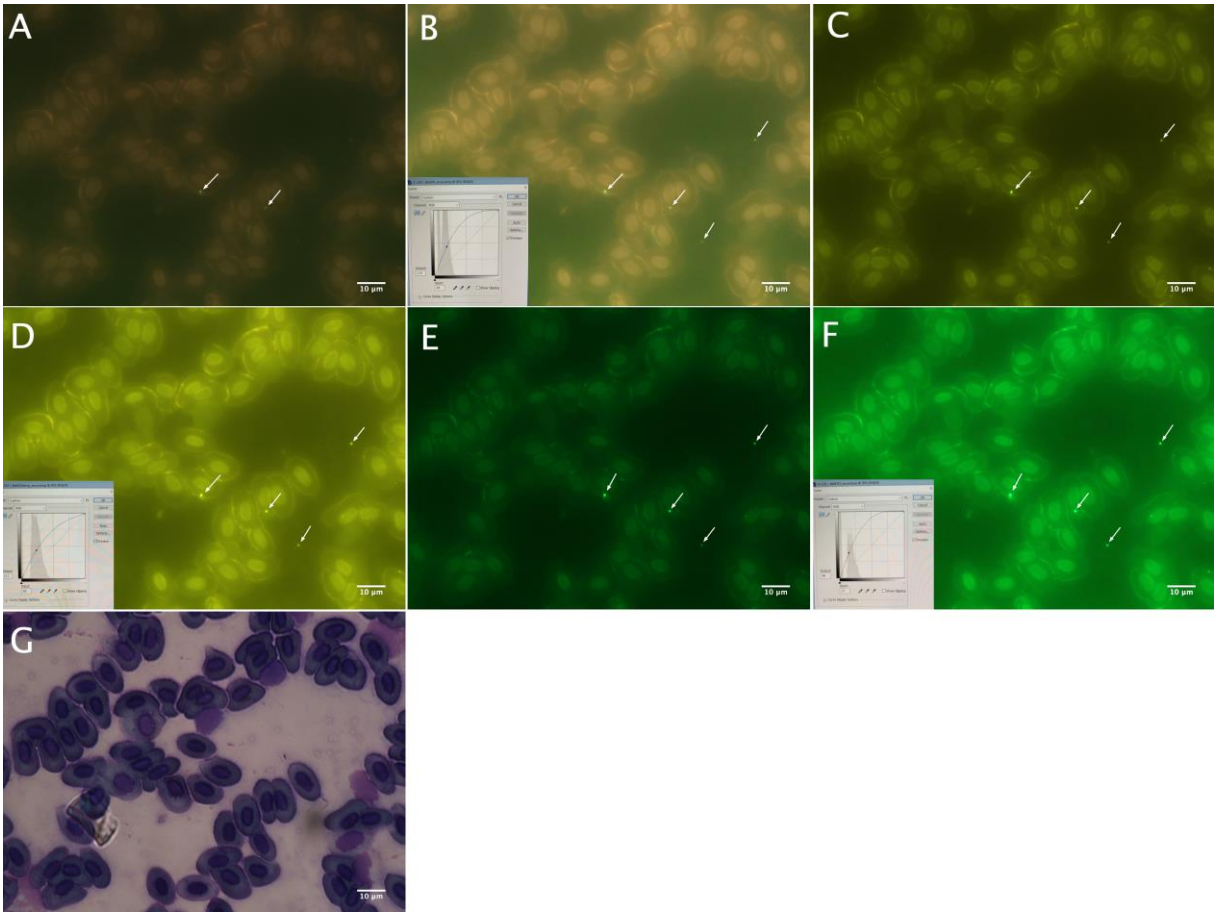

Figure S12.A. Original fluorescent Polyethylene terephthalate (PET) particles in a blood sample from the Atlantic salmon (*Salmo salar*) parr (A, C and E). A curve-function (Photoshop) is used to enhance the contrast in B, D and F. Changes in curve is presented in the lower left of these pictures (gray boxes). G) The original Hemacolor stained section used to make overlay with DFR (A). Fluorescence filters: A-B: DFR, C-D: B2A, E-F: B2E. G: light microscope, DIC. All pictures: 60x magnification.

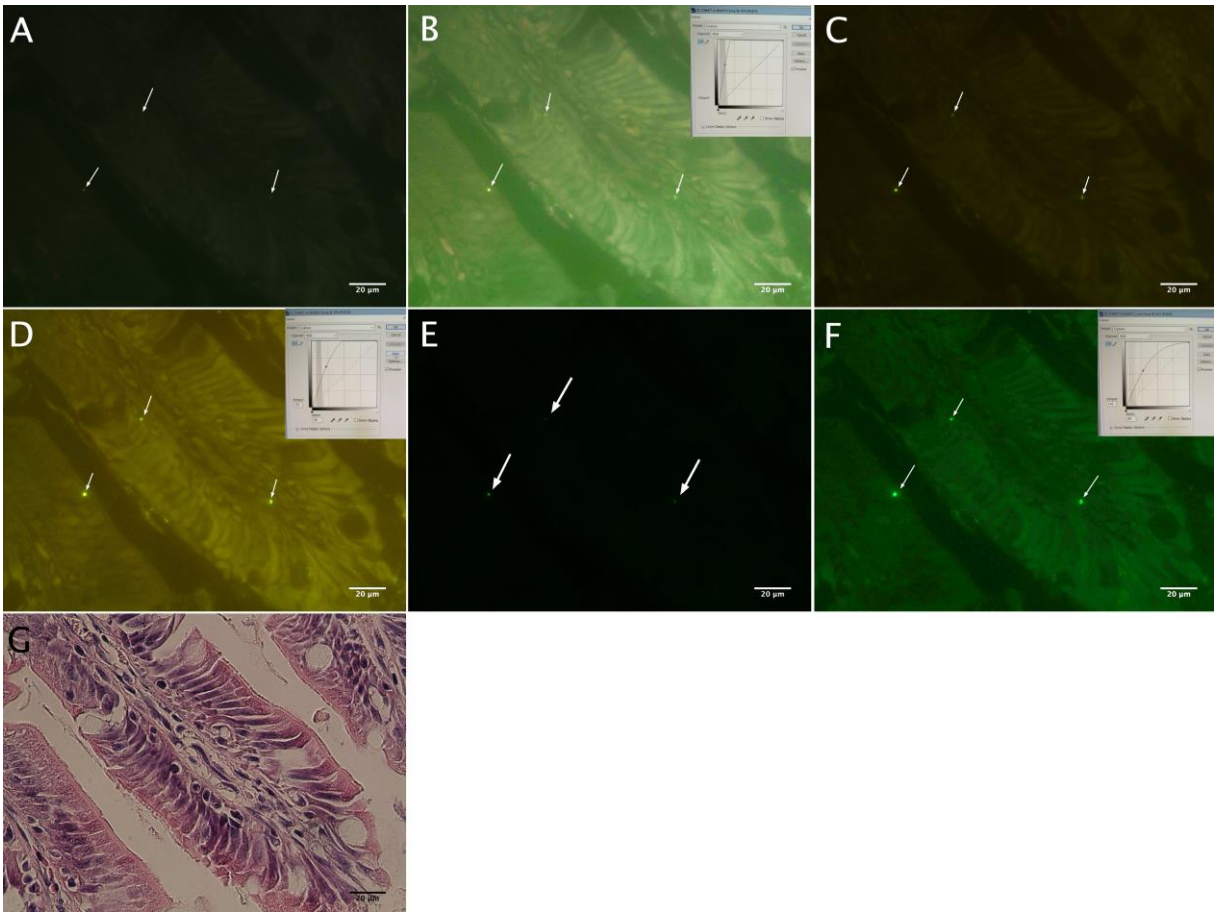

Figure S12.B. Original images of fluorescent Polyethylene terephthalate (PET) particles in two midgut mucosal folds of the Atlantic salmon (*Salmo salar*) parr, illustrated in A, C and E. A curve-function (Photoshop) is used to enhance the contrast between the background / particles and the tissue in B, D and F. Change in curve is presented in the upper right of these three images (gray boxes). G) is the original Hematoxylin & Eosin (HE) – stained section used for overlay with DFR (B). Fluorescence filters: A - B: DFR, C - D: B2A, E - F: B2E. G: light microscope (DIC). All pictures: 40x magnification

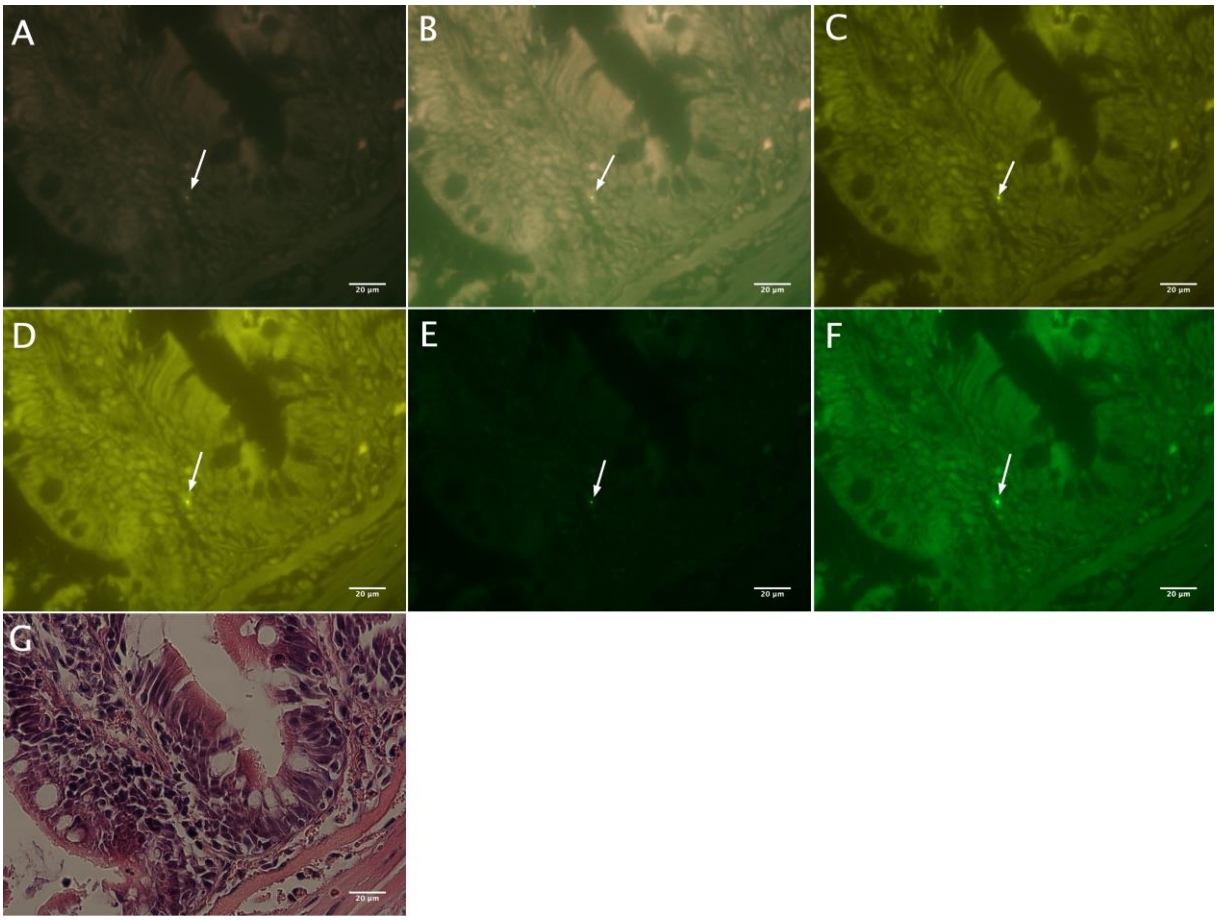

Figure S12.C. Original images of a fluorescent Polyethylene terephthalate (PET) particle in lamina propria / the basal end of a midgut mucosal fold of the Atlantic salmon (*Salmo salar*) parr (A, C and E). A curve-function (Photoshop) is used to enhance the contrast between the background / particles and the tissue. (Curve-modifications not available). G) The original Hematoxylin & Eosin (H&E) – stained section used for overlay with DFR (B). Fluorescent filters: A – B: DFR, C – D: B2A, E – F: B2E. G: light microscope (DIC).

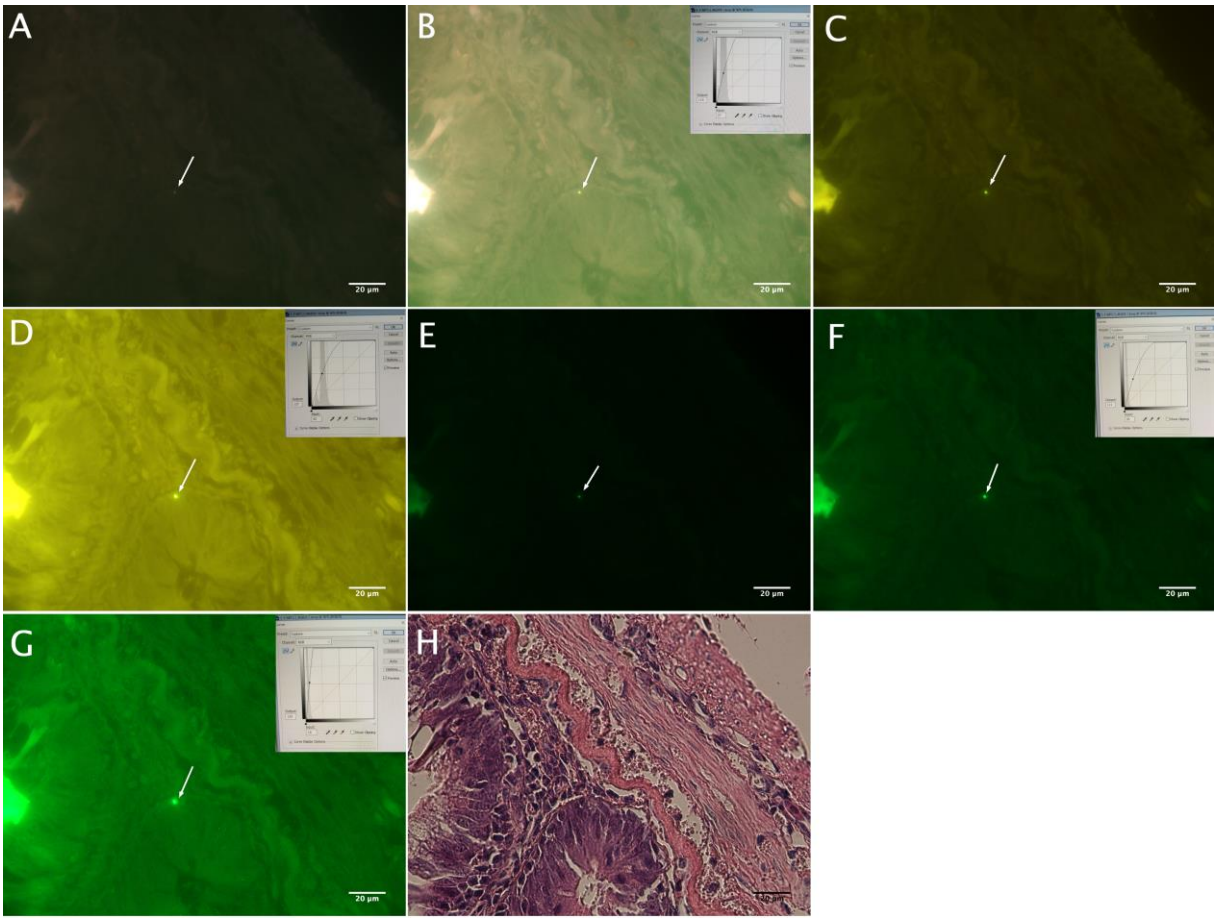

Figure S12.D. Original images of a fluorescent Polyethylene terephthalate (PET) particle in lamina propria / basal end of a hindgut mucosal fold from the Atlantic salmon (*Salmo salar*) parr (A, C and E). A curve-function (Photoshop) is used to enhance the contrast between the background / particle and the tissue in B, D, F and G. The change in curve is presented in the upper right of these images (gray boxes). F was used to make overlay with the original Hematoxylin & Eosin (H&E) – stained section (H). Fluorescence filters: A – B: DFR, C – D: B2A, E – F: B2E. H: light microscope (DIC).

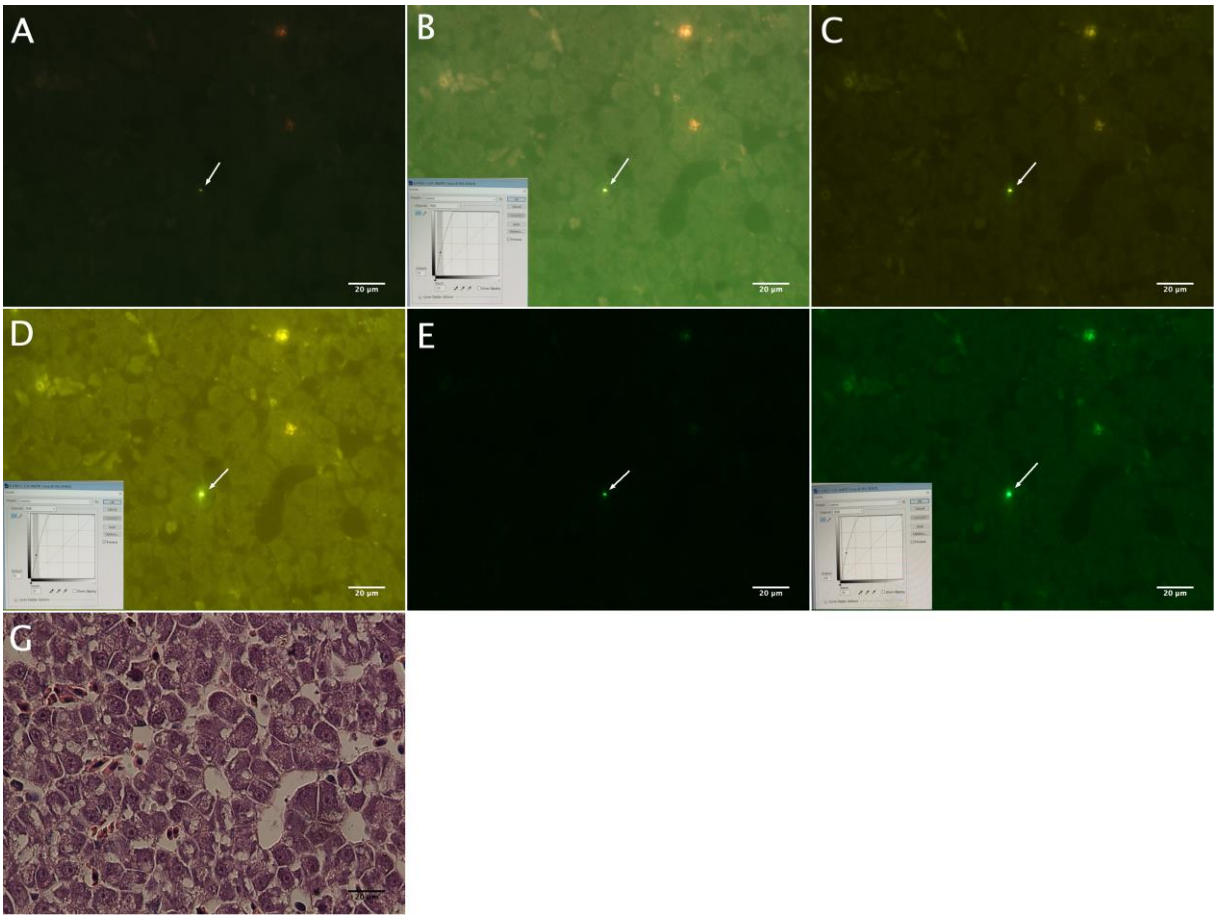

Figure S12.E. Original images of a fluorescent Polyethylene terephthalate (PET) particle in liver of the Atlantic salmon (*Salmo salar*) parr (A, C and E). A curve-function (Photoshop) is used to enhance the contrast between the background/particle and tissue in B, D and F. The change in curve is presented in the lower left of these pictures (gray boxes). G) is the original Hematoxylin & Eosin (H&E) – stained section used to make overlay with DFR. Fluorescent filters: A – B: DFR, C – D: B2A, E – F: B2E. G) light microscope (DIC).

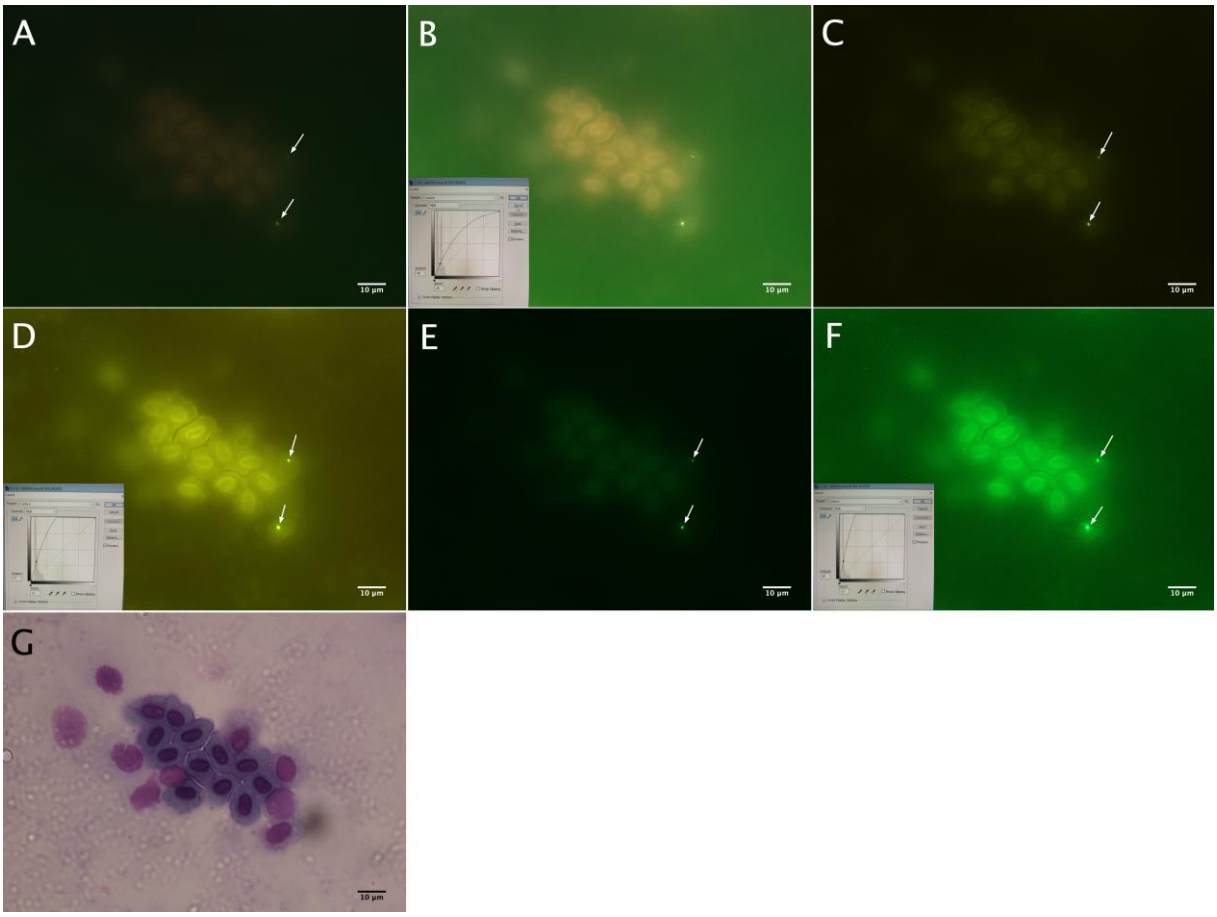

Figure S12.F. Fluorescent Polyethylene terephthalate (PET) particles in a blood sample of the Atlantic salmon (*Salmo salar*) parr. A, C and E is the original images, taken with fluorescent filters DFR, B2A and B2E, respectively. A curve-function (Photoshop) is used in B, D and F to enhance the contrast between the background/particle and the tissue. The change in curve is presented in the lower left of these pictures (gray boxes). G is the original Hematoxylin & Eosin (H&E) stained section used for overlay. G is taken with light microscopy (DIC).

Gina Almas Gundersen

Master's thesis Trondheim 2019

NTNU
Kunnskap for en bedre verden